



**SYNTHESIS AND BIOLOGICAL EVALUATION OF NOVEL 1,4-
DISUBSTITUTED-1,2,3-TRIAZOLE DERIVATIVES**

**A THESIS SUBMITTED TO
THE GRADUATE SCHOOL OF NATURAL AND APPLIED SCIENCES
OF
GAZI UNIVERSITY**

BY

Mustafa Nabeel Mirdan MIRDAN

**IN PARTIAL FULFILLMENT OF THE REQUIREMENTS
FOR
THE DEGREE OF MASTER OF SCIENCE
IN
CHEMISTRY**

JULY 2019

The thesis study titled “SYNTHESIS AND BIOLOGICAL EVALUATION OF NOVEL 1,4-DISUBSTITUTED-1,2,3-TRIAZOLE DERIVATIVES” is submitted by Mustafa Nabeel Mirdan MIRDAN in partial fulfillment of the requirements for the degree of Master of Science/Doctor of Philosophy in the Department of Chemistry, Gazi University by the following committee.

Supervisor: Prof. Dr. AliyeAlaylı ALTUNDAŞ

Chemistry Department, Gazi University

I certify that this thesis is a Master of Science thesis in terms of quality and content

Chairman: Assoc. Prof. EbruAKTAN

Chemistry Department, Gazi University

I certify that this thesis is a Master of Science thesis in terms of quality and content

Member: Assist. Prof. ÇağatayDENGİZ

Chemistry Department, University

I certify that this thesis is a Master of Science thesis in terms of quality and content

Date: 25/07/2019

I certify that this thesis, accepted by the committee, meets the requirements for being a Master of Science Thesis.

.....

Prof. Dr. Sena YAŞYERLİ

Dean of Graduate School of Natural and Applied Sciences

ETHICAL STATEMENT

I hereby declare that in this thesis study I prepared in accordance with thesis writing rules of Gazi University Graduate School of Natural and Applied Sciences;

- All data, information and documents presented in this thesis have been obtained within the scope of academic rules and ethical conduct,
 - All information, documents, assessments and results have been presented in accordance with scientific ethical conduct and moral rules,
 - All material used in this thesis that are not original to this work have been fully cited and referenced,
 - No change has been made in the data used,
 - The work presented in this thesis is original,
- or else, I admit all loss of rights to be incurred against me.

Signature

Mustafa Nabeel Mirdan MIRDAN

25/07/2019

SYNTHESIS AND BIOLOGICAL EVALUATION OF NOVEL 1,4-DISUBSTITUTED-
1,2,3-TRIAZOLE DERIVATIVES

(M. Sc. Thesis)

Mustafa Nabeel Mirdan MIRDAN

GAZI UNIVERSITY

GRADUATE SCHOOL OF NATURAL AND APPLIED SCIENCES

July 2019

ABSTRACT

In this thesis, a series of novel 1,4-disubstituted-1,2,3-triazole derivatives were synthesized the target molecules production followed click chemistry and three-component one-pot synthetic methods. In the synthesis of those compounds, the substituents on the aromatic rings were composed of electron-donating and electron-withdrawing groups. These compounds were biologically evaluated in vitro on xanthine oxidase (XO) inhibition. 1-ethynyl-4-methoxybenzene and 2-ethynylthiophene were synthesized in two steps by brominating and elimination reactions from para-methoxy benzaldehyde and thiophene carbaldehyde. Fifteen, 1,4-disubstituted-1,2,3-triazoles were synthesized form [3 + 2] cycloaddition reactions of substituted alkynes in the presence of Cu (II) catalyst with aryl azides formed after reduction, halogenation, and replacement reactions steps from substituted benzaldehydes. The structure of the synthesized compounds was examined using physical and FT-IR, ¹H-NMR, and ¹³C-APT-NMR spectroscopic methods. Inhibition effect of these compounds on XO enzyme was investigated according to Worthington method by measuring uric acid formation at 290 nm in vitro. (5-Bromothiophen-2-yl) – (1-(3-fluorobenzyl) -1*H*-1,2,3-triazol-4-yl) methanone, and (5-Bromothiophen-2-yl) – (1-(4-methoxybenzyl)-1*H*-1,2,3-triazol-4-yl) methanone compounds showed the highest IC₅₀ value: 0.93 ± 0.020 μM and 0.99 ± 0.043 μM compared to allopurinol positive standard.

ScienceCode : 20114
KeyWords : 1,2,3-triazole, xanthine oxidase
PageNumber : 93
Supervisor : Prof. Dr. Aliye ALTUNDAS

1,4-DİSÜBSTİTÜE-1,2,3-TRİAZOL TÜREVLERİNİN SENTEZİ BE BİYOLOJİK
ETKİLERİNİN İNCELENMESİ
(Yüksek Lisans Tezi)

Mustafa Nabeel Mirdan MIRDAN

GAZİ ÜNİVERSİTESİ
FEN BİLİMLERİ ENSTİTÜSÜ

Temmuz 2019

ÖZET

Bu tezde, 1,4-disüstitüe-1,2,3-triazol türevlerinden oluşan bir dizi bileşik sentezlendi. Hedef moleküllerin eldesinde, klik kimya ve üç bileşenli tek kap sentez yöntemleri kullandı. Bileşiklersentezinde armatik halkalardaki substitüentler elektron veren ve elektron çeken gruplar olarak dizayn edildi. Sentealenen triazol bileşiklerindeki substitüenterin ksantin oksidaz (XO) enzim inhibisyonu üzerine etikleri in vitro olarak inceşendi. Para-Metoksibenzaldhit be tiyofen karbaldehitden bromlama ve ayrılma tepkimeleri ile iki basamakta 1-etinil-4-metoksibenzen ve 2-etiniltiyofen sentezlendi. Ayrıca substitüe benzaldehitlerden indergeme, halojenleme ve yer deęiştirme tepkime basamaklarından sonra oluşturulan arilazürler ile ilgili alkinlerin Cu (II) katalizörü varlığında [3 + 2] sikokatılma tepkimelerinden onbeş tane 1,4-disubstitüe-1,2,3-triazol sentezlendi. Sentezlenen bileşiklerin yapıları, fiziksel ve FT-IR, ¹H-NMR ve ¹³C-APT-NMR spektroskopik yöntemleri kullanılarak aydınlatıldı. Bileşiklerin XO enzimi üzerine inhibisyon etkisi in-vitro olarak ürik asit oluşumunun 290 nm de ölçülmesiyle Worthington metoduna göre incelenmiştir . (5-Bromotiyofen-2-il) – (1-(3-florobenzil)-1*H*-1,2,3-triazol-4-il) metanon ve (5-Bromotiyofen-2-il)–(1-(4-metoksibenzil)-1*H*-1,2,3-triazol-4-il) metanon bileşiklerinin allopurinol pozitif standardına göre IC₅₀: 0.93 ± 0.020 µM ve 0.99 ± 0.043 µM deęerleriyle en yüksek inhibisyon etkisi gösterdiği bulunmuştur.

BilimKodu : 20114
AnahtarKelimeler : 1,2,3-triazol, ksantin oksadase
SayfaAdedi : 93
Danışman : Prof. Dr. Aliye ALTUNDAŞ

ACKNOWLEDGMENTS

Firstly, I am ever grateful to Allah, the Creator, and the Guardian, and to whom I owe my very existence.

Foremost, I would like to offer my thanks and appreciation to my supervisor Pro. Dr. Aliye ALTUNDAŞ for continued support and guidance during my master study. This thesis would not be completed without her support.

Besides my advisors, I would like to express my thanks to my thesis committee members Assoc. Prof. Ebru AKTAN and Assist. Prof. Çağatay DENGİZ for their advice, support, and helpful feedback.

Best my gratitude to my dear father, mother, and sister for their unlimited support, patience and encouragement.

Finally, I thank our assistant Güler YAĞIZ, and fellow student Yunus TURKMEN, spectrum examiner Dr. Burcu AYDINER, and teaching assist. Doğukan DOYDUK who have not forgotten me. Thank you to everyone who encouraged me during the difficult periods of study, which reduced my stress.

CONTENTS

	Pages
ABSTRACT.....	iv
ÖZET	v
ACKNOWLEDGMENTS	vi
CONTENTS.....	vii
LIST OF FIGURES	xi
LIST OF SCHEMES.....	xiv
LIST OF TABLES.....	xv
LIST OF ABBREVIATIONS.....	xvii
1. INTRODUCTION.....	1
2. MATERIAL AND METHODS.....	21
2.1. Chemicals.....	21
2.2. Equipment.....	21
2.3. Methods.....	21
2.3.1. Corey-Fuchs reaction.....	21
2.3.2. Synthesis of azido methyl derivatives from aldehydes.....	22
2.3.3. Click reaction.....	23
2.3.4. Three component one-pot method.....	23
2.3.5. Sample preparation for biological evaluation.....	23
3. EXPERIMENTAL.....	25
3.1. General procedure for alkyne synthesis.....	25
3.1.1. 2,2-Dibromovinyl synthesis.....	25
3.1.2. Alkyne synthesis.....	26
3.2. General procedure for the synthesis of azido methyl derivatives.....	27
3.2.1. Synthesis of (4-nitrophenyl) methanol (compound e).....	27
3.2.2. Synthesis of 1-(azidomethyl)-4-nitrobenzene (compound f).....	28

	Pages
3.2.3.Synthesis alcohols (compound g - n).....	29
3.2.4.Synthesis of azidomethyl derivatives (compound o - v).....	30
3.3. Click reaction procedure for triazole synthesis.....	30
3.3.1.Synthesis of 1-(2-fluorobenzyl)-4-(4-methoxyphenyl)-1 <i>H</i> -1,2,3-triazole (21)	31
3.3.2.Synthesis of 1-(3-fluorobenzyl)-4-(4-methoxyphenyl)-1 <i>H</i> -1,2,3-triazole (22)	31
3.3.3.Synthesis of 1-(4-fluorobenzyl)-4-(4-methoxyphenyl)-1 <i>H</i> -1,2,3-triazole (23)	32
3.3.4.Synthesis of 1-(2,4-difluorobenzyl)-4-(4-methoxyphenyl)- 1 <i>H</i> -1,2,3-triazole (24).....	32
3.3.5.Synthesis of 1-(3,4-difluorobenzyl)-4-(4-methoxyphenyl)- 1 <i>H</i> -1,2,3-triazole (25).....	32
3.3.6.Synthesis of 1-(2,5-difluorobenzyl)-4-(4-methoxyphenyl)- 1 <i>H</i> -1,2,3-triazole (26).....	33
3.3.7.Synthesis of 1-(4-methoxyphenyl)-4-(4-nitrobenzyl)-1 <i>H</i> -1,2,3-triazole (27)	33
3.3.8.Synthesis of 1-(3-fluorobenzyl)-4-(thiophen-2-yl)-1 <i>H</i> -1,2,3-triazole (28)	34
3.3.9.Synthesis of 1-(2,5-difluorobenzyl)-4-(thiophen-2-yl)-1 <i>H</i> -1,2,3-triazole (29)	34
3.3.10.Synthesis of 1-(3,5-difluorobenzyl)-4-(thiophen-2-yl)- 1 <i>H</i> -1,2,3-triazole (30).....	34
3.3.11.Synthesis of 1-(4-nitrobenzyl)-4-(thiophen-2-yl)-1 <i>H</i> -1,2,3-triazole (31)	35
3.4.Three component one-pot procedure for triazole synthesis	35
3.4.1.Synthesis of (1-(3-fluorobenzyl)-1 <i>H</i> -1,2,3-triazole-4-yl) (5-methylthiophen-2-yl)methanone (32).....	36
3.4.2.Synthesis of (1-(3,5-difluorobenzyl)-1 <i>H</i> -1,2,3-triazole-4-yl) (5-methylthiophen-2-yl)methanone (33).....	36
3.4.3.Synthesis of (5-bromothiophen-2-yl)(1-(3-fluorobenzyl)- 1 <i>H</i> -1,2,3-triazole-4-yl) methanone (34).....	37

	Pages
3.4.4. Synthesis of (5-bromothiophen-2-yl)(1-(4-methoxybenzyl)-1 <i>H</i> -1,2,3-triazole-4-yl) methanone (35)	37
4. CONCLUSION	39
4.1. Spectroscopic analysis of triazole compounds	39
4.1.1. FT-IR, ¹ H-NMR, ¹³ C-APT-NMR spectroscopy analysis results of 1-(2-fluorobenzyl)-4-(4-methoxyphenyl)-1 <i>H</i> -1,2,3-triazole (21)	39
4.1.2. FT-IR, ¹ H-NMR, ¹³ C-APT-NMR spectroscopy analysis results of 1-(3-fluorobenzyl)-4-(4-methoxyphenyl)-1 <i>H</i> -1,2,3-triazole (22)	42
4.1.3. FT-IR, ¹ H-NMR, ¹³ C-APT-NMR spectroscopy analysis results of 1-(4-fluorobenzyl)-4-(4-methoxyphenyl)-1 <i>H</i> -1,2,3-triazole (23)	45
4.1.4. FT-IR, ¹ H-NMR, ¹³ C-APT-NMR spectroscopy analysis results of 1-(2,4-difluorobenzyl)-4-(4-methoxyphenyl)-1 <i>H</i> -1,2,3-triazole (24)	48
4.1.5. FT-IR, ¹ H-NMR, ¹³ C-APT-NMR spectroscopy analysis results of 1-(3,4-difluorobenzyl)-4-(4-methoxyphenyl)-1 <i>H</i> -1,2,3-triazole (25)	51
4.1.6. FT-IR, ¹ H-NMR, ¹³ C-APT-NMR spectroscopy analysis results of 1-(2,5-difluorobenzyl)-4-(4-methoxyphenyl)-1 <i>H</i> -1,2,3-triazole (26)	54
4.1.7. FT-IR, ¹ H-NMR, ¹³ C-APT-NMR spectroscopy analysis results of 4-(4-methoxyphenyl)-1-(4-nitrobenzyl)-1 <i>H</i> -1,2,3-triazole (27)	57
4.1.8. FT-IR, ¹ H-NMR, ¹³ C-APT-NMR spectroscopy analysis results of 1-(3-fluorobenzyl)-4-(thiophen-2-yl)-1 <i>H</i> -1,2,3-triazole (28)	60
4.1.9. FT-IR, ¹ H-NMR, ¹³ C-APT-NMR spectroscopy analysis results of 1-(2,5-difluorobenzyl)-4-(thiophen-2-yl)-1 <i>H</i> -1,2,3-triazole (29)	63
4.1.10. FT-IR, ¹ H-NMR, ¹³ C-APT-NMR spectroscopy analysis results of 1-(3,5-difluorobenzyl)-4-(thiophen-2-yl)-1 <i>H</i> -1,2,3-triazole (30)	66
4.1.11. FT-IR, ¹ H-NMR, ¹³ C-APT-NMR spectroscopy analysis results of 1-(4-nitrobenzyl)-4-(thiophen-2-yl)-1 <i>H</i> -1,2,3-triazole (31)	69
4.1.12. FT-IR, ¹ H-NMR, ¹³ C-APT-NMR spectroscopy analysis results of (1-(3-fluorobenzyl)-1 <i>H</i> -1,2,3-triazol-4-yl)(5-methylthiophen-2-yl) methanone (32)	72
4.1.13. FT-IR, ¹ H-NMR, ¹³ C-APT-NMR spectroscopy analysis results of (1-(3-fluorobenzyl)-1 <i>H</i> -1,2,3-triazol-4-yl)(5-methylthiophen-2-yl) methanone (33)	75
4.1.14. FT-IR, ¹ H-NMR, ¹³ C-APT-NMR spectroscopy analysis results of (5-bromothiophen-2-yl)(1-(3-fluorobenzyl)-1 <i>H</i> -1,2,3-triazol-4-yl) methanone (34)	78

	Pages
4.1.15. FT-IR, ¹ H-NMR, ¹³ C-APT-NMR spectroscopy analysis results of (5-bromothiophen-2-yl)(1-(4-methoxybenzyl)-1 <i>H</i> -1,2,3-triazol-4-yl) methanone (35).....	81
4.2. Biological analysis of triazole compounds	84
4.3. Conclusion	87
REFERENCES	89
CURRICULUM VITAE	93



LIST OF FIGURES

Figure	Pages
Figure 1.1. Triazole isomers	1
Figure 1.2. An earlier model of CuAAC.....	2
Figure 1.3. Modern mechanistic proposal for CuAAC reaction.....	3
Figure 1.4. Proposed intermediates in the catalytic cycle of the RuAAC reaction	4
Figure 1.5. Li's view for the reaction course.....	6
Figure 1.6. Ramachary's vision for the reaction pathway.....	6
Figure 1.7. Rozin's proposed mechanism	7
Figure 1.8. Ali's proposed mechanism.....	8
Figure 1.9. Rademann's proposed mechanism.....	9
Figure 1.10. The postulated mechanism for base-catalyzed synthesis of 1,5-disubstituted-1,2,3-triazoles.....	10
Figure 1.11. Triazole as amide surrogate.....	12
Figure 1.12. Triazole as amide surrogate.....	12
Figure 1.13. Triazole as ester group surrogate.....	13
Figure 1.14. Triazole as ester group surrogate.....	14
Figure 1.15. Triazole as carboxylic acid group surrogate.....	15
Figure 1.16. Triazole as olefin group surrogate.....	16
Figure 1.17. Triazole as olefin group surrogate.....	16
Figure 1.18. Triazole as a heterocyclic surrogate	18
Figure 1.19. Xanthine oxidase inhibitors.....	19
Figure 1.20. The molecules we planned to synthesize in this thesis.....	19
Figure 4.1. FT-IR spectrum of compound 21	39
Figure 4.2. ¹ H-NMR spectrum of compound 21.....	40
Figure 4.3. APT-NMR spectrum of compound 21	41
Figure 4.4. FT-IR spectrum of compound 22	42
Figure 4.5. ¹ H-NMR spectrum of compound 22.....	43

Figure	Pages
Figure 4.6. APT-NMR spectrum of compound 22	44
Figure 4.7. FT-IR spectrum of compound 23	45
Figure 4.8. ¹ H-NMR spectrum of compound 23.....	46
Figure 4.9. APT-NMR spectrum of compound 23	47
Figure 4.10. FT-IR spectrum of compound 24	48
Figure 4.11. ¹ H-NMR spectrum of compound 24.....	49
Figure 4.12. APT-NMR spectrum of compound 24	50
Figure 4.13. FT-IR spectrum of compound 25	51
Figure 4.14. ¹ H-NMR spectrum of compound 25.....	52
Figure 4.15. APT-NMR spectrum of compound 25	53
Figure 4.16. FT-IR spectrum of compound 26	54
Figure 4.17. ¹ H-NMR spectrum of compound 26.....	55
Figure 4.18. ¹³ C-NMR spectrum of compound 26	56
Figure 4.19. FT-IR spectrum of compound 27	57
Figure 4.20. ¹ H-NMR spectrum of compound 27.....	58
Figure 4.21. APT-NMR spectrum of compound 27	59
Figure 4.22. FT-IR spectrum of compound 28	60
Figure 4.23. ¹ H-NMR spectrum of compound 28.....	61
Figure 4.24. APT-NMR spectrum of compound 28	62
Figure 4.25. FT-IR spectrum of compound 29	63
Figure 4.26. ¹ H-NMR spectrum of compound 29.....	64
Figure 4.27. APT-NMR spectrum of compound 29	65
Figure 4.28. FT-IR spectrum of compound 30	66
Figure 4.29. ¹ H-NMR spectrum of compound 30.....	67
Figure 4.30. APT-NMR spectrum of compound 30	68
Figure 4.31. FT-IR spectrum of compound 31	69

Figure	Pages
Figure 4.32. ^1H -NMR spectrum of compound 31.....	70
Figure 4.33. APT-NMR spectrum of compound 31	71
Figure 4.34. FT-IR spectrum of compound 32	72
Figure 4.35. ^1H -NMR spectrum of compound 32.....	73
Figure 4.36. APT-NMR spectrum of compound 32	74
Figure 4.37. FT-IR spectrum of compound 33	75
Figure 4.38. ^1H -NMR spectrum of compound 33.....	76
Figure 4.39. ^{13}C -NMR spectrum of compound 33	77
Figure 4.40. FT-IR spectrum of compound 34	78
Figure 4.41. ^1H -NMR spectrum of compound 34.....	79
Figure 4.42. APT-NMR spectrum of compound 34	80
Figure 4.43. FT-IR spectrum of compound 35	81
Figure 4.44. ^1H -NMR spectrum of compound 35.....	82
Figure 4.45. APT-NMR spectrum of compound 35	83

LIST OF SCHEMES

Scheme	Pages
Scheme 1. Corey-Fuchs reaction to access 1-ethynyl-4-methoxy benzene.....	22
Scheme 2. Corey-Fuchs reaction to access 2-ethynylthiophene.....	22
Scheme 3. Aldehyde to azido methylbenzenes.....	22
Scheme 4. Click reaction	23
Scheme 5. Cross-Dehydrogenative coupling reaction.....	23



LIST OF TABLES

Tables	Pages
Table 1.1. R groups on the synthesized molecules	20
Table 3.1. Physical data of 1-(2,2-dibromovinyl)-4-methoxybenzene	25
Table 3.2. Physical data of 2-(2,2-dibromovinyl) thiophene	26
Table 3.3. Physical data of 1-ethynyl-4-methoxybenzene	27
Table 3.4. Physical data of 2-ethynyl thiophene	27
Table 3.5. Physical data of (4-nitrophenyl) methanol	28
Table 3.6. Physical data of 1-(azidomethyl)-4-nitrobenzene	28
Table 3.7. Physical data for compounds g – n	29
Table 3.8. Physical data for compounds o – v	30
Table 3.9. Physical data of 1-(2-fluorobenzyl)-4-(4-methoxyphenyl)-1 <i>H</i> -1,2,3- triazole	31
Table 3.10. Physical data of 1-(3-fluorobenzyl)-4-(4-methoxyphenyl)-1 <i>H</i> - 1,2,3-triazole	31
Table 3.11. Physical data of 1-(4-fluorobenzyl)-4-(4-methoxyphenyl)-1 <i>H</i> - 1,2,3-triazole	32
Table 3.12. Physical data of 1-(2,4-difluorobenzyl)-4-(4-methoxyphenyl)-1 <i>H</i> - 1,2,3-triazole	32
Table 3.13. Physical data of 1-(3,4-difluorobenzyl)-4-(4-methoxyphenyl)-1 <i>H</i> - 1,2,3-triazole	33
Table 3.14. Physical data of 1-(2,5-difluorobenzyl)-4-(4-methoxyphenyl)-1 <i>H</i> - 1,2,3-triazole	33
Table 3.15. Physical data of 1-(4-methoxyphenyl)-4-(4-nitrobenzyl)-1 <i>H</i> - 1,2,3-triazole	33
Table 3.16. Physical data of 1-(3-fluorobenzyl)-4-(thiophen-2-yl)-1 <i>H</i> -1,2,3-triazole ...	34
Table 3.17. Physical data of 1-(2,5-difluorobenzyl)-4-(thiophen-2-yl)-1 <i>H</i> - 1,2,3-triazole	34
Table 3.18. Physical data of 1-(3,5-difluorobenzyl)-4-(thiophen-2-yl)-1 <i>H</i> - 1,2,3-triazole	35
Table 3.19. Physical data of 1-(4-nitrobenzyl)-4-(thiophen-2-yl)-1 <i>H</i> -1,2,3-triazole	35

Tables	Pages
Table 3.20. Physical data of (1-(3-fluorobenzyl)-1 <i>H</i> -1,2,3-triazole-4-yl)(5-methylthiophen-2-yl)methanone	36
Table 3.21. Physical data of (1-(3,5-difluorobenzyl)-1 <i>H</i> -1,2,3-triazole-4-yl)(5-methylthiophen-2-yl)methanone	36
Table 3.22. Physical data of (5-bromothiophen-2-yl)(1-(3-fluorobenzyl)-1 <i>H</i> -1,2,3-triazole-4-yl) methanone.....	37
Table 3.23. Physical data of (5-bromothiophen-2-yl)(1-(4-methoxybenzyl)-1 <i>H</i> -1,2,3-triazole-4-yl) methanone.....	37
Table 4.1. Selected FT-IR spectrum data of compound 21	39
Table 4.2. Selected FT-IR spectrum data of compound 22	42
Table 4.3. Selected FT-IR spectrum data of compound 23	45
Table 4.4. Selected FT-IR spectrum data of compound 24	48
Table 4.5. Selected FT-IR spectrum data of compound 25	51
Table 4.6. Selected FT-IR spectrum data of compound 26	54
Table 4.7. Selected FT-IR spectrum data of compound 27	57
Table 4.8. Selected FT-IR spectrum data of compound 28	60
Table 4.9. Selected FT-IR spectrum data of compound 29	63
Table 4.10. Selected FT-IR spectrum data of compound 30	66
Table 4.11. Selected FT-IR spectrum data of compound 31	69
Table 4.12. Selected FT-IR spectrum data of compound 32	72
Table 4.13. Selected FT-IR spectrum data of compound 33	75
Table 4.14. Selected FT-IR spectrum data of compound 34	78
Table 4.15. Selected FT-IR spectrum data of compound 35	81
Table 4.16. Xanthine oxidase inhibition values.....	85

LIST OF ABBREVIATIONS

Abbreviations and symbols which are used in this thesis, with their meanings, are elaborated down-below.

Symbols Meanings

δ Chemical shift

Abbreviations Meanings

$^1\text{H-NMR}$	^1H - Nuclear Magnetic Resonance
$^{13}\text{C-APT NMR}$	^{13}C -“Attached Proton Test” Nuclear Magnetic Resonance
CBr_4	Tetrabromomethane
CuAAC	Copper(I)-catalyzed azide-alkyne cycloaddition
$\text{Cu}(\text{NO}_3)_2 \cdot 3\text{H}_2\text{O}$	Copper (II) nitrate trihydrate
$\text{CuSO}_4 \cdot 5\text{H}_2\text{O}$	Copper (II) sulfate pentahydrate
DCM	Dichloromethane
DMF	Dimethyl formamide
EtOAc	Ethyl acetate
FT-IR	Attenuated Total Reflection Fourier Transform Infrared Spectrometer
NaBH_4	Sodium borohydride
NaN_3	Sodium azide
Na_2SO_4	Sodium sulfate
$n\text{-BuLi}$	Normal butyllithium
PBr_3	Tribromophosphine
PPh_3	Triphenylphosphine
$t\text{-BuLi}$	Tertiary butyllithium
TMEDA	Tetramethylethylenediamine

1. INTRODUCTION

Triazole are heterocyclic aromatic compounds containing three nitrogen and two carbon atoms in five-membered rings (see Figure 1.1). This journey begins when *P. Griess*, 1864 pioneered organic azide chemistry synthesis. His research left the door wide open for follow-up studies. One of which was 1,2,3-triazole moiety synthesis. The first analogy of triazole moiety comes from nitrile imine interaction with dienophile group such as isocyanate. This reaction, however, turns out to be energetically unfavorable [1], and for the sake of clarity, 1,2,4-triazole synthesis is out of this thesis' scope. Alternatively, A. Michael, who is known for Michael addition, reported an easy strategy to synthesize 1,2,3-triazoles by combining acetylenes with alkyl azides [2]. What fascinated organic chemists at that time to spend more effort to develop this reaction was α -bond formation at the end of the cycloaddition. Regioselectivity, however, posed a problem even for brilliant scientists. Various explanations, such as steric and electronic hindrance, aroused to articulate the reason behind such poor regioselectivity. Several decades of devoted work have been invested to get a better regioselectivity with higher yields, but few of them have solved this mystery.

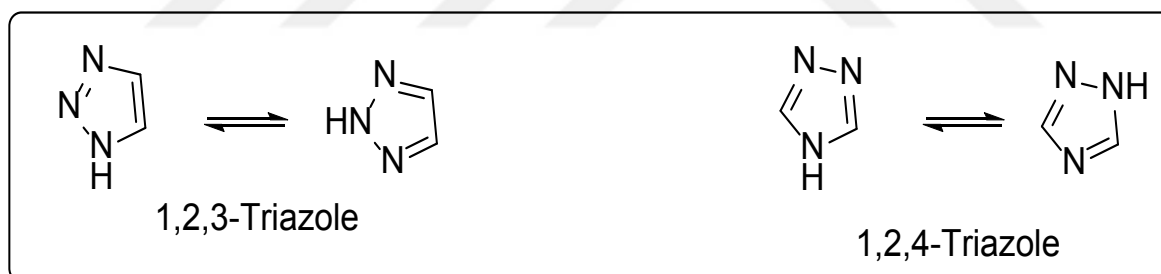


Figure 1.1. Triazole isomers

The challenging questions were why a mixture of products are observed in the synthesis of 1,2,3-triazoles, and how to get one type of product over the other. A theoretical study conducted by Sharpless, et al. [3] in 2005, showed that the energy barrier for transition state of both 1,4- and 1,5-disubstituted-1,2,3-triazoles are very close in values of 25.7 and 26 kcal/mol, respectively, which explains the equal amount of two products in one reaction. Various experimental approaches represented by individual works of Rostovtsev, et al. [4], Meldal, et al. [5] in 2002, and Boren, et al. [6] in 2008 emerged to get only one product on the expense of the other one. Copper-catalyzed azide-alkyne-cycloaddition (CuAAC) method, on the contrary to Huisgen thermal approach, gives only 1,4-disubstituted-1,2,3-

triazoles. Boren method, on the other hand, uses the ruthenium-catalyst system to get 1,5-disubstituted-1,2,3-triazoles. The theoretical explanation of these observations will be the subject of the following discussion.

Regiospecificity was Husigen method's problem, knowing that Sharpless, et al. [3] decided to run a theoretical study to have a deeper understanding and to solve the mystery behind it. Density functional theory (DFT) calculations that mentioned earlier showed how close both products are in transition-state energy-barrier with the sub-kilocalorie difference in units. After being found out that copper (II)/ascorbate system is adequate to bring one of the product's transition-energy-barrier down, the author examined the type of ligands needed to the reaction medium. Through their study, the author noticed that water has dual functionalities: it serves as a suitable solvent due to its higher polarity; and it serves as a thermodynamically stable ligand to copper metal center until it is replaced by azide moiety. According to the DFT studies on CuAAC method, activation energy of 1,4-disubstituted-1,2,3-triazole is lowered from 25.7 to 18.7 kcal/mol, which means that 1,4-disubstituted-1,2,3-triazole formation is preferred by seven order of magnitude. Experimental result reported in 2002 shows that primer, secondary, tertiary, and aryl azide reacts with alkyne in excellent yield. However, the mechanistic proposal was not clear until 2013 [7]. However, for the reader's benefit, Sharpless mechanism is represented in Figure 1.2 [3].

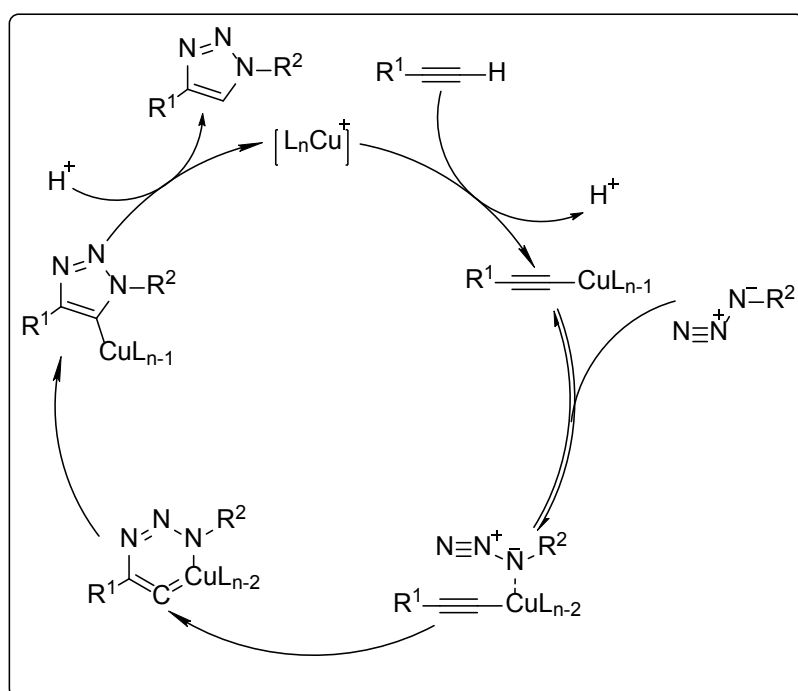


Figure 1.2. An earlier model of CuAAC

After reviewing suggested mechanistic pathways for 1,4-disubstituted-1,2,3-triazole ring formation, Worrell, et al. [7] ran several experiments to provide a more elaborate mechanistic picture. Based on weak π -interaction of the copper metal ion with alkyne moiety, which suggested earlier, the author followed precise procedure to produce copper (I) N-heterocyclic substituted acetylide. Treatment of copper (I)-acetylide with a substituted azide in the absence of soluble-exogenous-copper catalyst formed triazole ring within 20 min and confirmed by real-time heat-follow reaction calorimetry. When the same reaction was run in the absence of catalyst no product formation was confirmed. After that, the author hypothesized that each copper atom involved in triazole ring formation acts individual. To prove this hypothesis, the author used copper enriched catalyst isotope (^{63}Cu) with naturally abundant copper (I)-acetylide (69:31). According to the results, the author noticed that the copper (I) isotope, which attached to triazole ring get enriched of about 50% which negates their earlier hypothesis. Therefore, the author decides to run another experiment to determine at which stage the naturally abundant copper (I) get enriched; first, from known polynuclear catalyst, no enrichment occurred according to the time of flight mass spectrometry (TOF-MS); second, the author examined the idea of performing the reaction with trace-amount of cases; third, the author assumed that isotope enrichment occurs by substituted azide addition to π -interacted enriched copper at copper (I)-acetylide. At this stage, triazolide ring intermediate forms followed by fast NHC exchange between two copper atoms with one acting as ligand donor to the more oxidized copper atom. Figure 1.3 represents the latest proposal on CuAAC-reaction mechanism.

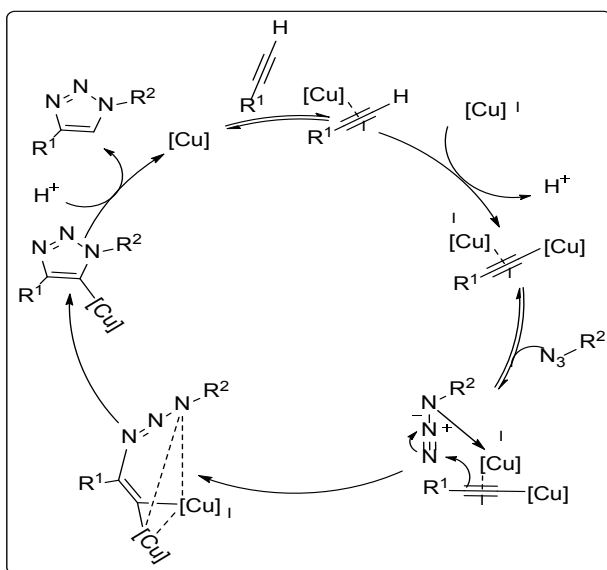


Figure 1.3. Modern mechanistic proposal for CuAAC reaction

Boren, et al. [6] wanted to prove that it is possible to obtain 1,5-disubstituted-1,2,3-triazoles alone by using ruthenium-catalysts. The author's idea was based on earlier studies of successful benzene formation from acetylenes by Ru-catalyst. Through this study, it was found that ruthenium-catalyzed azide-alkyne-cycloaddition (RuAAC) can tolerate not only terminal but also internal alkyne moiety. The mechanistic pattern suggests that the new bond was formed between electron-rich carbon of alkyne and terminal nitrogen of azide, and this type of binding requires perfect position of chloride ligand; either by forming a hydrogen bond with a specific type of alkyne substituent or by the electronic effect of alkyne. Even though there reported method succeeded in 1,5-disubstituted-1,2,3-triazole formation, it was reported in two cases where tetra-azadiene and cyclo-pentatriene complexes were formed with ruthenium metal that prevented triazole formation. To explain why these byproducts were formed, the author optimized the amount of components used, and the addition pattern of components to the reaction medium. It was also reported that longer time necessary with secondary azide component transformation to triazole ring, while tertiary-azide resulted in no triazole ring formation. In conclusion, the author proved that 1,5-di and 1,4,5-trisubstituted-1,2,3-triazole formation are possible and proposed a simple mechanistic pathway for their formation, as shown in Figure 1.4.

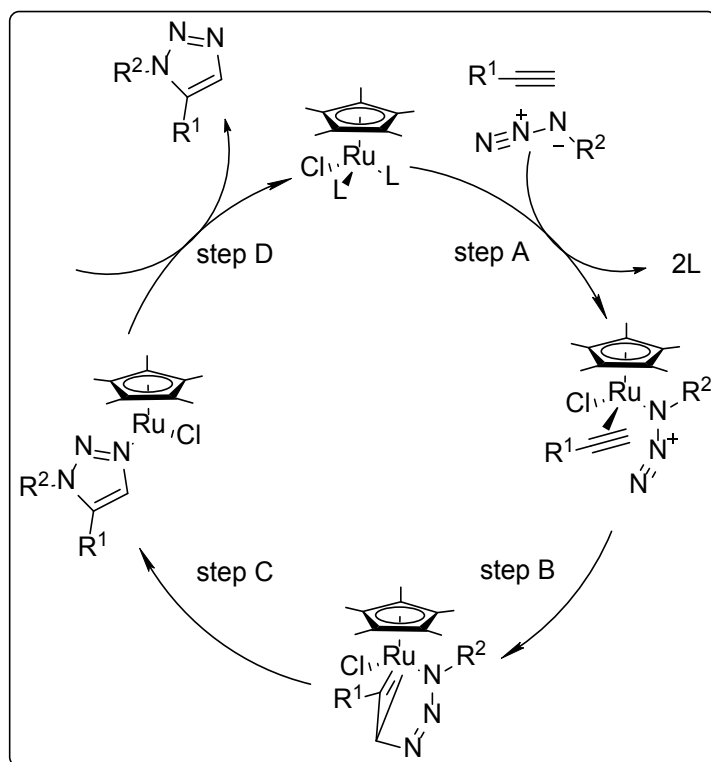


Figure 1.4. Proposed intermediates in the catalytic cycle of the RuAAC reaction

With its excellent regioselectivity under ambient condition, triazole click chemistry was utilized as a biolabeling agent to visualize protein activity in living cells as Staudinger and strain promoted [3+2] cycloadditions do. While evaluating those two compared to CuAAC, it was reported an interesting activity for biomolecular labeling in exocellular protein samples. However, CuAAC-triazole caused living cell's death and intervening in protein-labeled bioanalysis [8-10]. Since CuAAC triazoles may yield incorrect indications in-situ, some scientists suggested running a preliminary-bioactivity-test for the 1,2,3-triazoles in smaller-scale [11]. Others created new synthetic methods to eliminate copper and ruthenium metal usage while retaining regioselectivity. To provide alternative synthetic pathways applicable for large- and small-scale of bio isosteric reactions. The suggestion of recent paces of research can be narrowed into four sub-groups: organo-catalyzed enamine mediated-azide cycloaddition [12, 13]; azide and active methylene binding through base-promoted cycloaddition [14, 15]; reaction of α -keto-phosphorous-ylides with aryl azides [16, 17]; or tetramethylammonium hydroxide use to bind alkyne with azide moieties [18]. Each sub-division are discussed in brief.

Li, et al. [12] and Ramachary, et al. [13] examined the influence of enamine-mediated organo-catalysts on 1,4-disubstituted-1,2,3-triazole production. Accordingly, they found out that dienamine serves as HOMO-rising dipolarophile. When they run different trials to determine a proper base to be used in the course of the reaction, it was found out that DBU is the required catalyst for Ramachary and Li's methods, Li additionally mixed DBU with diethylamine dissolved in DMSO to get the best results. The effect of both electron-withdrawing-groups and electron-donating-groups on azides and aldehydes were also evaluated. Eventually, the research furnished an alternative synthetic pathway for 1,4-disubstituted triazole with an excellent yield. Li, for instance, reported the use of α,β -unsaturated aliphatic aldehyde chains to give a mixture of Z-E isomers, and the use of alkyl azide turns out to be not efficient. Ramachary, on the other hand, reported the use of aliphatic chain aldehydes with almost similar results compared to that of Li obtained. Both groups concluded that the final product yield is dependent on both the length of the aldehyde chains and the presence of the electron-donating group on both components. When we compare both synthetic methods, Ramachary managed to obtain 1,4-disubstituted-1,2,3-triazoles in 30 min while Li synthesized them in 5 h at room temperature. The mechanistic explanation for triazole ring formation is depicted in Figures 1.5 and 1.6.

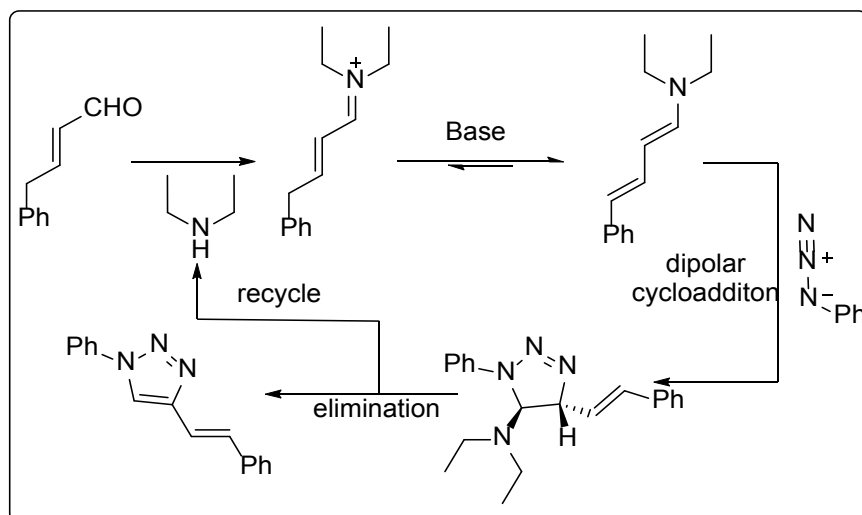


Figure 1.5. Li's view for the reaction course

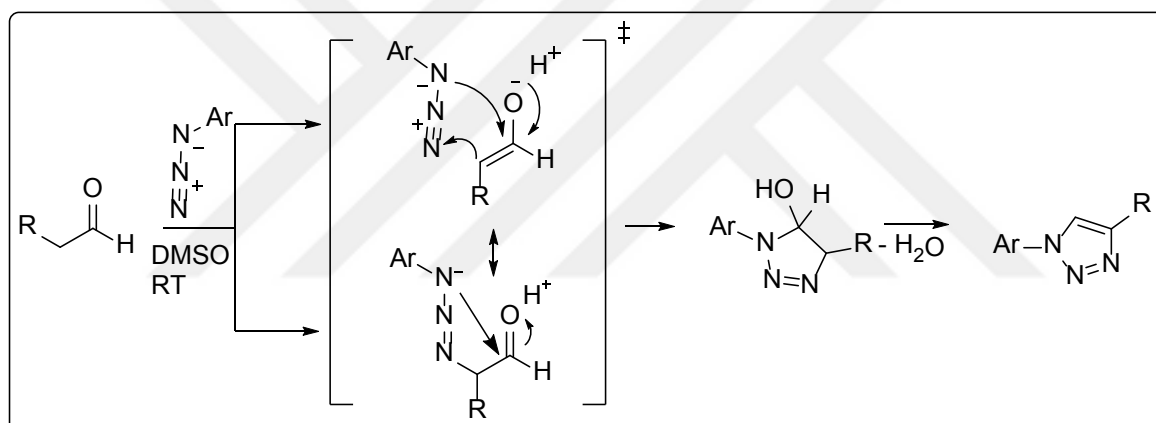


Figure 1.6. Ramachary's vision for the reaction pathway

Next, researchers like Rozin, et al. [15], and Ali, et al. [14] investigated the effect of activated methylene on regioselectivity. Utilization of both variously substituted 1-trifluoromethyl-1,3-dicarbonyl, or malononitrile all provides an electron-rich olefin intermediate. Carbon with double bond adjacent to this electron withdrawing group is always a preferred site for N 1 of azide moiety to form a new bond with it, Rozin proved this proposal with the data gained from ^{13}C NMR. When examined the deprotonation state of both carbonyl groups with and without triethyl amine presence, it was found out that carbonyl group next to trifluoromethyl functional group is the only deprotonated one. Ali, on the other hand, trusted a DFT calculations to determine the exact pathway. The results of the calculations were in favor of olefin group adjacent to electron withdrawing group with 23.5 kcal/mol, while the other pathway disfavored with 11.6 kcal/mol. The authors agreed on some facts, for example,

it is necessary to have an electron-withdrawing group attached to azide moiety for better yield, and their method was applicable in thermal base mediated conditions. On the other hand, they disagreed on solvent selection Rozin, for instance, reported an inverse relation between product yields when solvent used, while Ali used DBU in DMSO. Ali obtained 1,4-disubstituted- while Rozin accessed 1,4,5-trisubstituted-1,2,3-triazoles. Figure 1.7 and 1.8 represents the postulated mechanisms.

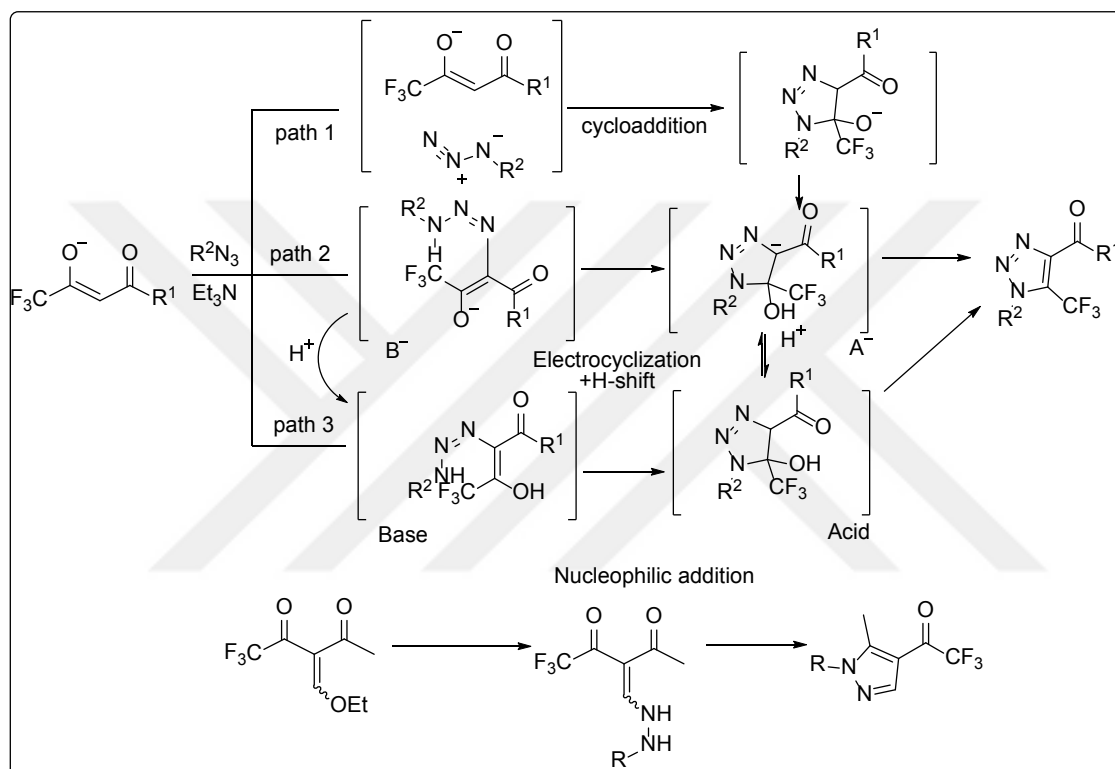


Figure 1.7. Rozin's proposed mechanism

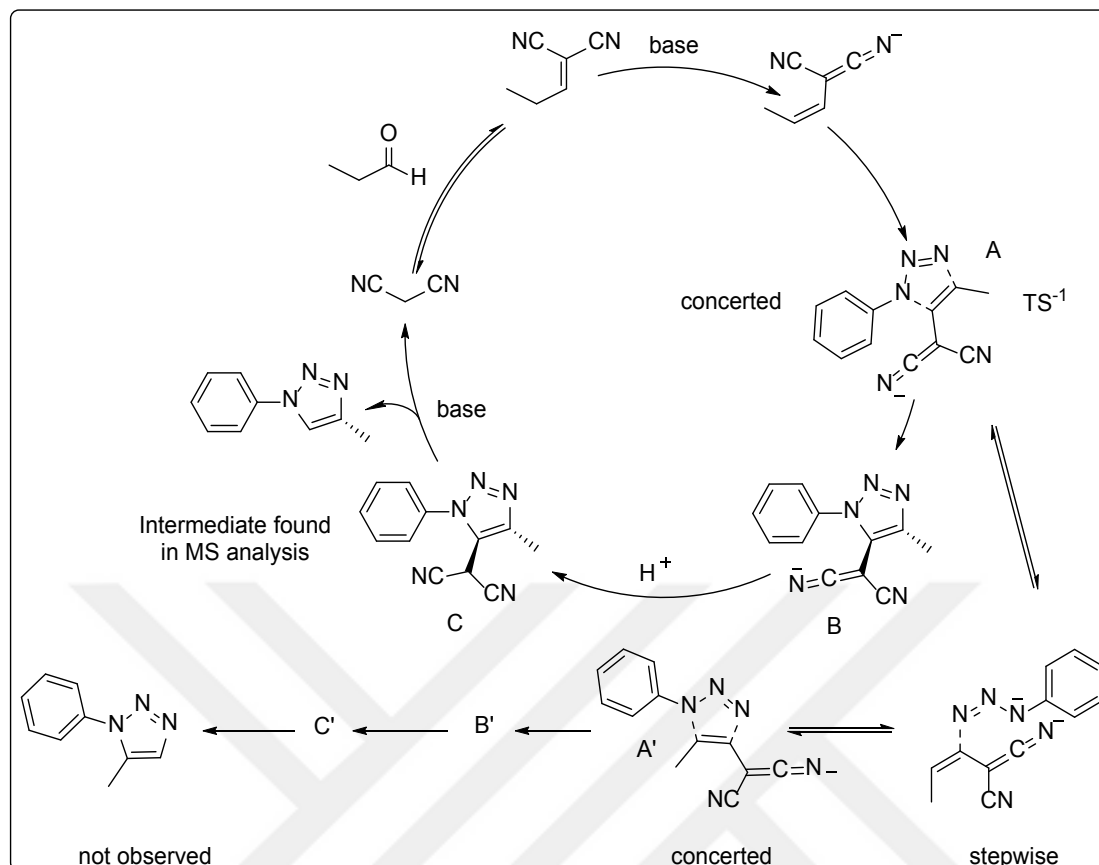


Figure 1.8. Ali's proposed mechanism

Rademann, et al. [16, 17] explored the possibility of synthesizing pseudo-cis-peptide by 1,5-disubstituted-1,2,3-triazole on a solid support. They initially mentioned cis-peptide formation through the lactamization step of linear peptide containing a triazole ring attached to the solid support. First, the author attached tert-butyl phosphorene ylidene to resin. Then elongation of the peptide chain takes place on N-terminal. The mechanistical suggestion was that trifluoroacetic acid must be used, after the desired linear peptide begin formed so that C-terminal of phosphorene ylidene gets decarboxylated. After N-terminal being transformed into azide, the LUMO of N 3 can form a ring with the HOMO of C-terminal of phosphorane ylide, which is electron rich olefin. Subsequently, N 1 of azide moiety attacks carbonyl group to form 1,5-disubstituted-1,2,3-triazole ring. The author examined the peptide sequence length effect to conclude that diphosphoranylidene always gives dimeric cis-peptide it follows stepwise reaction mechanism, while triphosphoranylidene gives monomeric cis-peptide after conducting the reaction on high-cross-linked resin following concerted reaction mechanism. The synthesized products were confirmed using LCMS and 2D NMR. On another occasion, the author performed the same reaction to confirm which configuration

does 1,5-disubstituted-1,2,3-triazole prefer when used as a click ligation agent of linear peptides. After synthesizing these products, a molecular dynamics simulation was run on them to find out that 1,5-disubstituted-1,2,3-triazole prefers turn-like configuration in solution. Figure 1.9 demonstrates the proposed mechanism.

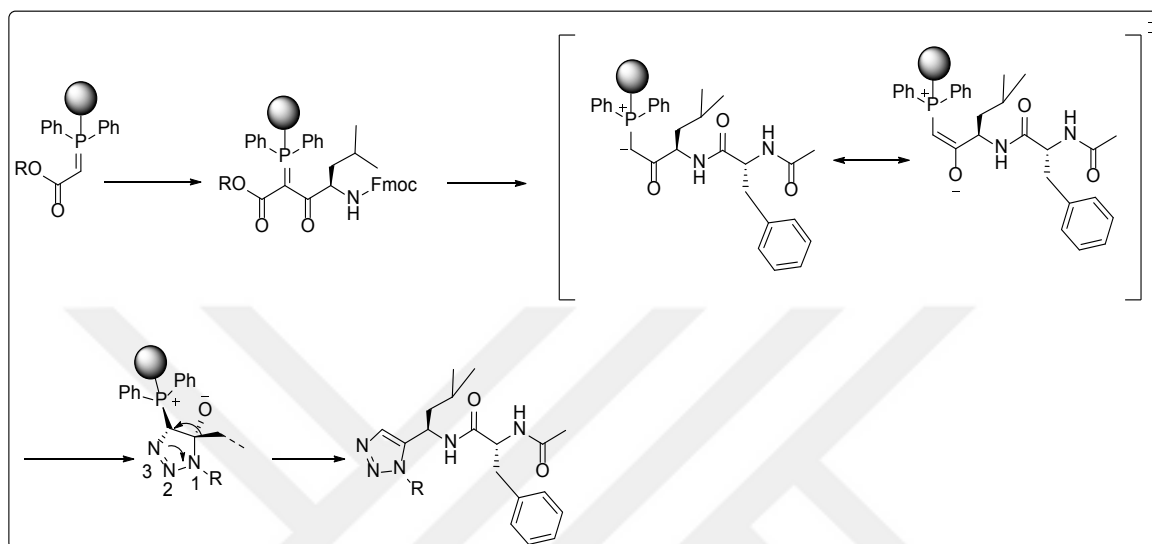


Figure 1.9. Rademann's proposed mechanism.

Kwok, et al. [18] employed an idea of dissolving acetylene in a basic medium to form acetylide intermediate to get 1,5-disubstituted-1,2,3-triazole ring with a variety of aryl substituted azides at room temperature. Previous reports mentioned the use of lithium or magnesium metals to form acetylides, the author, on the other hand, proposed that acetylene has a quite acidic behavior in DMSO. Accordingly, acetylide should be obtained upon exposure to base. Indeed, the author used tetramethylammonium hydroxide for the acetylene deprotonation. The formed acetylide attacks to terminal nitrogen and triazole ring closure occur through 6π -electron cyclization process. Subsequently, protonated DMSO gets deprotonated by giving away hydrogen to get stabilized 1,5-disubstituted-1,2,3-triazole. The author managed to synthesize 1,5-disubstituted-1,2,3-triazole even starting from electron-rich aryl azides in excellent yields. The postulated mechanism is shown in Figure 1.10.

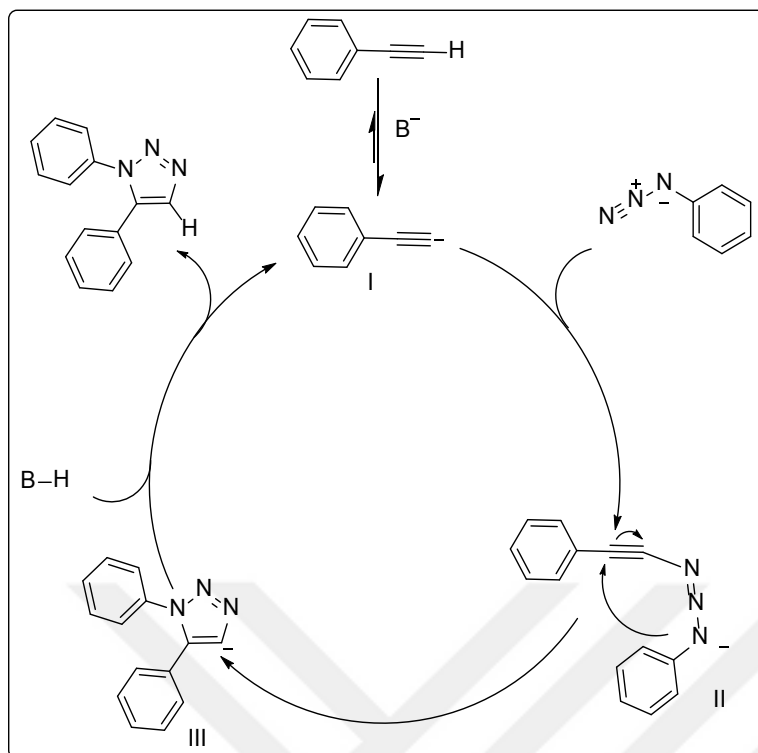


Figure 1.10. The postulated mechanism for base-catalyzed synthesis of 1,5-disubstituted-1,2,3-triazoles

After both metal-catalyzed and metal free pathways being investigated, 1,2,3-triazoles were tested in vivo domain. Following Sharpless and Meldal methods, by Letschert, et al. [19], and following retro-Diels-Alder method for metal-free cycloaddition reaction by van Berkel, et al. [20] 1,4,5-trisubstituted triazoles were successfully obtained in vivo. Attributes like; stability under pH ranging from 4-12, redox reaction intolerance, chemo- and regio-selectivity, polarity, and hydrogen bond donating and accepting ability made 1,4-disubstituted-1,2,3-triazoles a valuable tool for bioorganic chemists to use. Having a unique structural feature in addition to those mentioned earlier, triazoles, as several studies suggested [21-29], may mimic the biological role played by amides, an ester bonds, carboxylic acids, olefins, and other heterocyclic functional groups to reduce drug resistance. With this foundation in hand, we faced with the question of choosing either 1,4-di- or 1,5-di-substituted triazole to synthesize, and which specific biological group to target.

Massarotti, et al. [30] reviewed protein date base (pdb) cases in which 1,4-di- and 1,5-di-substituted triazoles form a complex structure with DNA and peptide units to refine the pharmacophoric role played by them. Concerns about molecular recognition, metabolic and

biological stability, and solubility were the author's evaluation criterion for deciding which one suits better as a novel bioactive compound. Besides having an aromatic index equal to that of benzene, the N-3 atom on the triazole ring also displays a hydrogen bond accepting affinity with a total of 4 pdb cases for the 1,4-disubstituted-1,2,3-triazole; carbon 4, however, shows hydrogen donating affinity, even if it is a weak bond, with a total of 7 pdb cases for 1,4-disubstituted-1,2,3-triazole. Moreover, 1,4-disubstituted-1,2,3-triazole ring had two types of π -stacking interaction, namely face-face in two instances and edge-face in one instance while 1,5- had one type of π -stacking interaction of edge-face in one instance. Forming these types of bonds will assure targeted protein stability and drug efficacy. The author, then, analyzed the cases where 1,4-disubstituted-1,2,3-triazole formed a bond to the amino-acid binding site to show that 1,4-disubstituted-1,2,3-triazole prefers binding to hydrophobic residues over polar ones. While evaluating 1,4-di and 1,5-disubstituted-1,2,3-triazole's metabolic stability, the author derived some conclusions like; electron donor group substituted 1,4-disubstituted is more stable towards oxidative demethylation than 1,5-disubstituted, electron withdrawing group presence leads to 1,4-being resistant to biotransformation, having metabolically labile substituents (e.g. methyl group on the aromatic ring) leads to aromatic ring hydroxylation. Metabolically stable 1,4-disubstituted-1,2,3-triazoles do not form toxic amines in vivo. Finally, 1,4-disubstituted-1,2,3-triazole shows best results in terms of in vitro solubility.

Based on the information provided by Massarotti, we set the 1,4-disubstituted-1,2,3-triazole as our synthetic target for their overall attributes in vitro and in vivo. To determine which functional group to target we, first, studied some crucial cases mentioned in the paper of Bonandi, et al. [31], in which both 1,4-di and 1,5-di-substituted-1,2,3-triazoles enhanced or compressed the biological efficacy as a bio isostere:

Triazole as amide group surrogate

Brik, et al. [21] reported the synthesis of both 1 and 2 as typical examples of the efficient amide replacement with triazole ring. These analogues, synthesized through Sharpless and Meldal methods, provided a more stable derivatives of amprenavir based on computational modeling. These calculations indicated that N-2 of triazole rings, which replaces carbonyl group, forms a hydrogen bond with a water molecules that further forms a hydrogen bond with HIV-1 protease, and C5 of triazole, which replaces amine group in the original

compound, forms a hydrogen bond with Gly27 peptide oxygen on biological evaluation with this mutant type of disease. Figure 1.11 contains the original compound next to functional group replaced compounds.

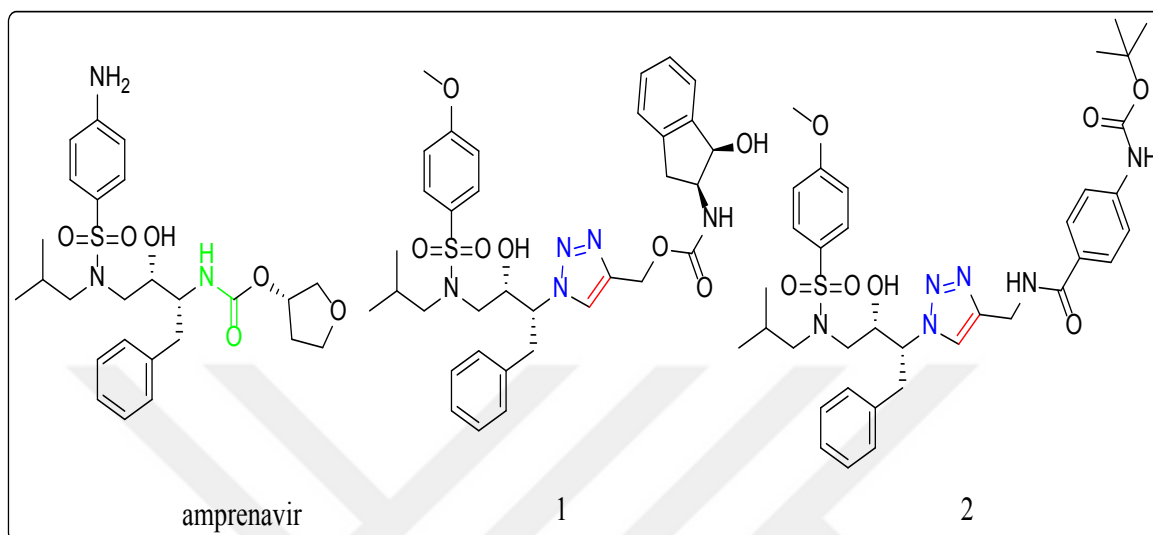


Figure 1.11. Triazole as amide surrogate

Monceaux, et al. [22] on the contrary, reported that biological activities went down by 1000 threshold upon amide-anti-1,2,3-triazole replacement. To have an elaborate picture of such discouraging result, the author ran a molecular docking test between reference compound 3 and compound 4. The results showed that the attached group at C-4 is aligned with 3, but the attached group at N-1 is tilted making the secondary amine group bridge formation with D228 carboxylate impossible. Docked module indicated the reason for a reduced biological activity of 4 against BACE1. Figure 1.12 contains the original compound next to functional group replaced compounds.

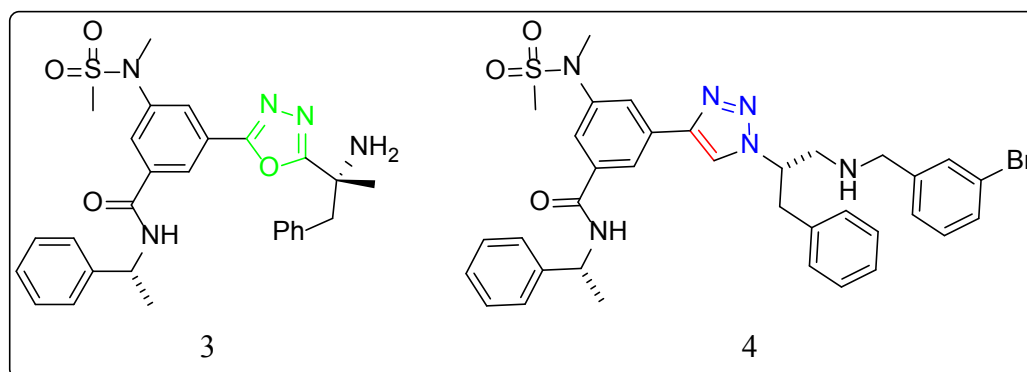


Figure 1.12. Triazole as amide surrogate

Triazole as ester group surrogate

Imperio, et al. [23] proposed an alternative synthetic strategy in which lactone of natural products like Steganacin and Podophyllotoxin which spotted as a weak joint for its possible metabolic degradation by that a massive loss in the efficacy, to be replaced with a triazole moiety. As biological analysis showed, these compounds form bonds with active colchicine sites bringing about microtubule inhibition. Others reported these compounds to display anticancer activity. To utilize the ruthenium catalyzed method, the author synthesized 1,5-disubstituted-1,2,3-triazole analogues of the lactone rings of both deoxy-podophyllotoxin and Stegane. While biologically evaluating the triazole analogues of these natural products podophyllotoxin analogue was proven to have IC₅₀ value superior to its original compound. Then anti-tubulin assay was run no podophyllotoxin and 5 with combretastatin C-4 and paclitaxel to suggest that podophyllotoxin analogue possess the same anti-tubulin affinity as the original compound does. Figure 1.13 contains the original compounds next to functional group replaced compounds.

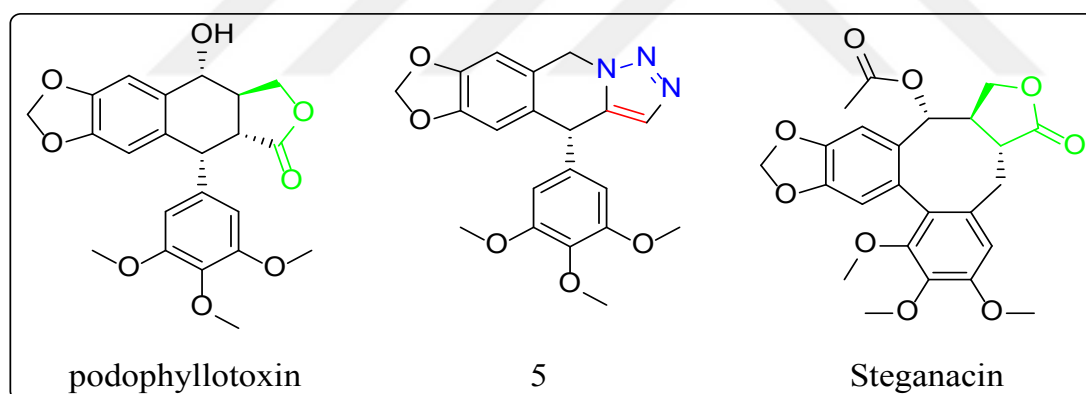


Figure 1.13. Triazole as ester group surrogate

In another study reported by Li, et al. [24] on replacing ester group in β -D-glucogallin (BGG) with a robust surrogate that tolerates neutral and acidic medium without being decomposed and that inhibits specifically diabetic eye disease. The absence of sorbitol dehydrogenase cause sorbitol accumulation, which is responsible for several diseases, one of which is diabetic eye disease. The author attempted to replace ester with amide triazole, and other groups, and then the author examined the effect of linker length on AKR1B1 inhibition. While evaluating triazole as amide surrogate, amide analogue gave comparable inhibition results to that of BGG, triazole, however, failed to reduce AKR1B1 inhibition. The author's

theory behind triazole's weak inhibition was the carbonyl group absence, while molecular modeling suggested that triazole moiety causes inversion of analogue interaction with specified pocket. Both bioassay and molecular modeling indicated that produced analogue effect gets reduced as linker groups length increased. Figure 1.14 contains the original compounds next to functional group replaced compounds.

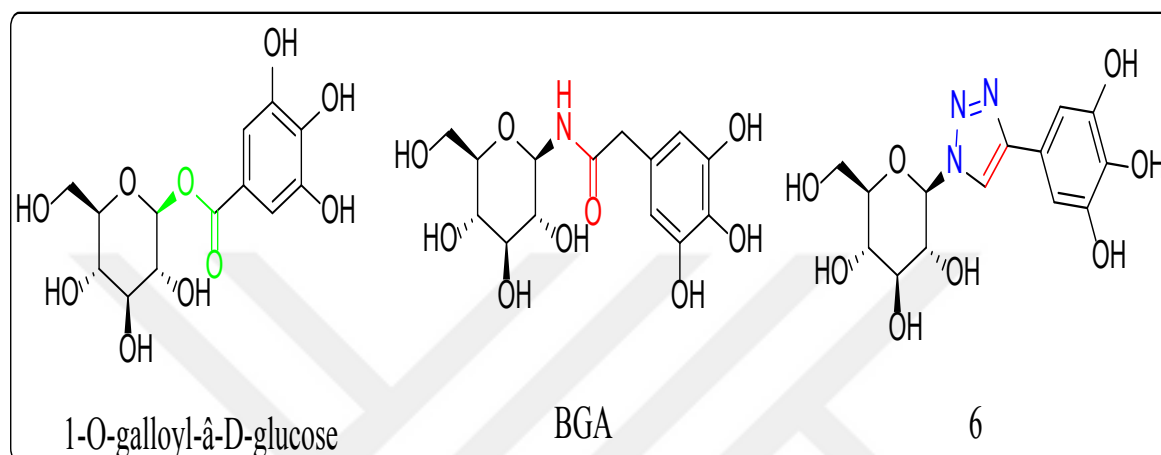


Figure 1.14. Triazole as ester group surrogate

Triazole as carboxylic acid group surrogate

Pippione, et al. [25] have suggested N-substituted hydroxy triazoles as carboxylic bio isosteres based on data gathered from pKa and CLogP. Through analysis, the author found that the position of substitution on the N atom has a significant effect on pKa values of the bio isostere. From that the author aimed to construct triazole analogue inhibitor of AMPA receptor and OvCHT1, which is known for causing blindness (*Onchocerca volvulus* chitinase), by providing a mimetic structure with IC₅₀ value comparable or better than those existing drugs. Triazole inhibitor analogue of AMPA receptor succeeded to maintain equal pKa value while failed to provide inhibition scale equal to that of the existing one. But triazole analogues of MDG-1-33A (namely; 7, 8, 9) managed to maintain a comparable pKa value and to have an IC₅₀ value at the nanomolar range. (Figure 1.15)

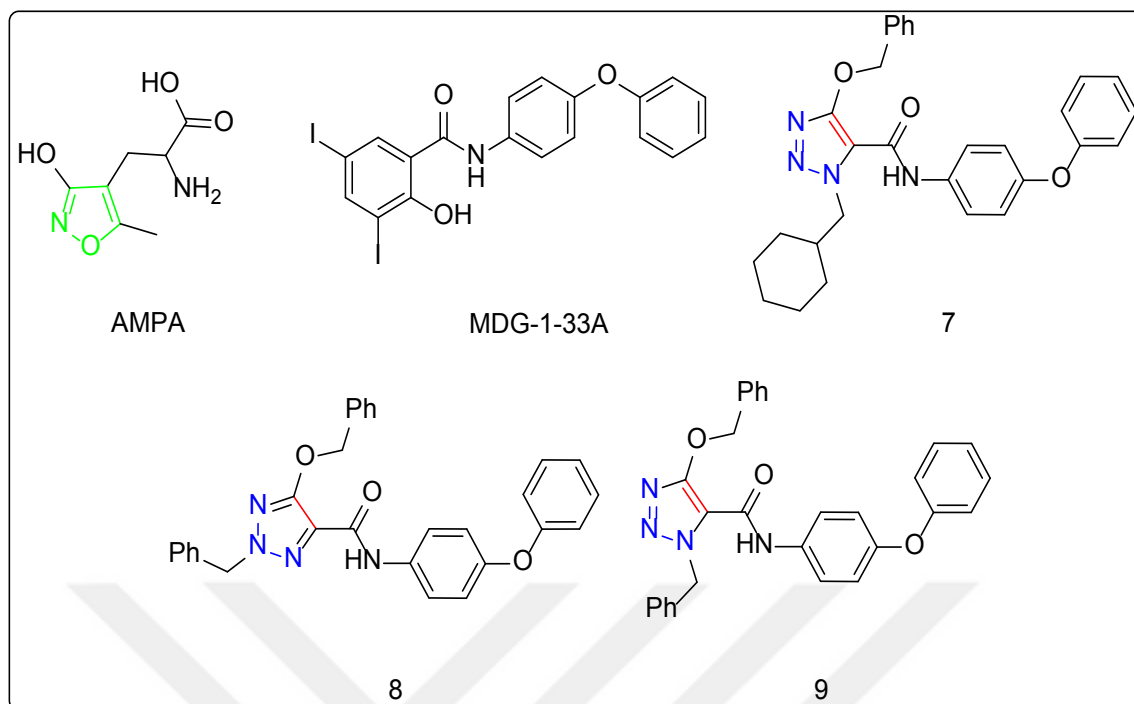


Figure 1.15. Triazole as carboxylic acid group surrogate

Triazole as olefin group surrogate

Beale, et al. [26] have examined the possibility of replacing the cis-stilbene bridge with a soluble and more stable surrogate to dismantle the vascular system of cancer cells. At first, the author examined the nitrogen position concerning a trimethoxy substituted aryl ring. When biologically evaluated triazole analogue of combretastatin A-4 (CA-4): N atom adjacent to the trimethoxy aryl ring showed inhibitory activity with IC₅₀ value 35 nM in the 1,5-disubstituted form; while flipping the ring downgraded inhibitory activity to 410 nM; replacing 1,5-disubstituted triazole with 1,4-isomer, on the other hand, resulted in IC₅₀ value fall to 1,3 μM; extending the bridge length results also in activity fall as well; utilizing 1,2,4-triazole, alternatively, gave better IC₅₀ value of 25 nM compared to 1,2,3-triazole analogue with carbon atom was next to the trimethoxy phenyl ring and the N atom positioned next to 3-hydroxy-4-methoxy aryl ring as seen in the figure 1.16. Next, the author tested the idea of replacing two of the methoxy groups on the trimethoxy ring with halogen atoms such as bromine and iodine. A test on cell growth-inhibition was run on SK-OV-3 cell line by comparing CA-4, 10, 11, 12, at 3 nM concentration resulted in 31, 72, 88, 44 %, respectively, of micro-tubulin interference which meant that dibrominated CA-4 triazole analogue had a superior interference to that of reference compound CA-4, at concentration 15 nM compound

42 showed cell arrest value of 84 %. When these analogues tested for inhibiting tubulin polymerization, 10 inhibited a hundred pre-cent of the polymerization CA-4, on the other hand, inhibited fifty-eight pre-cent of it. The biological assay on Human-umbilical-vein-endothelial-cell line using CA-4, 10, 11, 12 resulted in IC₅₀ values exceeded to equal to CA-4 value with 1, 1.7, 2.2 nM, respectively. Finally, the author ran a molecular modeling assay of their products using colchicine binding sites to have an elaborated picture of the way triazole analogue would interact with binding sites. Molecular modeling results showed that the hydroxy position alongside the 4-methoxy atom at B ring results in more stable hydrogen bond formation, which was the case for compound 10 and 12.

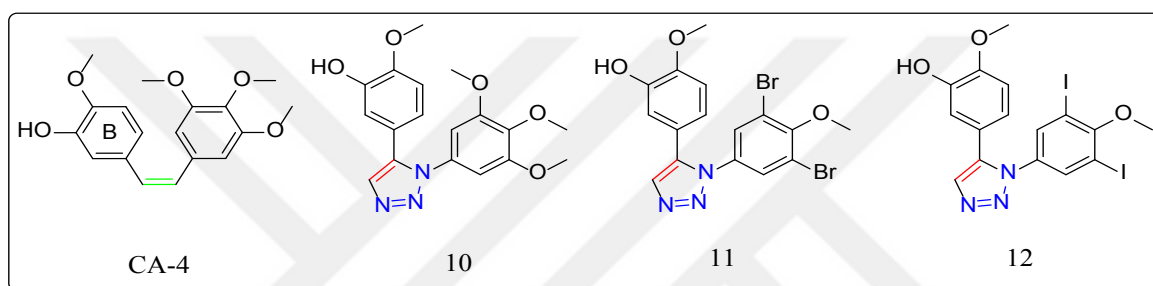


Figure 1.16. Triazole as olefin group surrogate

From successful cases of chalcone, and anti-tubulin olefinic double bond replacement, Mesenzani, et al. [27] came with the idea of replacing double bonds with 1,4-di-, 4,5-di-substituted-1,2,3-triazoles, and 1,5-disubstituted tetrazoles (figure 1.17). The author ran two biological tests; one of them was on neuroblastoma-cell-line (SH-SY5Y), and the second one was on cell arrest at G2/M phase. From these two assays, they concluded that compound 13, 14 ynone showed anti-tubulin characteristics while all triazole and tetrazole analogues failed. Cell arrest tests showed that compound 15 has as potency to be reference drug.

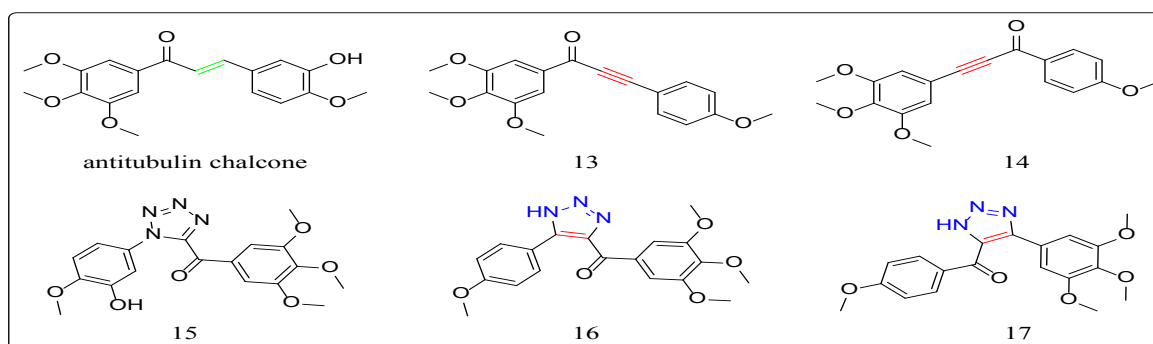


Figure 1.17. Triazole as olefin group surrogate

Triazole as a heterocyclic surrogate

Suzuki, et al. [28, 29] targeted histone deacetylase 8 inhibitors (HDAC 8) based on reports of specific cell growth regulation of T-cell lymphoma and neuroblastoma. Earlier attempts to synthesize selective triazole inhibitors of this enzyme were not successful. By dissecting the chemical structure of vorinostat, which consisted of three components zinc-binding-group (hydroxamate), a linker, and anilide cap, 120 triazole derivatives were synthesized and evaluated their effect against HDAC 8 of HeLa cancer cell line. Subsequently, the author ran a test to determine copper (I) presence on the overall inhibition with vorinostat as a reference drug. No significant effect on HDAC 8 inhibition was observed. From the 120 triazole analogues, the author found out that two compounds have comparable activity to that of PCI-34051 at 0.3 μ M against HDAC 8. Weak efficacy exerted by those two compounds against total HDACs at higher concentration while showing comparable results to PCI-34051 which is HDAC 8 selective inhibitor. Compound 18 possessed an IC_{50} value of 70 nM compared to PCI-34051 value of 310 nM. This compound was submitted to molecular modeling using HDAC 8-complex of CRA-A crystal as a template. From molecular modeling results it was concluded that 1,2,3-triazole linker controls the configuration of 18 in binding site within HDAC 8 enzyme and by doing so 18 takes U like shape assuring phenyl thio-methyl group binding to hydrogen bonds formed, and CH- π bound formation with triazole ring. On another occasion, the author explored the idea of replacing triazole ring with six- and five-membered rings to evaluate HDAC 8 inhibition on the accumulation of acetyl-cohesin in HeLa cell and on T-cell lymphoma inhibition considering HH, MT4, Jurkat, and HuT78 types. Biological examination of enzymatic efficacy on compound 20, in anti-triazole conformation, showed IC_{50} values of 53 nM, which is a better than that of compound 18. These compounds (18, 19, 20) then submitted to cell assay to determine acetyl accumulation compound 19, having a thiazole ring instead, exerted acceptable results of acetyl accumulation while the other two had unexpected participation. Finally, these compounds were tested for the T-cell lymphoma inhibition. Compound 19 again had superior results to that of compound 18. Figure 1.18 contains the original compounds next to functional group replaced compounds.

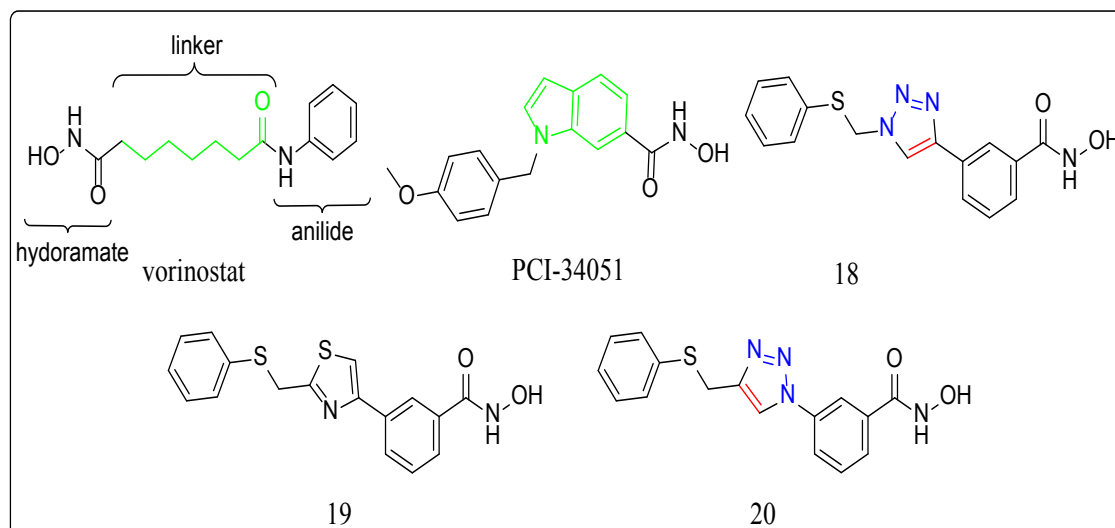


Figure 1.18. Triazole as a heterocyclic surrogate

Among the cases we reviewed, a complete replacement of Allopurinol's purine ring with thiazole moiety of Febuxostat afforded improvement in the IC_{50} value from $7.56 \mu M$ to 16 nM . Such an enhancement has received our attention (figure 1.17). These drugs are prescribed for patients suffering from hyperuricemia condition when pharmacological therapy is needed to alleviate uric acid accumulation in the blood. This condition is identified by over- or under-excretion of uric acid. Overproduction of uric acid consequently crystallized and precipitate in joints and nearby tissues. The elevated uric acid level in the blood, as proposed, can provoke xanthine oxidoreductase enzyme to increase uric acid formation. The mechanism at which uric acid elevation can cause disorders is unknown but is hypothesized to follow oxidative stress mechanism. The primary threat of uric acid accumulation comes from the antioxidant and prooxidant nature of it, in which prooxidant nature can reduce the nitric-oxide level in veins, leading to chronic-heart-failure, and increase reactive-oxygen-species formation, which reacts with nitric oxide to form peroxy-nitrite free-radical [32]. Another study also describes reactive-oxygen-species as a critical cause of inflammation, cancer, etc. [33]. Even though both drugs performed well as xanthine oxidase inhibitor studies showed that 20-40 % of the patient using allopurinol and 45-67 % using febuxostat of the patients reached acceptable uric acid level in blood, that means new treatment is still required [34]. Others evaluated both drugs for toxicity. Accordingly, febuxostat is less toxic compared to allopurinol [35].

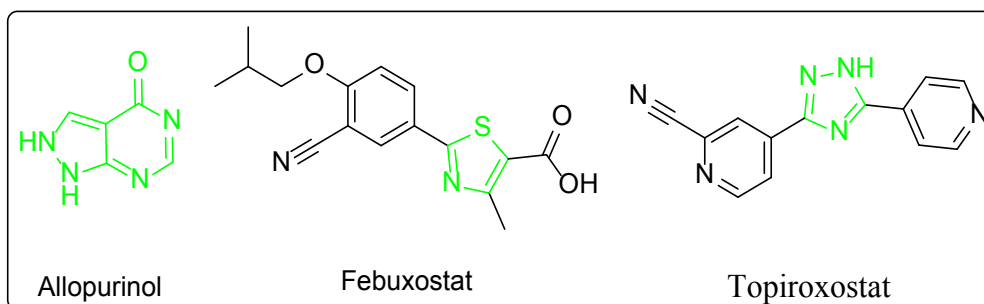


Figure 1.19. Xanthine oxidase inhibitors

Recent expansion of xanthine oxidase inhibitor family to compound containing triazoles such as Topiroxostat [36] in the figure 1.19. Competitive research concerning the uric acid level reduction in the blood, [37] earlier report mentioned having N-2 substituted 1,2,3-triazole with an IC_{50} value of 84 nM motivated us to create a research project. Thus, we focused on synthesizing 1,4-disubstituted-1,2,3-triazoles on smaller-scale and biologically evaluated several structures. At the final stage, we will synthesize target compound on a larger scale depending on the bioassay results. Figure 1.20 contains the molecules we planned to synthesize in this thesis. While table 1 contains the R groups on the synthesized molecules.

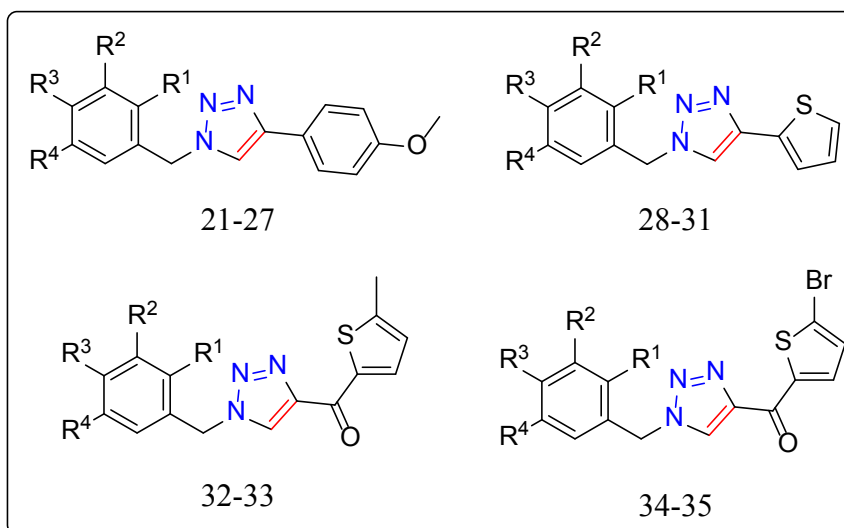


Figure 1.20. The molecules we planned to synthesize in this thesis

Table 1.1. R groups on the synthesized molecules

21	$R^1 = F$	$R^2 = H$	$R^3 = H$	$R^4 = H$
22	$R^1 = H$	$R^2 = F$	$R^3 = H$	$R^4 = H$
23	$R^1 = H$	$R^2 = H$	$R^3 = F$	$R^4 = H$
24	$R^1 = F$	$R^2 = H$	$R^3 = F$	$R^4 = H$
25	$R^1 = H$	$R^2 = F$	$R^3 = F$	$R^4 = H$
26	$R^1 = F$	$R^2 = H$	$R^3 = H$	$R^4 = F$
27	$R^1 = H$	$R^2 = H$	$R^3 = NO_2$	$R^4 = H$
28	$R^1 = H$	$R^2 = F$	$R^3 = H$	$R^4 = H$
29	$R^1 = F$	$R^2 = H$	$R^3 = H$	$R^4 = F$
30	$R^1 = H$	$R^2 = F$	$R^3 = H$	$R^4 = F$
31	$R^1 = H$	$R^2 = H$	$R^3 = NO_2$	$R^4 = H$
32	$R^1 = H$	$R^2 = F$	$R^3 = H$	$R^4 = H$
33	$R^1 = H$	$R^2 = F$	$R^3 = H$	$R^4 = F$
34	$R^1 = H$	$R^2 = F$	$R^3 = H$	$R^4 = H$
35	$R^1 = H$	$R^2 = F$	$R^3 = OMe$	$R^4 = F$

2. MATERIAL AND METHODS

2.1. Chemicals

Triphenylphosphine (PPh₃), tetra bromomethane (CBr₄), sodium ascorbate, copper (II) sulfate pentahydrate (CuSO₄·5H₂O), 4-methoxybenzaldehyde, 1-(5-methylthiophen-2-yl)ethan-1-one, 1-(5-bromothiophen-2-yl)ethan-1-one, 1-(thiophen-2-yl)ethan-1-one, sodium azide (NaN₃), dimethyl formamide (DMF), *n*-butyl lithium (*n*-BuLi), *t*-butyl lithium (*t*-BuLi), dichloromethane (DCM), ethyl acetate (EA), *n*-hexane, tribromo phosphine (PBr₃), sodium borohydride (NaBH₄), diethyl ether, copper (II) nitrate trihydrate (Cu(NO₃)₂·3H₂O), sodium sulfate (Na₂SO₄), tetramethylethylenediamine (TMEDA).

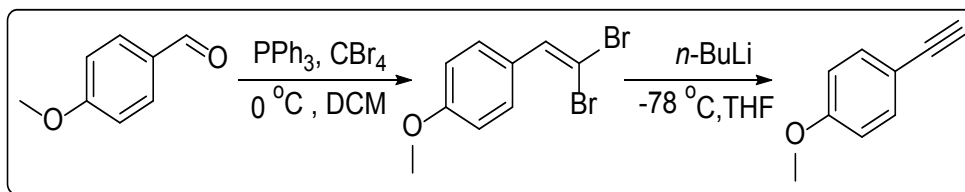
2.2. Equipment

- A) ¹H-NMR spectra were recorded at 300 MHz.
- B) ¹³C-NMR spectra were recorded at 75 MHz.
- C) Mattson- 1000 FT-IR was used for FT-IR analysis.
- D) The melting point for samples was taken by Stuart melting point smp30.

2.3. Methods

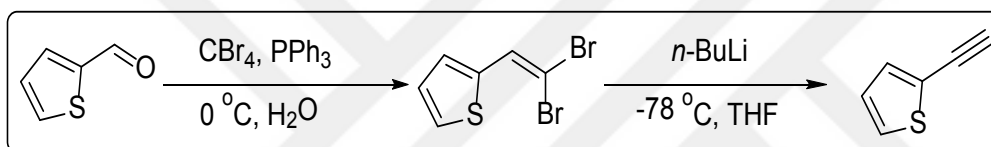
2.3.1. Corey-Fuchs reaction

This method can be used to synthesize 4-methoxyphenylacetylene and 2-ethynylthiophene starting from corresponding aldehydes. The conversion process is executed in two steps. First substituted para-methoxy benzaldehydes were converted with the help of tetra bromomethane and triphenylphosphine to (2,2-dibromovinyl)-4-methoxy benzene. Subsequently, the product of the first step converted to ethynyl para-methoxy benzene moiety in the presence of *n*-butyl lithium [38]. The product of this method demonstrated in scheme 1 down-below.



Scheme 1. Corey-Fuchs reaction to access 1-ethynyl-4-methoxy benzene

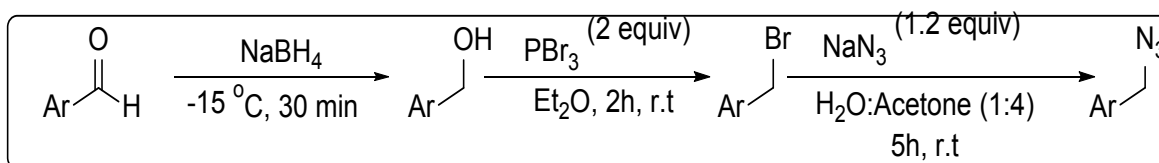
Alternatively, Corey-Fuchs reaction was employed in the transformation of thiophene-2-carboxaldehyde to 2-ethynylthiophene. First, thiophene-2-carboxaldehyde was converted to 2-(2,2-dibromovinyl) thiophene as mentioned above. Eventually, 2-(2,2-dibromovinyl) thiophene was transformed to 2-ethynylthiophene. The product of this method demonstrated in scheme 2 down-below.



Scheme 2. Corey-Fuchs reaction to access 2-ethynylthiophene

2.3.2. Synthesis of azido methyl derivatives from aldehydes

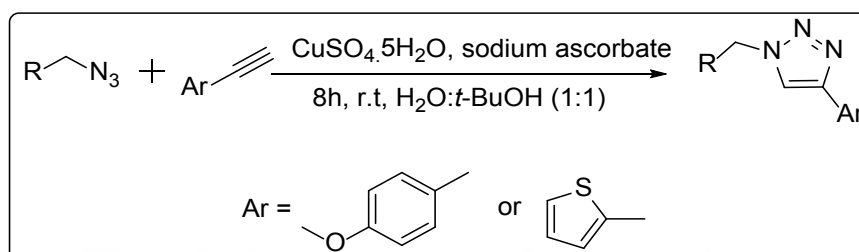
This sequence of reactions follows several transformation phases. It was initiated with aldehyde group reduction to alcohol moiety by NaBH_4 . In the next step, the alcohol group was brominated using PBr_3 in diethyl ether. Finally, bromide group was transformed into corresponding azides via NaN_3 in a mixed medium of water and acetone. The product of this method demonstrated in scheme 3 down-below.



Scheme 3. Aldehyde to azido methylbenzenes

2.3.3. Click reaction

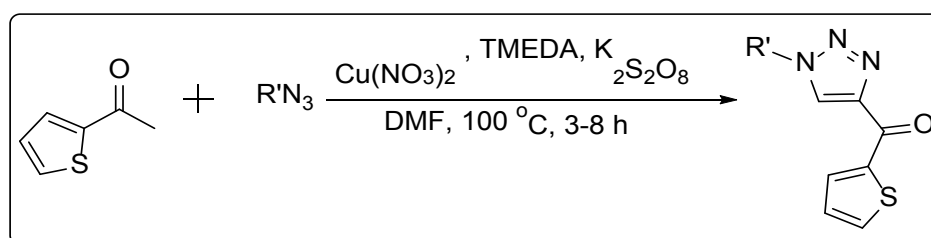
Click-reaction combines alkynes and azides. Combination process takes place at room temperature with the assistance of copper (II) sulfate and sodium ascorbate in a mixture of water and *tert*-butanol. The product of this method demonstrated in scheme 4 down-below.



Scheme 4. Click reaction

2.3.4. Three component one-pot method

4-aryl methanone substituted 1,2,3-triazole derivatives were synthesized following this method. The product formation in this reaction requires a carbon source to be added (namely, DMF). First, $\text{K}_2\text{S}_2\text{O}_8$ oxidizes methyl group of DMF moiety which activates the reaction. Then, oxidized DMF subsequently attacks ketone moiety. The reaction between the intermediate and benzyl azide gives the desired product. The product of this method demonstrated in scheme 5 down-below.



Scheme 5. Cross-Dehydrogenative coupling reaction

2.3.5. Sample preparation for biological evaluation

Enzyme inhibition was determined by quantifying the amount of uric acid produced from xanthine in the reaction mixture. Fifteen different compounds of 1,4-disubstituted 1,2,3-

triazole were used as an inhibitor for Xanthine Oxidase (XO) by observing the decrease in the uric acid formation at 294 nm. The reaction mixtures contained 0.2U XO, phosphate buffer (50mM, pH 7.4), different concentration of tested compounds and 1 mM xanthine was added to initiate the reaction, xanthine was prepared freshly. 0.2U XO was prepared with 0.2 N ammonium sulfate. The reaction mixture was incubated for 10min at 37 °C before added xanthine, and then xanthine was added to start the reaction, the activity was measured by Shimadzu UV-1601 at wavelength 294 nm. All the experiments were performed in triplicates, then the average of three reading was taken. the tested compound was dissolved in DMSO as stock, then diluted with phosphate buffer (50 mM, pH 7.4) the last concentration of DMSO in the reaction mixture was less than (0.001%), and this ratio had no effect on the enzyme activity. Allopurinol was used as a positive control. Then the IC₅₀ of XO was founded in terms to decrease in uric acid formation as compared to the formation in the absence of inhibitor.

3. EXPERIMENTAL

3.1. General procedure for alkyne synthesis

Alkyne synthesis takes two consecutive steps to give the desired product. First di-brominated of aldehyde group. Next di-brominated group gets reduced to afford target alkynes.

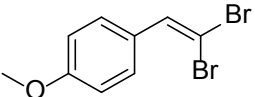
3.1.1. 2,2-Dibromovinyl synthesis

To prepare the 2,2-dibromovinyl product, tetra bromomethane (CBr_4) and triphenyl phosphine (PPh_3) was dissolved in dry dichloromethane and stirred for 30 min at 0 °C under argon atmosphere. In the next step, starting material (namely, para-methoxy benzaldehyde, and thiophene carbaldehyde) was added to the mixture. The crude stirred for an additional 1 or 2 h. Product formation confirmed by TLC checked. Finally, the reaction was quenched with ice, the organic layer was extracted with DCM, dried over (Na_2SO_4), filtered, and the solvent evaporated. Purification was done using column chromatography on silica gel by eluting it with (EtOAc/Hex 1:10 eq.),

Synthesis of 1-(2,2-dibromovinyl)-4-methoxybenzene (compound a)

Compound **a** was synthesized following the procedure described in 3.1.1. by dissolving CBr_4 (7.71 g, 29 mmol; 2 eq.) and PPh_3 (4.9 g, 14.7 mmol; 4 eq.) in dry DCM (11 mL), and para-methoxy benzaldehyde (1 g, 7.3 mmol; 1 eq.) added to the mixture. After the completion of the reaction, mixture was extracted with 60 mL of DCM.

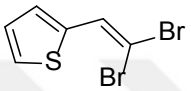
Table 3.1. Physical data of 1-(2,2-dibromovinyl)-4-methoxybenzene

Compound a	Melting point(°C)	Yield(%)
	Liquid	72

Synthesis of 2-(2,2-dibromovinyl) thiophene (compound b)

Compound **b** was synthesized following the procedure described in 3.1.1. compound **b** preparation required CBr_4 (3.7 g, 11.1 mmol; 1.25 eq.) and PPh_3 (5.9 g, 22.3 mmol; 2.5 eq.) to be dissolved in dry DCM (13 mL) and thiophene carbaldehyde (1 g, 9 mmol; 1 eq.). The mixture stirred for 2 h after addition. The crude was purified by column chromatography.

Table 3.2. Physical data of 2-(2,2-dibromovinyl) thiophene

Compound b	Melting point(°C)	Yield(%)
	Liquid	88

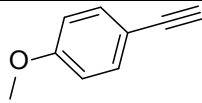
3.1.2. Alkyne synthesis

The titled compounds **c** and **d**, as seen below, prepared by dissolving dibromo vinyl in dry THF and *n*-BuLi (1.6 M solution in pentane) was added to the mixture. The mixture then was stirred for 1,5 h at -78 °C. Then, the mixture was brought to room temperature and stirred additional 1 h. the reaction was quenched with ammonium chloride (NH_4Cl), extracted with EtOAc, the organic layer was dried over Na_2SO_4 , filtered, and then the solvent was evaporated. The residue was purified by column chromatographed on SiO_2 (EtOAc/Hex; 1:4) to yield the target compound.

Synthesis of 1-ethynyl-4-methoxybenzene (compound c)

Compound **c** was synthesized following the procedure described in 3.2.1. compound **c** preparation required 1-(2,2-dibromovinyl)-4-methoxybenzene (1.54 g, 5.3 mmol; 1 eq.) to be dissolved in dry THF (13 mL) and *n*-BuLi (7.4 mmol, 5 mL; 1.4 eq.) was added to the mixture. The mixture was extracted using EtOAc (50 mL).

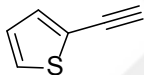
Table 3.3. Physical data of 1-ethynyl-4-methoxybenzene

Compound c	Melting point(°C)	Yield(%)
	Liquid	97

Synthesis of 2-ethynylthiophene (compound d)

2-Ethynyl thiophene was synthesized using corresponding dibromo compound (2.1 g, 7.8 mol; 1 eq.) and *n*-BuLi (15.7 mol, 9.8 mL; 2 eq.) in dry THF (28 mL) at -78 °C. This mixture was stirred for 2 h. Then, the mixture was extracted with DCM (2 x 80 mL).

Table 3.4. Physical data of 2-ethynyl thiophene

Compound d	Melting point(°C)	Yield(%)
	Liquid	75

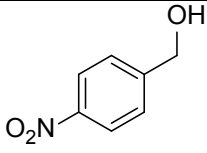
3.2. General procedure for the synthesis of azido methyl derivatives

The synthesis of azido methyl derivatives takes three steps to obtain desired products - the first step is the reduction of the aldehyde group to corresponding alcohol. Next, the alcohol group gets brominated and then it was converted into azido moiety.

3.2.1. Synthesis of (4-nitrophenyl) methanol (compound e)

First, para-nitro-substituted benzaldehyde (0.2 g, 1.3 mmol; 1 eq.) was added into a round bottom flask; filled with methanol (20 mL) and the content stirred at room temperature. Then, NaBH₄ (0.033 g, 0.87 mmol; 0.66 eq.) was added slowly, and the reaction mixture was stirred for 30 min. reaction was monitored using TLC. The mixture, then, was poured on crushed ice and extracted with EtOAc:H₂O (4:1 eq.). The separated organic layer dried over Na₂SO₄ and the solvent was evaporated to get our product.

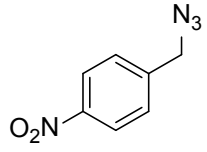
Table 3.5. Physical data of (4-nitrophenyl) methanol

Compound e	Melting point(°C)	Yield(%)
	95	70

3.2.2. Synthesis of 1-(azidomethyl)-4-nitrobenzene (compound f)

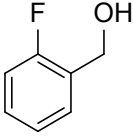
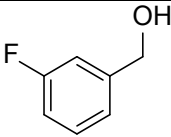
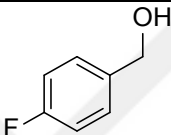
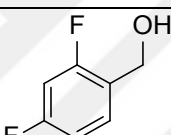
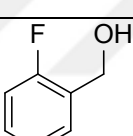
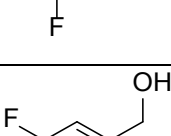
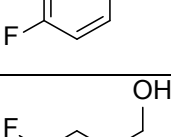
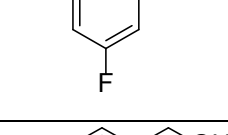
(4-nitrophenyl) methanol (0.14 g, 0.92 mmol; 1 eq.) was dissolved in diethyl ether (5 mL), and (2 eq.) of PBr_3 (0.5 g, 1.8 mmol) was added into this mixture dropwise. After confirming reaction completion using TLC, the content was poured into water and was extracted with diethyl ether (3 x 20 mL). Finally, the separated organic layer was dried over Na_2SO_4 and the excess organic solvent was evaporated to be used in the next step without further purification. 1-(bromomethyl)-4-nitrobenzene (1 eq.) was dissolved in H_2O :Acetone (5 mL; 1:4) and NaN_3 (0.076 g, 1.2 mmol; 1.5 eq.) was added to this mixture. After stirring the content for 5 h at room temperature, the mixture was diluted with water then was extracted with diethyl ether (3 x 20 mL). All the organic layers get combined and dried over Na_2SO_4 . The excess organic solvent was removed on evaporation, and the final product purified using flash chromatography eluting with DCM.

Table 3.6. Physical data of 1-(azidomethyl)-4-nitrobenzene

Compound f	Melting point(°C)	Yield(%)
	Liquid	71

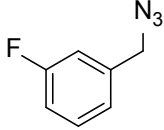
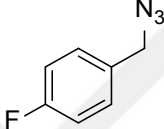
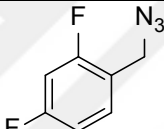
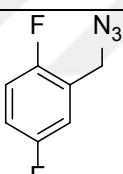
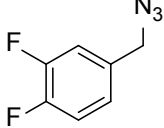
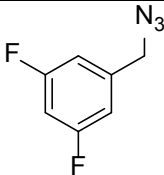
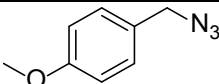
3.2.3. Synthesis alcohols (compound g - n)

Table 3.7. Physical data for compounds g – n

Compound name	formula	Melting point(°C)	Yield(%)
(2-fluorophenyl) methanol (g)		Liquid	98
(3-fluorophenyl) methanol (h)		Liquid	85
(4-fluorophenyl) methanol (i)		Liquid	77
(2,4- Difluorophenyl) methanol (j)		Liquid	76
(2,5- Difluorophenyl) methanol (k)		Liquid	97
(3,4- Difluorophenyl) methanol (l)		Liquid	99
(3,5- Difluorophenyl) methanol (m)		Liquid	84
(4-Methoxyphenyl) methanol (n)		Liquid	90

3.2.4. Synthesis of azidomethyl derivatives (compound o - v)

Table 3.8. Physical data for compounds o – v

Compound name	Formula	Melting point(°C)	Yield(%)
1-(Azidomethyl)-2-fluorobenzene (o)		Liquid	39
1-(Azidomethyl)-3-fluorobenzene (p)		Liquid	59
1-(Azidomethyl)-4-fluorobenzene (q)		Liquid	63
1-(Azidomethyl)-2,4-difluorobenzene (q)		Liquid	76
2-(Azidomethyl)-1,4-difluorobenzene (s)		Liquid	98
4-(Azidomethyl)-1,2-difluorobenzene (t)		Liquid	82
1-(Azidomethyl)-3,5-difluorobenzene (u)		Liquid	97
1-(Azidomethyl)-4-methoxybenzene (v)		Liquid	88

3.3. Click reaction procedure for triazole synthesis

Target compounds (21-27 and 28-31), as seen below, were prepared by dissolving 1-ethynyl-4-methoxybenzene or 2-ethynylthiophene (1 eq.) in the mixed solvent of tert-butanol and

water (6 mL; 1:1) with various substituted azides (1 eq.). Copper sulfate pentahydrate ($\text{CuSO}_4 \cdot 5\text{H}_2\text{O}$) (0.35 eq.) were catalyst mixed with sodium ascorbate (0.35 eq.) were then added to the reaction medium. The reaction mixture was stirred roughly for 8 h at room temperature. The reaction was monitored by TLC. The reaction mixture was poured into brine, was extracted with DCM (50 mL) and dried over Na_2SO_4 . The organic phase was evaporated by vacuum and the crude mixture was purified using column chromatography on silica gel (DCM/*n*-hexane) gave target products.

3.3.1. Synthesis of 1-(2-fluorobenzyl)-4-(4-methoxyphenyl)-1*H*-1,2,3-triazole (21)

Compound 21 (0.07 g) was obtained using 1-ethynyl-4-methoxybenzene (compound c) (0.1 g, 0.8 mol), and 2-fluorobenzyl azide (compound o) (0.114 g, 0.75 mol), $\text{CuSO}_4 \cdot 5\text{H}_2\text{O}$ (0.066 g, 0.27 mol), and sodium ascorbate (0.052 g, 0.27 mol).

Table 3.9. Physical data of 1-(2-fluorobenzyl)-4-(4-methoxyphenyl)-1*H*-1,2,3-triazole

Compound 21	Melting point(°C)	Yield(%)
	132	33

3.3.2. Synthesis of 1-(3-fluorobenzyl)-4-(4-methoxyphenyl)-1*H*-1,2,3-triazole (22)

Compound 22 (0.1 g) was obtained using 1-ethynyl-4-methoxybenzene (compound c) (0.15 g, 0.11 mol), and 3-fluorobenzyl azide (compound p) (0.172 g, 0.11 mol), $\text{CuSO}_4 \cdot 5\text{H}_2\text{O}$ (0.1 g, 0.4 mol), and sodium ascorbate (0.08 g, 0.4 mol).

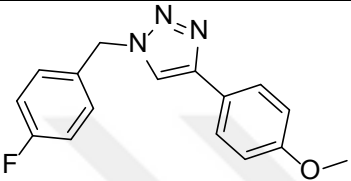
Table 3.10. Physical data of 1-(3-fluorobenzyl)-4-(4-methoxyphenyl)-1*H*-1,2,3-triazole

Compound 22	Melting point(°C)	Yield(%)
	145	31

3.3.3. Synthesis of 1-(4-fluorobenzyl)-4-(4-methoxyphenyl)-1*H*-1,2,3-triazole (23)

Compound 23 (0.3 g) was obtained using 1-ethynyl-4-methoxybenzene (compound c) (0.15 g, 0.11 mol), and 4-fluorobenzyl azide (compound q) (0.172 g, 0.113 mol), CuSO₄·5H₂O (0.1 g, 0.4 mol), and sodium ascorbate (0.08 g, 0.4 mol).

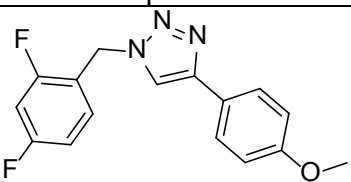
Table 3.11. Physical data of 1-(4-fluorobenzyl)-4-(4-methoxyphenyl)-1*H*-1,2,3-triazole

Compound 23	Melting point(°C)	Yield(%)
	157	93

3.3.4. Synthesis of 1-(2,4-difluorobenzyl)-4-(4-methoxyphenyl)-1*H*-1,2,3-triazole (24)

Compound 24 (0.058 g) was obtained using 1-ethynyl-4-methoxybenzene (compound c) (0.055 g, 0.041 mol), and 2,4-difluorobenzyl azide (compound r) (0.07 g, 0.041 mol), CuSO₄·5H₂O (0.036 g, 0.014 mol), and sodium ascorbate (0.029 g, 0.014 mol).

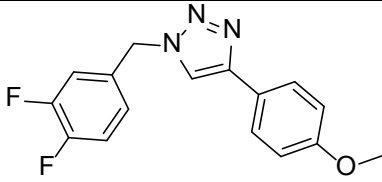
Table 3.12. Physical data of 1-(2,4-difluorobenzyl)-4-(4-methoxyphenyl)-1*H*-1,2,3-triazole

Compound 24	Melting point(°C)	Yield(%)
	150	46

3.3.5. Synthesis of 1-(3,4-difluorobenzyl)-4-(4-methoxyphenyl)-1*H*-1,2,3-triazole (25)

Compound 25 (0.13 g) was obtained using 1-ethynyl-4-methoxybenzene (compound c) (0.16 g, 0.12 mol), and 3,4-difluorobenzyl azide (compound s) (0.2 g, 0.12 mol), CuSO₄·5H₂O (0.1 g, 0.04 mol), and sodium ascorbate (0.08 g, 0.04 mol).

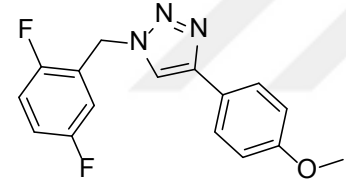
Table 3.13. Physical data of 1-(3,4-difluorobenzyl)-4-(4-methoxyphenyl)-1*H*-1,2,3-triazole

Compound 25	Melting point(°C)	Yield(%)
	160	37

3.3.6. Synthesis of 1-(2,5-difluorobenzyl)-4-(4-methoxyphenyl)-1*H*-1,2,3-triazole (26)

Compound 26 (0.16 g) was obtained using 1-ethynyl-4-methoxybenzene (compound c) (0.16 g, 0.12 mol), and 2,5-difluorobenzyl azide (compound t) (0.2 g, 0.12 mol), CuSO₄·5H₂O (0.1 g, 0.04 mol), and sodium ascorbate (0.08 g, 0.04 mol).

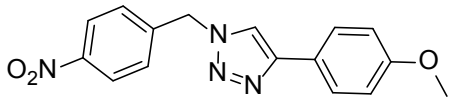
Table 3.14. Physical data of 1-(2,5-difluorobenzyl)-4-(4-methoxyphenyl)-1*H*-1,2,3-triazole

Compound 26	Melting point(°C)	Yield(%)
	90	45

3.3.7. Synthesis of 1-(4-methoxyphenyl)-4-(4-nitrobenzyl)-1*H*-1,2,3-triazole (27)

Compound 27 (0.116 g) was obtained using 1-ethynyl-4-methoxybenzene (compound c) (0.174 g, 0.13 mol), and 1-(azidomethyl)-4-nitrobenzene (compound f) (0.235 g, 0.13 mol), CuSO₄·5H₂O (0.11 g, 0.04 mol), and sodium ascorbate (0.09 g, 0.04 mol).

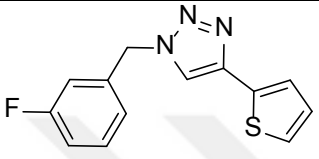
Table 3.15. Physical data of 1-(4-methoxyphenyl)-4-(4-nitrobenzyl)-1*H*-1,2,3-triazole

Compound 27	Melting point(°C)	Yield(%)
	140	28

3.3.8. Synthesis of 1-(3-fluorobenzyl)-4-(thiophen-2-yl)-1*H*-1,2,3-triazole (28)

Compound 28 (0.05 g) was obtained using 2-ethynyl thiophene (compound d) (0.143 g, 0.13 mol), and 3-fluorobenzyl azide (compound p) (0.2 g, 0.13 mol), CuSO₄·5H₂O (0.115 g, 0.04 mol), and sodium ascorbate (0.091 g, 0.04 mol).

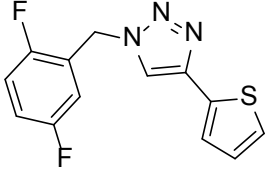
Table 3.16. Physical data of 1-(3-fluorobenzyl)-4-(thiophen-2-yl)-1*H*-1,2,3-triazole

Compound 28	Melting point(°C)	Yield(%)
	97-100	16

3.3.9. Synthesis of 1-(2,5-difluorobenzyl)-4-(thiophen-2-yl)-1*H*-1,2,3-triazole (29)

Compound 29 (0.3 g) was obtained using 2-ethynyl thiophene (compound d) (0.128 g, 0.12 mol), and 2,5-difluorobenzyl azide (compound r) (0.2 g, 0.12 mol), CuSO₄·5H₂O (0.1 g, 0.04 mol), and sodium ascorbate (0.08 g, 0.04 mol).

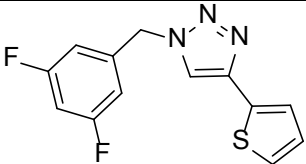
Table 3.17. Physical data of 1-(2,5-difluorobenzyl)-4-(thiophen-2-yl)-1*H*-1,2,3-triazole

Compound 29	Melting point(°C)	Yield(%)
	87	92

3.3.10. Synthesis of 1-(3,5-difluorobenzyl)-4-(thiophen-2-yl)-1*H*-1,2,3-triazole (30)

Compound 30 (0.23 g) was obtained using 2-ethynyl thiophene (compound d) (0.13 g, 0.12 mol), and 3,5-difluorobenzyl azide (compound v) (0.2 g, 0.12 mol), CuSO₄·5H₂O (0.1 g, 0.04 mol), and sodium ascorbate (0.08 g, 0.04 mol).

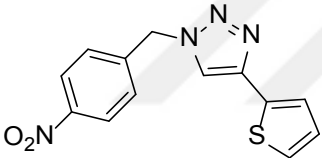
Table 3.18. Physical data of 1-(3,5-difluorobenzyl)-4-(thiophen-2-yl)-1*H*-1,2,3-triazole

Compound 30	Melting point(°C)	Yield(%)
	135-140	71

3.3.11. Synthesis of 1-(4-nitrobenzyl)-4-(thiophen-2-yl)-1*H*-1,2,3-triazole (31)

Compound 31 (0.09 g) was obtained using 1-ethynyl thiophene (compound d) (0.11 g, 0.1 mol), and 1-(azidomethyl)-4-nitrobenzene (compound u) (0.183 g, 0.1 mol), CuSO₄·5H₂O (0.09 g, 0.04 mol), and sodium ascorbate (0.07 g, 0.04 mol).

Table 3.19. Physical data of 1-(4-nitrobenzyl)-4-(thiophen-2-yl)-1*H*-1,2,3-triazole

Compound 31	Melting point(°C)	Yield(%)
	115	31

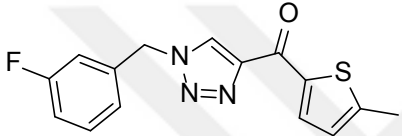
3.4. Three component one-pot procedure for triazole synthesis

To prepare target compounds (32-35) as seen below, 1-(5-methyl thiophene-2-yl)ethan-1-one or 1-(5-bromothiophene-2-yl)ethan-1-one (1 eq.) have to be dissolved in DMF and react with (1.5 eq.) of variously substituted azido methyl benzene, copper nitrate (Cu(NO₃)₂·3H₂O) (0.2 eq.), potassium persulfate (K₂S₂O₈) (3 eq.), and tetramethylethanediamine (TMEDA) (0.2 eq.). The mixture then was stirred for a week at 100 °C in an oil bath. The reaction was monitored by TLC. After completion, the substance was poured into water, extracted with DCM, then the organic layer was dried over sodium sulfate (Na₂SO₄). Finally, the product was further dried by vacuum and purified by column chromatography on silica gel (EtOAc/Hex; 10:3 eq.). Recrystallization was done with (DCM) to get the target product after two days.

3.4.1. Synthesis of (1-(3-fluorobenzyl)-1*H*-1,2,3-triazole-4-yl)(5-methylthiophen-2-yl)methanone (32)

Compound 32 (0.09 g) was obtained using 3-fluorobenzyl azide (compound o) (0.2 g, 1.3 mol), and 1-(5-methylthiophen-2-yl) ethan-1-one (0.12 g, 0.8mol), DMF (5 mL), Cu(NO₃)₂·3H₂O (0.04 g, 0.176 mol), K₂S₂O₈ (0.62 g, 2.7 mol), and TMEDA (0.024 g, 0.18 mol).

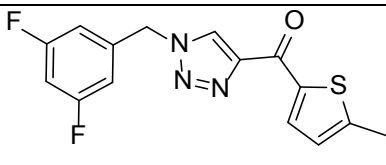
Table 3.20. Physical data of (1-(3-fluorobenzyl)-1*H*-1,2,3-triazole-4-yl)(5-methylthiophen-2-yl)methanone

Compound 32	Melting point(°C)	Yield(%)
	155	34

3.4.2. Synthesis of (1-(3,5-difluorobenzyl)-1*H*-1,2,3-triazole-4-yl)(5-methylthiophen-2-yl)methanone (33)

Compound 33 (0.167 g) was obtained using 3,5-difluorobenzyl azide (compound u) (0.19 g, 1.14 mol), and 1-(5-methylthiophen-2-yl) ethan-1-one (0.11 g, 0.76 mol), DMF (5 mL), Cu(NO₃)₂·3H₂O (0.04 g, 0.15 mol), K₂S₂O₈ (0.53 g, 2,3 mol), TMEDA (0.018 g, 0.15 mol).

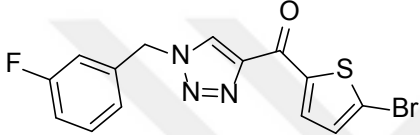
Table 3.21. Physical data of (1-(3,5-difluorobenzyl)-1*H*-1,2,3-triazole-4-yl)(5-methylthiophen-2-yl)methanone

Compound 33	Melting point(°C)	Yield(%)
	168-171	69

3.4.3. Synthesis of (5-bromothiophen-2-yl)(1-(3-fluorobenzyl)-1*H*-1,2,3-triazole-4-yl) methanone (34)

Compound 34 (0.167 g) was obtained using 3-fluorobenzyl azide (compound o) (0.2 g, 2 mol), and 1-(5-bromothiophen-2-yl) ethan-1-one (0.266 g, 1.3 mol), DMF (6.6 mL), Cu(NO₃)₂·3H₂O (0.064 g, 0.26 mol), K₂S₂O₈ (0.922 g, 4 mol), TMEDA (0.031 g, 0.26 mol).

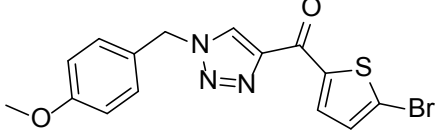
Table 3.22. Physical data of (5-bromothiophen-2-yl)(1-(3-fluorobenzyl)-1*H*-1,2,3-triazole-4-yl) methanone

Compound 34	Melting point(°C)	Yield(%)
	150	31

3.4.4. Synthesis of (5-bromothiophen-2-yl)(1-(4-methoxybenzyl)-1*H*-1,2,3-triazole-4-yl) methanone (35)

Compound 35 (0.167 g) was obtained using 4-methoxybenzyl azide (compound v) (0.27 g, 1.7 mol), and 1-(5-bromothiophen-2-yl) ethan-1-one (0.23 g, 1.1 mol), DMF (5.5 mL), Cu(NO₃)₂·3H₂O (0.08 g, 0.33 mol), K₂S₂O₈ (0.77 g, 3.3 mol), TMEDA (0.077 g, 0.33 mol).

Table 3.23. Physical data of (5-bromothiophen-2-yl)(1-(4-methoxybenzyl)-1*H*-1,2,3-triazole-4-yl) methanone

Compound 35	Melting point(°C)	Yield(%)
	168	82



4. CONCLUSION

4.1. Spectroscopic analysis of triazole compounds

4.1.1. FT-IR, $^1\text{H-NMR}$, $^{13}\text{C-APT-NMR}$ spectroscopy analysis results of 1-(2-fluorobenzyl)-4-(4-methoxyphenyl)-1*H*-1,2,3-triazole (21)

FT-IR spectrum data of compound 21

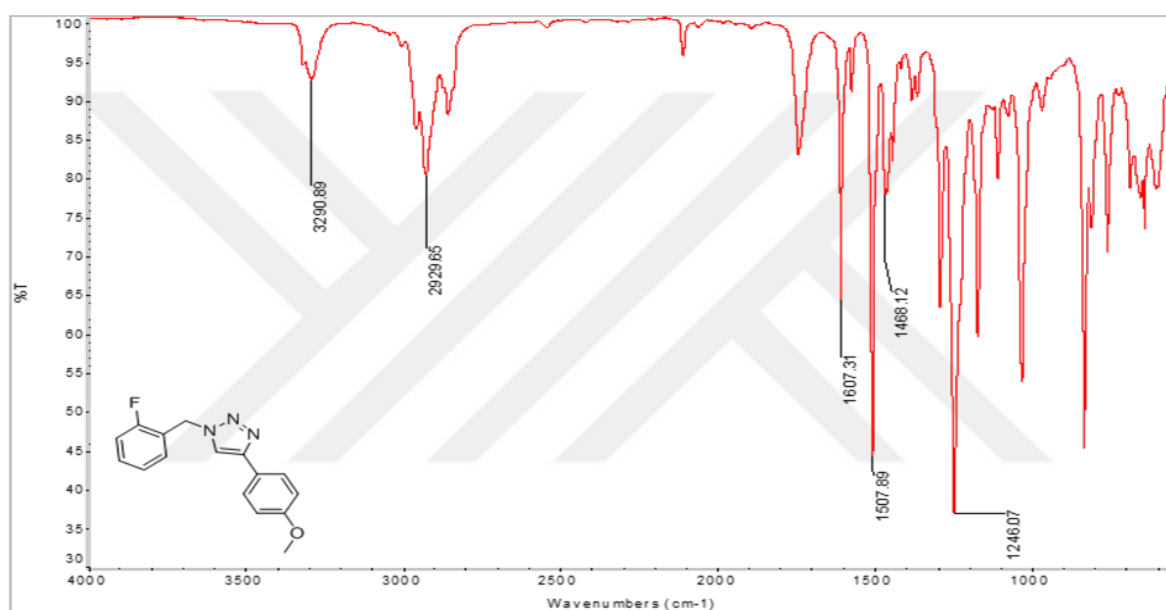


Figure 4.1. FT-IR spectrum of compound 21

Table 4.1. Selected FT-IR spectrum data of compound 21

$\bar{\nu}$ (cm^{-1})	Bonds
3291	Aromatic C-H bond's band
2930	Methyl C-H bond's band
1607-1507-1468	Aromatic C=C, N=N, C=N bond's band
1246	C-O-C bond's band

$^1\text{H-NMR}$ spectrum of compound 21

The target compound 21 was dissolved in deuteriochloroform (CDCl_3). From $^1\text{H-NMR}$ of an analyzed compound, as seen in figure 4.2, one can see the following δ of 3.83 ppm (s, 3H) belongs to $-\text{OCH}_3$ and of 5.62 ppm (s, 2H) belongs to $-\text{CH}_2$. The AA'XX' system of para-methoxybenzene ring can be seen at δ of 6.93 ppm (quasi d, $J = 8.8$ Hz, 2H) for hydrogen atoms next to the methoxy group (AA' part), while the XX' part appear at δ of 7.73 ppm (quasi d, $J = 8.8$ Hz, 2H). Hydrogen atoms of fluorine-substituted phenyl ring resonate at 7.33-7.11 ppm as following hydrogen atom at 5-position appears at δ of 7.11 (m, 1H), while hydrogen atom at 6-position appears at δ of 7.15 ppm (m, 1H), while hydrogen atoms at 3- and 4-positions appear at δ 7.33 ppm (m, 2H). Lastly, the hydrogen atom of triazole ring appears at δ of 7.67 ppm (s, 1H).

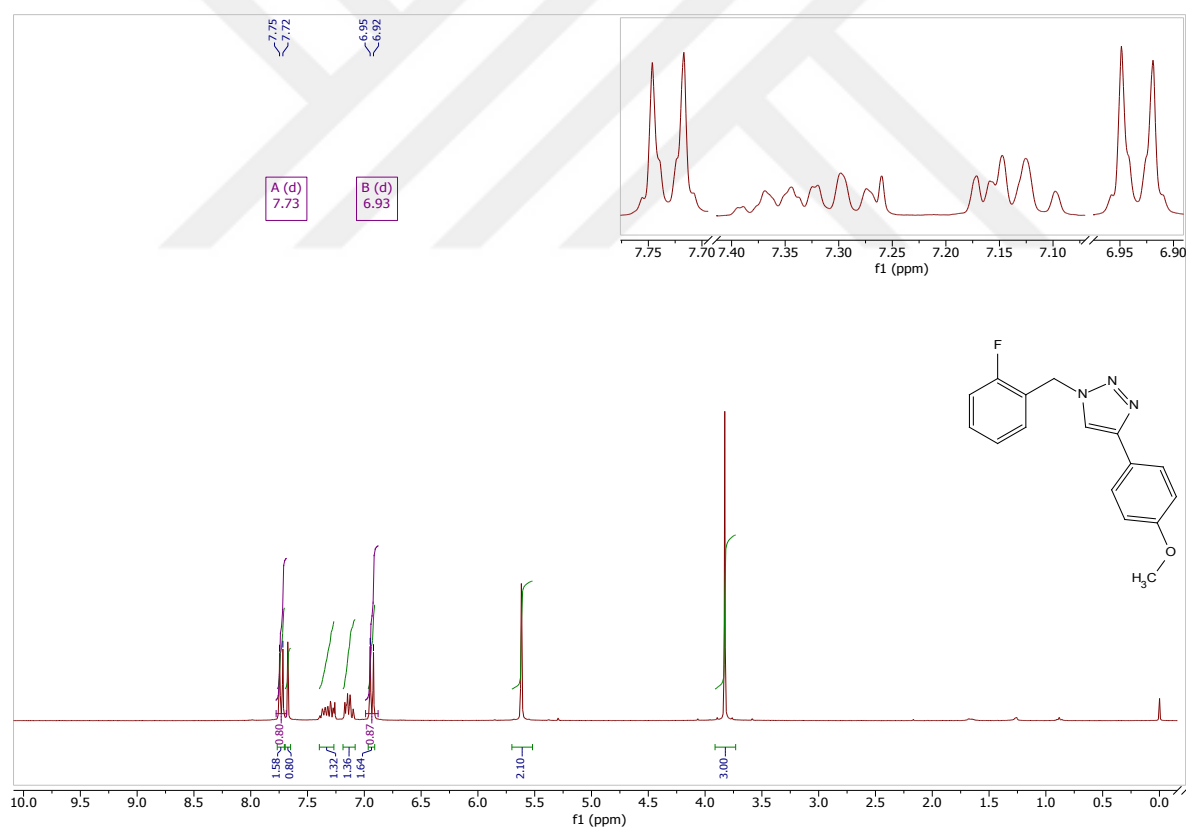


Figure 4.2. $^1\text{H-NMR}$ spectrum of compound 21

^{13}C -NMR spectrum of compound 21

The target compound 21 was dissolved in CDCl_3 . From APT-NMR of the analyzed compound, as seen in figure 4.3, one can see the following δ of 47.7 ppm belongs to methylene linker and of 55.4 ppm belongs to $-\text{OCH}_3$. The C-H carbon atoms near para-methoxy group can be seen at δ of 114.3 ppm, while the furthest two C-H atoms can be seen at δ of 127.1 ppm. Quaternary carbon atoms of para-methoxy benzene at 1-position appears at δ of 122.2 ppm while carbon at 4-position appears at 159.7 ppm. Carbon atoms of fluorine phenyl ring resonate at δ of 160.6-115.9 ppm as following: quaternary carbon atoms at 1- and 2-positions appear at δ 123.3 ppm and 160.6 ppm (d, $J = 247.2$ Hz), respectively. Carbon atom at 3-position appears at δ of 115.9 ppm (d, $J = 21.2$ Hz), carbon atom at 4-position appears at δ of 124.9 ppm (d, $J = 3.6$ Hz). Carbon atom at 5-position appears at δ of 119 ppm, carbon atom at 6-position, on the other hand, appears at δ of 130.6 ppm (d, $J = 3.2$ Hz). Lastly, carbon atom at 5-position of triazole ring appears at δ of 131 (d, $J = 8.0$ Hz) ppm, while the quaternary carbon atom at 4-position of triazole ring appears at δ of 148.2 ppm.

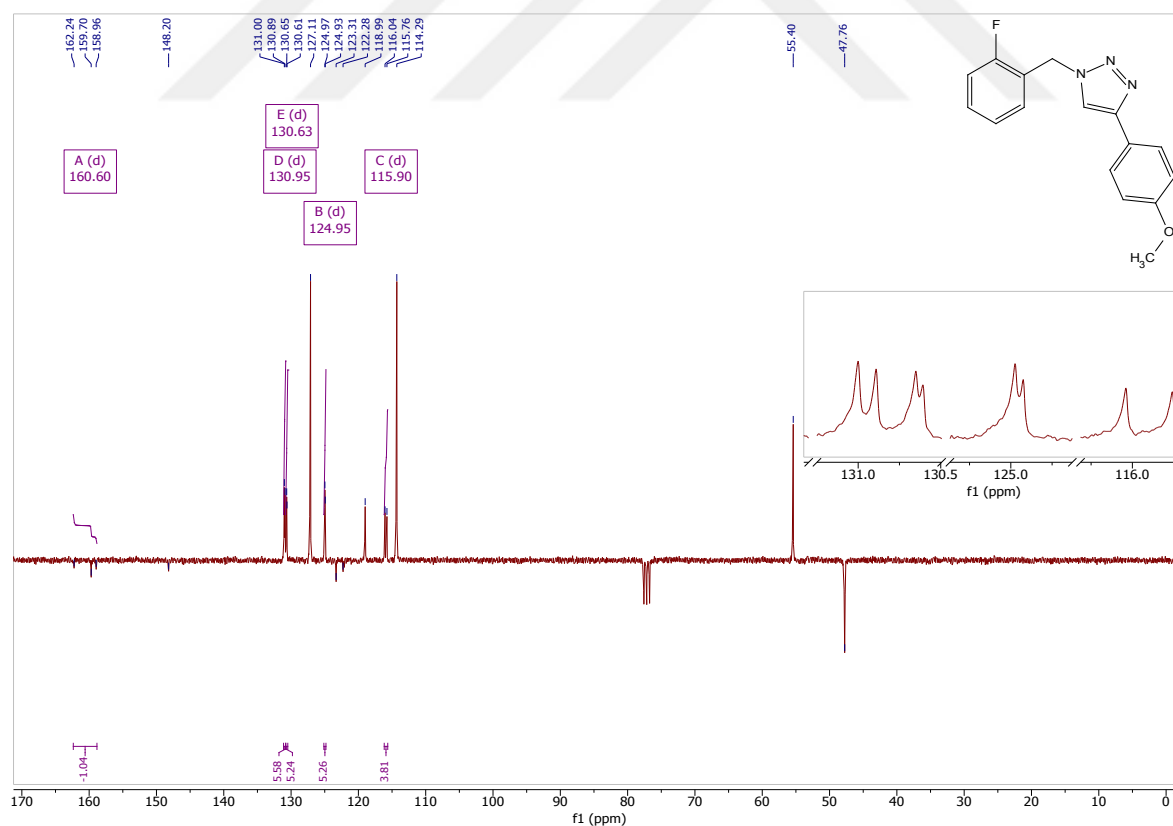


Figure 4.3. APT-NMR spectrum of compound 21

4.1.2. FT-IR, $^1\text{H-NMR}$, $^{13}\text{C-APT-NMR}$ spectroscopy analysis results of 1-(3-fluorobenzyl)-4-(4-methoxyphenyl)-1*H*-1,2,3-triazole (22)

FT-IR spectrum data of compound 22

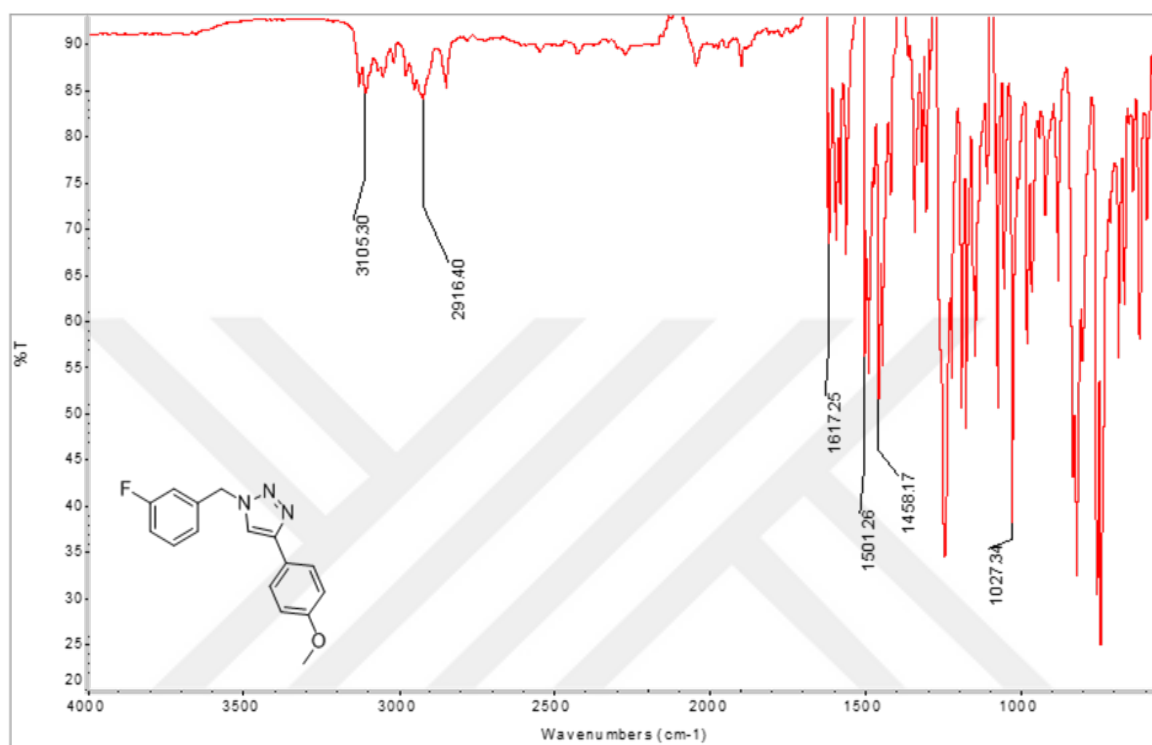


Figure 4.4. FT-IR spectrum of compound 22

Table 4.2. Selected FT-IR spectrum data of compound 22

$\bar{\nu}$ (cm ⁻¹)	Bonds
3105	Aromatic C-H bond's band
2916	Methyl C-H bond's band
1617-1501-1458	Aromatic C=C, N=N, C=N bond's band
1027	C-O-C bond's band

$^1\text{H-NMR}$ spectrum of compound 22

The target compound 22 was dissolved in CDCl_3 . From $^1\text{H-NMR}$ of an analyzed compound, as seen in figure 4.5, one can see the following δ of 3.82 ppm (s, 3H) belongs to $-\text{OCH}_3$ and of 5.55 ppm (s, 2H) belongs to $-\text{CH}_2$ hydrogen atoms. The AA' part of AA'XX' system

hydrogen atoms next to the methoxy group appear at δ of 6.94 (quasi d, $J = 8.8$ Hz, 2H) ppm for, while the XX' part appear at δ of 7.73 (quasi d, $J = 8.8$ Hz, 2H) ppm. Hydrogen atoms of the 3-fluorinephenyl ring appear as following: hydrogen atom at 2-position appears at δ of 7.00 (m, 1 H), and hydrogen atom at 4-position appears at δ of 7.07 ppm (m, 1H). The hydrogen atoms at 5-position appears at δ 7.35 ppm (m, 1H). The hydrogen atom at 6-position appears at δ of 7.04 ppm (m, 1H). Lastly, the hydrogen atom of triazole ring appears at δ of 7.67 ppm (s, 1H).

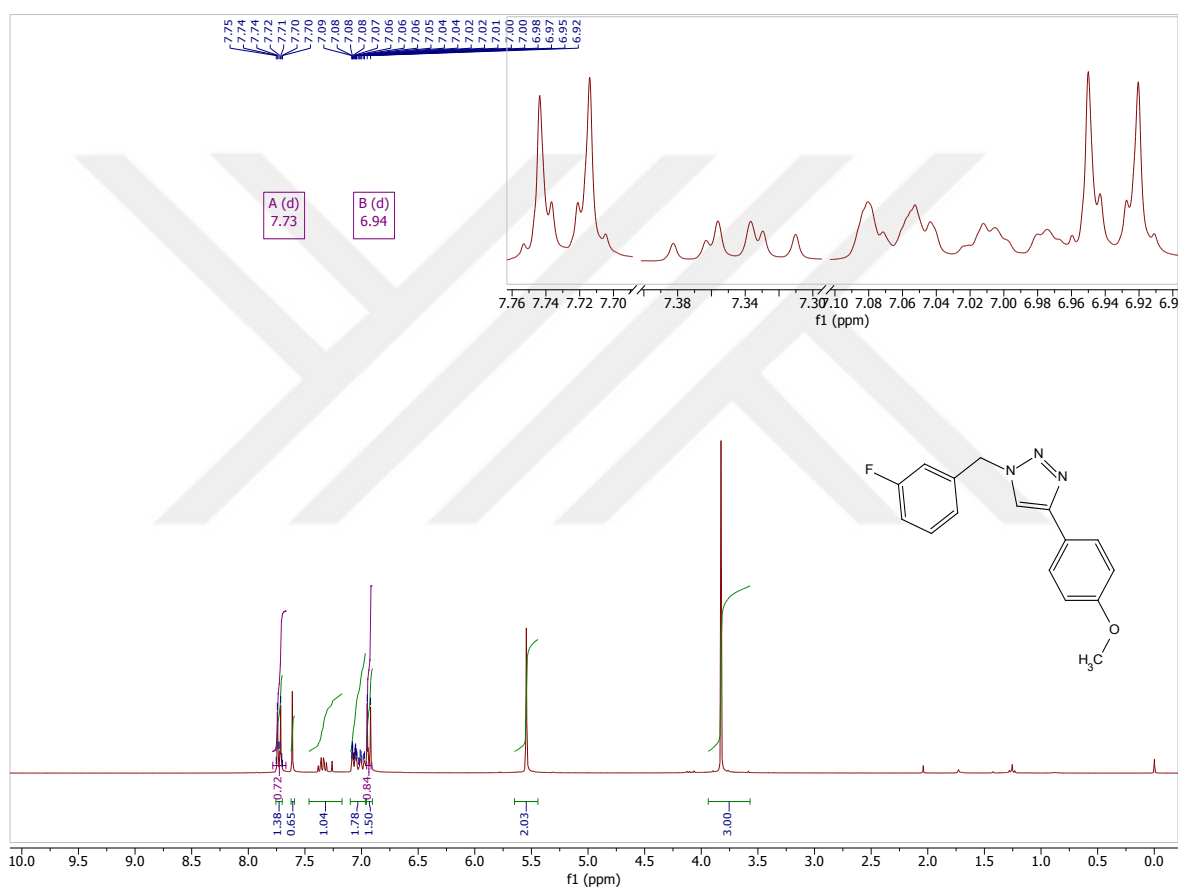


Figure 4.5. $^1\text{H-NMR}$ spectrum of compound 22

$^{13}\text{C-NMR}$ spectrum of compound 22

The target compound 22 was dissolved in CDCl_3 . From APT-NMR of the analyzed compound, as can be seen in figure 4.6, one can see the following δ of 53.5 ppm belongs to $-\text{OCH}_3$ and 55.4 ppm belongs to methylene linker. The C-H atoms near para-methoxy group can be seen at δ of 114.3 ppm, while the furthest two C-H atoms appear at δ of 127.1 ppm. Quaternary carbon atoms of para-methoxy benzene at 1-position appears at 123.0 ppm, while

carbon at 4-position appears at 159.7 ppm. Carbon atoms of fluorine phenyl ring resonate at 163.1 – 115.0 ppm as following: quaternary carbon atoms at 1- and 3-positions appear at δ of 137.3 (d, $J = 7.4$ Hz) ppm and of 163.1 (d, $J = 248$ Hz) ppm. Carbon atom at 2-position appears at δ of 115.0 (d, $J = 22.3$ Hz), carbon atoms at 4-position appears at δ of 115.8 (d, $J = 21.0$ Hz), and carbon atom at 5-position appears at δ of 123.6 (d, $J = 3.0$ Hz). Carbon atom 6-position appears at δ of 119 ppm. Lastly, carbon atom at 5-position of triazole ring appears at δ of 130.8 (d, $J = 8.3$ Hz) ppm, while the quaternary carbon atom at 4-position of triazole ring appears at δ of 148.6 ppm.

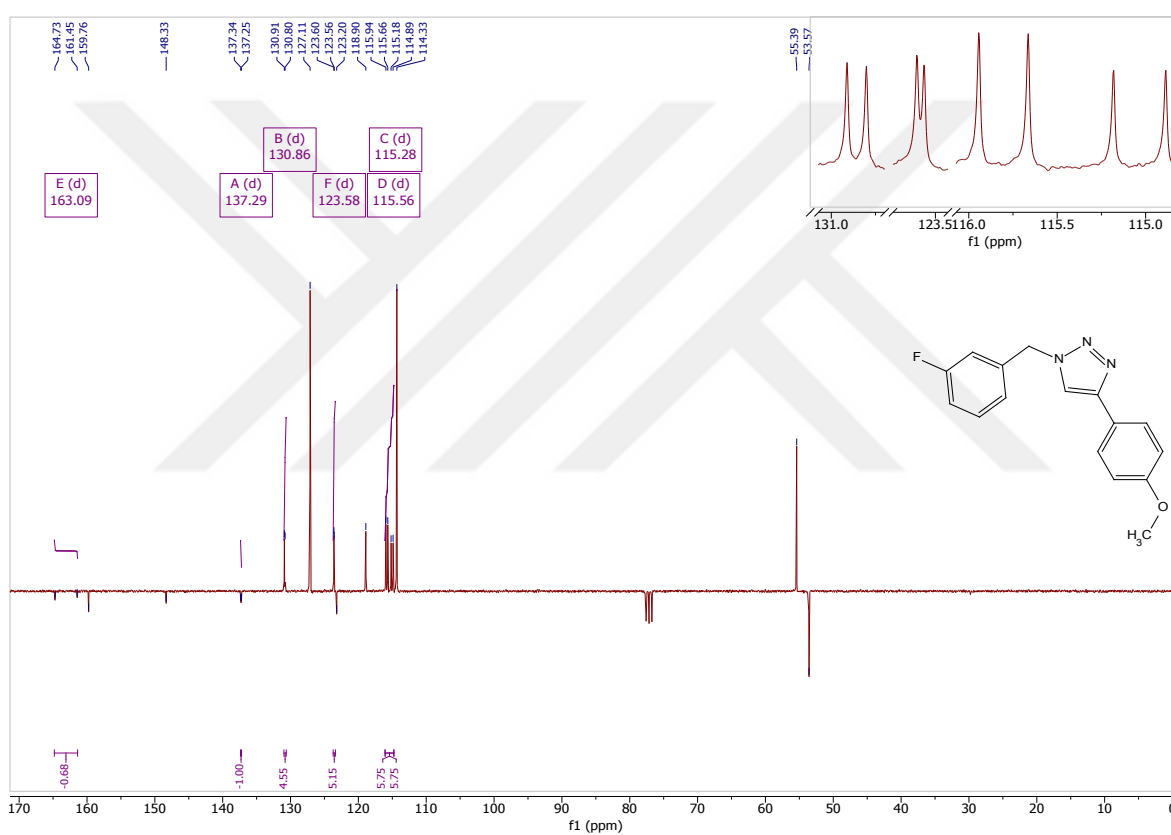


Figure 4.6. APT-NMR spectrum of compound 22

4.1.3. FT-IR, $^1\text{H-NMR}$, $^{13}\text{C-APT-NMR}$ spectroscopy analysis results of 1-(4-fluorobenzyl)-4-(4-methoxyphenyl)-1*H*-1,2,3-triazole (23)

FT-IR spectrum data of compound 23

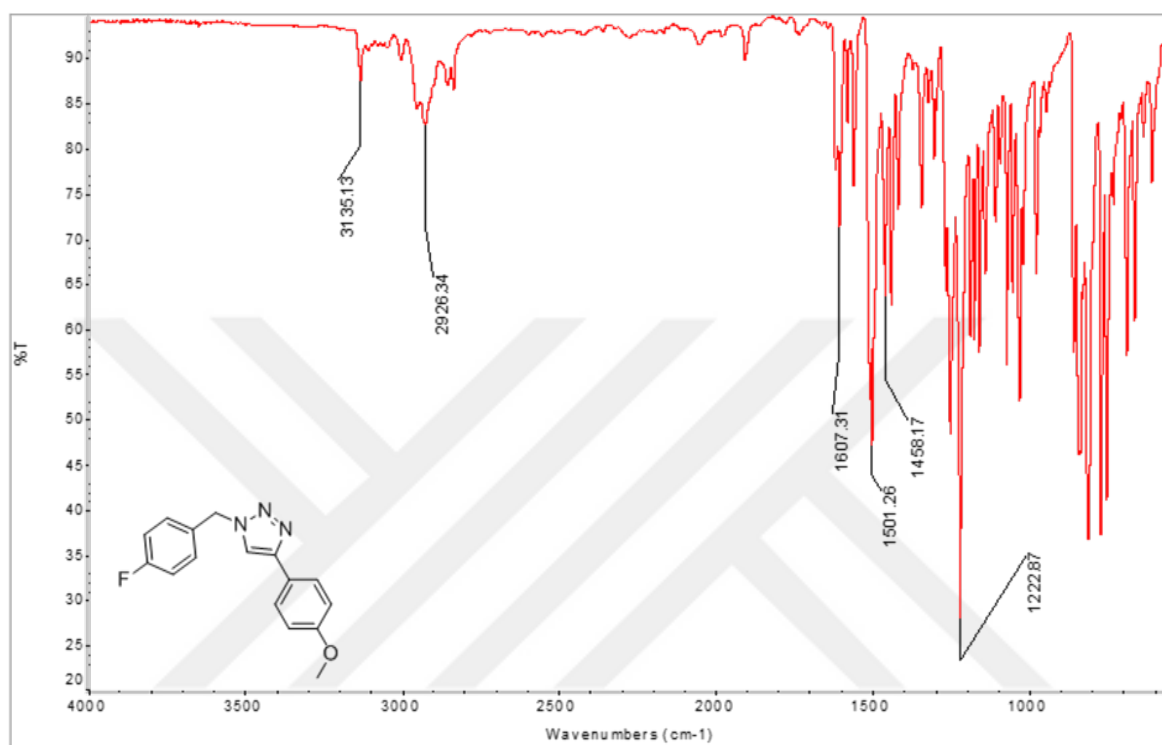


Figure 4.7. FT-IR spectrum of compound 23

Table 4.3. Selected FT-IR spectrum data of compound 23

$\bar{\nu}$ (cm $^{-1}$)	Bonds
3135	Aromatic C-H bond's band
2926	Methyl C-H bond's band
1607-1502-1458	Aromatic C=C, N=N, C=N bond's band
1222	C-O-C bond's band

$^1\text{H-NMR}$ spectrum of compound 23

The target compound 23 was dissolved in CDCl_3 . From $^1\text{H-NMR}$ of an analyzed compound, as seen in figure 4.8. One can see the following δ of 3.82 ppm (s, 3H) of $-\text{OCH}_3$ and of 5.65 ppm (s, 2H) of $-\text{CH}_2$. The AA'XX' system of hydrogen atoms of para-methoxy benzene ring

can be seen at δ of 6.94 (quasi d, $J = 8.8$ Hz, 2H) ppm for AA' part, while the XX' part appear at δ of 7.72 (quasi d, $J = 8.8$ Hz, 2H) ppm. In the middle appears the AA'XX' system of the 4-fluorophenyl ring as seen at δ of 7.08 (t, $J = 8.6$ Hz, 2H) ppm for the AA' part to methylene linker, while the XX' part appear at δ of 7.30 (dd, $J = 8.6, 5.3$ Hz, 2H) ppm. Lastly, the hydrogen atom of the triazole ring appears at δ of 7.57 (s, 1H).

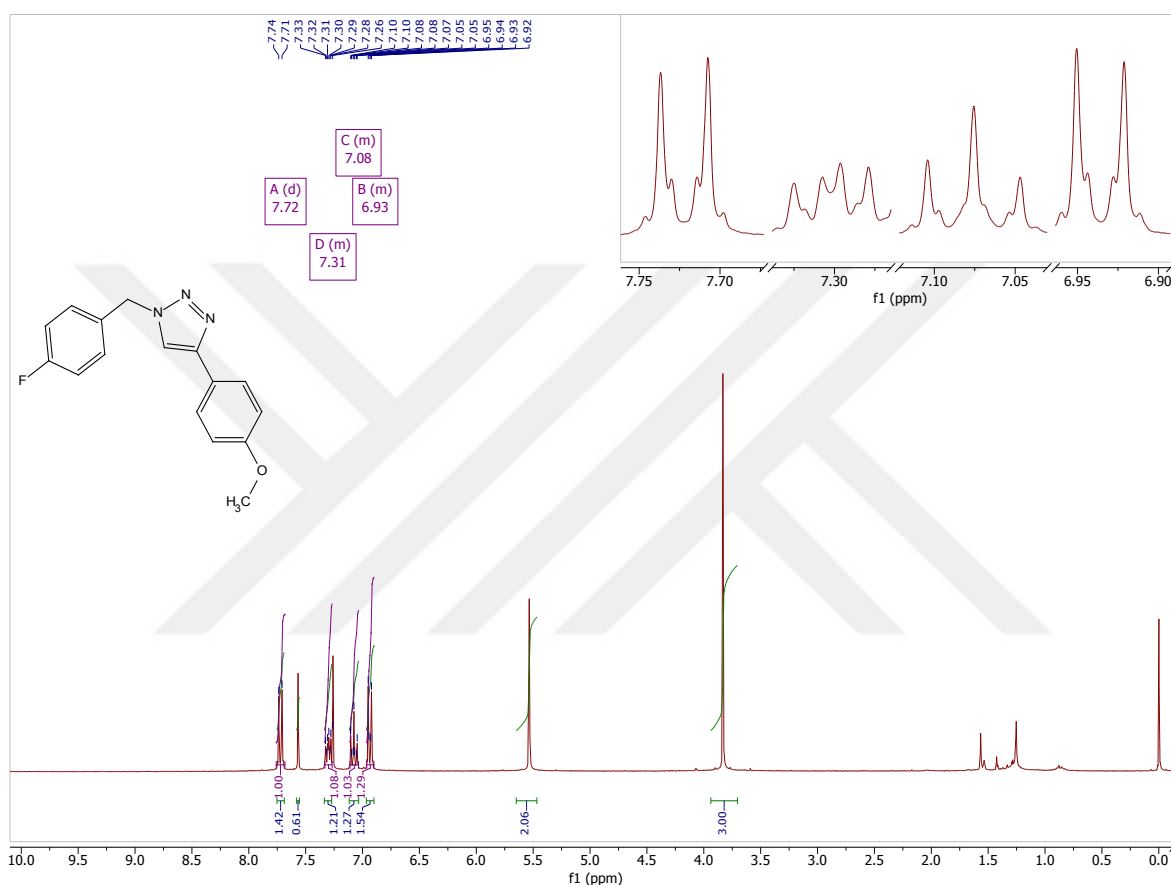


Figure 4.8. ^1H -NMR spectrum of compound 23

^{13}C -NMR spectrum of compound 23

The target compound 23 was dissolved in CDCl_3 . From APT-NMR of the analyzed compound, as seen in figure 4.9, one can see the following δ of 53.6 ppm belongs to $-\text{OCH}_3$ and of 55.5 ppm belongs to methylene linker. The C-H carbon atoms near para-methoxy group can be seen at δ of 114.0 ppm, while the furthest two C-H atoms appear at δ of 127.0 ppm. Quaternary carbon atoms of para-methoxy benzene at 1-position appears at δ of 123.3 ppm, while carbon at 4-position appears at 159.8 ppm. Carbon atoms of fluorine phenyl ring resonate at 161.5 – 116.3 ppm as following: quaternary carbon atoms at 1- and 4-positions

appear at δ of 130.8 (d, $J = 3.4$ Hz) ppm and of 163.0 (d, $J = 248$ Hz) ppm. Carbon atoms at 3- and 5-positions appear at δ of 116.3 (d, $J = 21.8$ Hz) ppm, carbon atoms at 2- and 6-positions appear at δ of 118.5 ppm. Lastly, carbon atom at 5-position of triazole ring appears at δ of 130.0 (d, $J = 8.4$ Hz) ppm, while the quaternary carbon atom at 4-position of triazole ring appears at δ of 148.2 ppm.

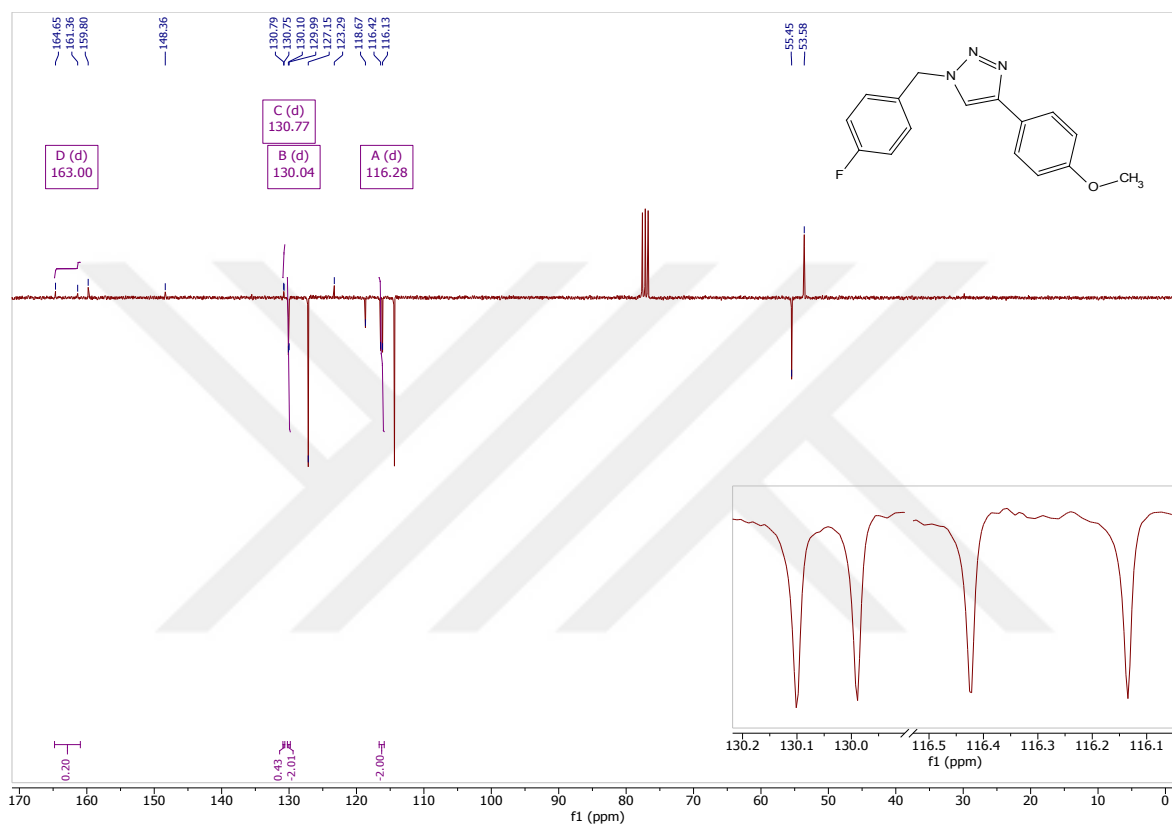


Figure 4.9. APT-NMR spectrum of compound 23

4.1.4. FT-IR, $^1\text{H-NMR}$, $^{13}\text{C-APT-NMR}$ spectroscopy analysis results of 1-(2,4-difluorobenzyl)-4-(4-methoxyphenyl)-1*H*-1,2,3-triazole (24)

FT-IR spectrum data of compound 24

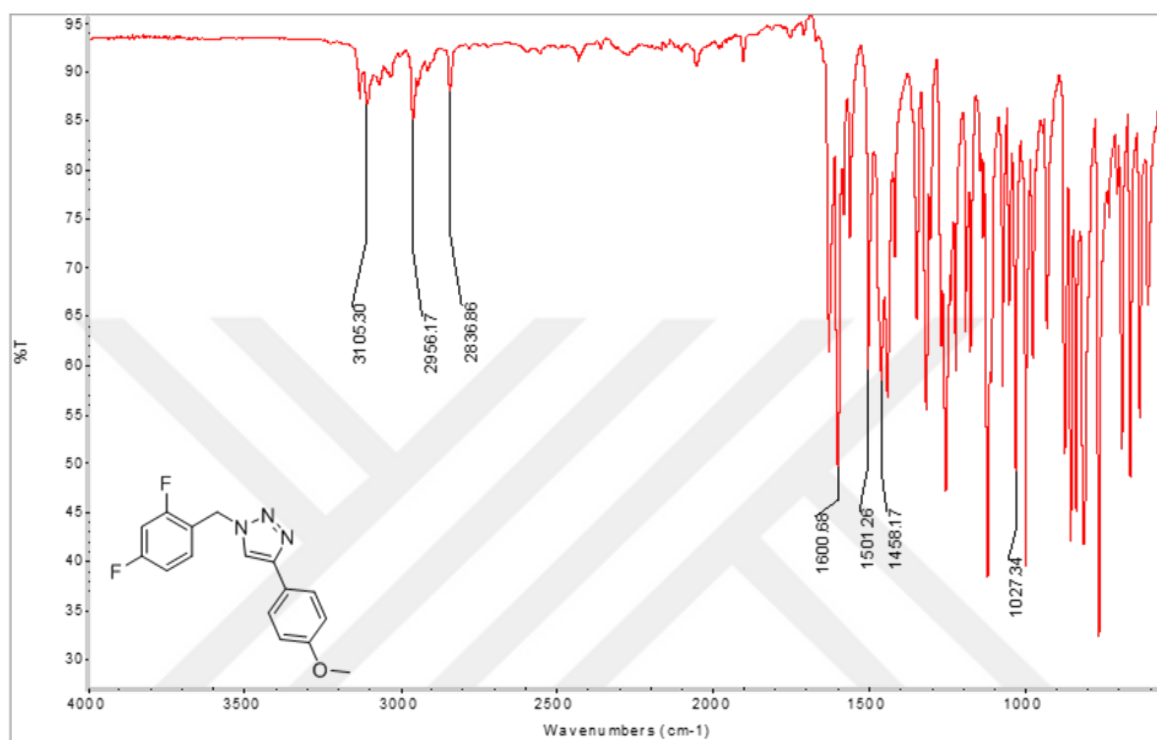


Figure 4.10. FT-IR spectrum of compound 24

Table 4.4. Selected FT-IR spectrum data of compound 24

$\bar{\nu}$ (cm^{-1})	Bonds
3105	Aromatic C-H bond's band
2956-2836	Methyl C-H bond's band
1601-1500-1458	Aromatic C=C, N=N, C=N bond's band
1027	C-O-C bond's band

$^1\text{H-NMR}$ spectrum of compound 24

The target compound 24 was dissolved in CDCl_3 . From $^1\text{H-NMR}$ of an analyzed compound, as seen in figure 4.11, one can see the following δ of 3.82 ppm (s, 3H) of OCH_3 and of 5.65 ppm (s, 2H) of CH_2 . The $\text{AA}'\text{XX}'$ system of hydrogen atoms of para-methoxy benzene ring

can be seen at δ of 6.93 (quasi d, $J = 8.8$ Hz, 2H) ppm for hydrogen atoms next to the methoxy group, while the other two appear at δ of 7.73 (quasi d, $J = 8.8$ Hz, 2H). Hydrogen atoms of 2,4-difluoro phenyl ring appear as following: the hydrogen atom which located between two fluorine atoms appear at δ of 6.87 ppm (m, 1H), hydrogen atom at 5-position appears at δ of 7.33 ppm (m, 1H), hydrogen atom at 6-position appears at δ of 7.00 ppm (m, 1H). lastly, the hydrogen atom of triazole ring appears at δ of 7.67 ppm (s, 1H).

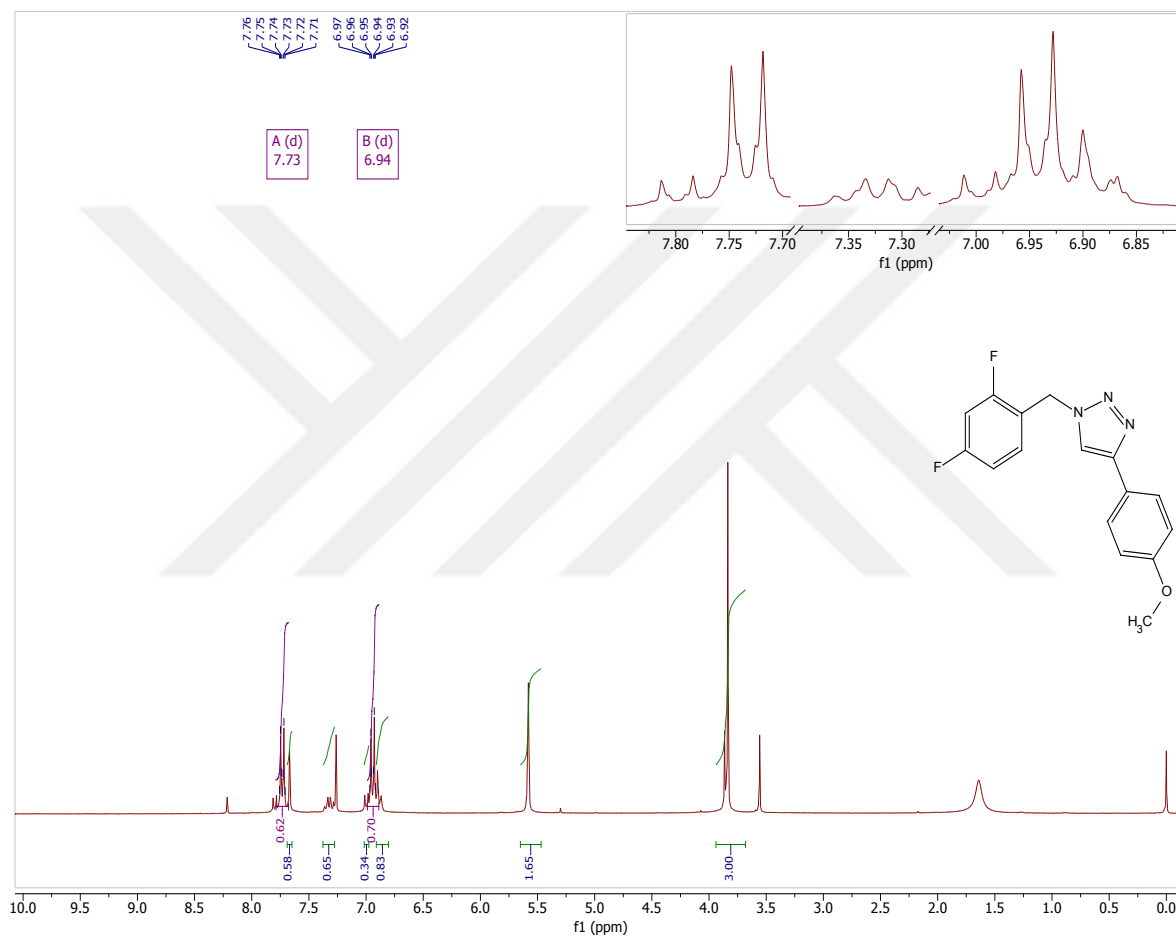


Figure 4.11. ^1H -NMR spectrum of compound 24

^{13}C -NMR spectrum of compound 24

The target compound 24 was dissolved in CDCl_3 . From APT-NMR of the analyzed compound, as seen in figure 4.12, one can see the following δ of 47.3 ppm belongs to methylene linker and of 55.5 ppm belongs to $-\text{OCH}_3$. The C-H carbon atoms near para-methoxy group can be seen at δ of 114.4 ppm, while the furthest two C-H atoms appear at δ of 127.2 ppm. Quaternary carbon atoms of para-methoxy benzene at 1-position appears at δ

of 123.1 ppm, while carbon at 4-position appears at δ of 159.9 ppm. Carbon atoms of fluorine phenyl ring resonate at δ of 161.5 – 104.5 ppm as following: quaternary carbon atoms at 1-, 2- and 4-positions appear at δ of 126.6 ppm, of 161.0 ppm, and of 163.4 ppm. Carbon atom at 3-position appears at δ of 104.5 (dd, $J = 25.1$ Hz) ppm, carbon atom at 5-position appears at δ of 131.8 (dd, $J = 9.9, 4.8$ Hz). Lastly, carbon atom at 5-position of triazole ring appears at δ of 118.9 ppm, while the quaternary carbon atom at 4-position appears at δ of 148.2 ppm.

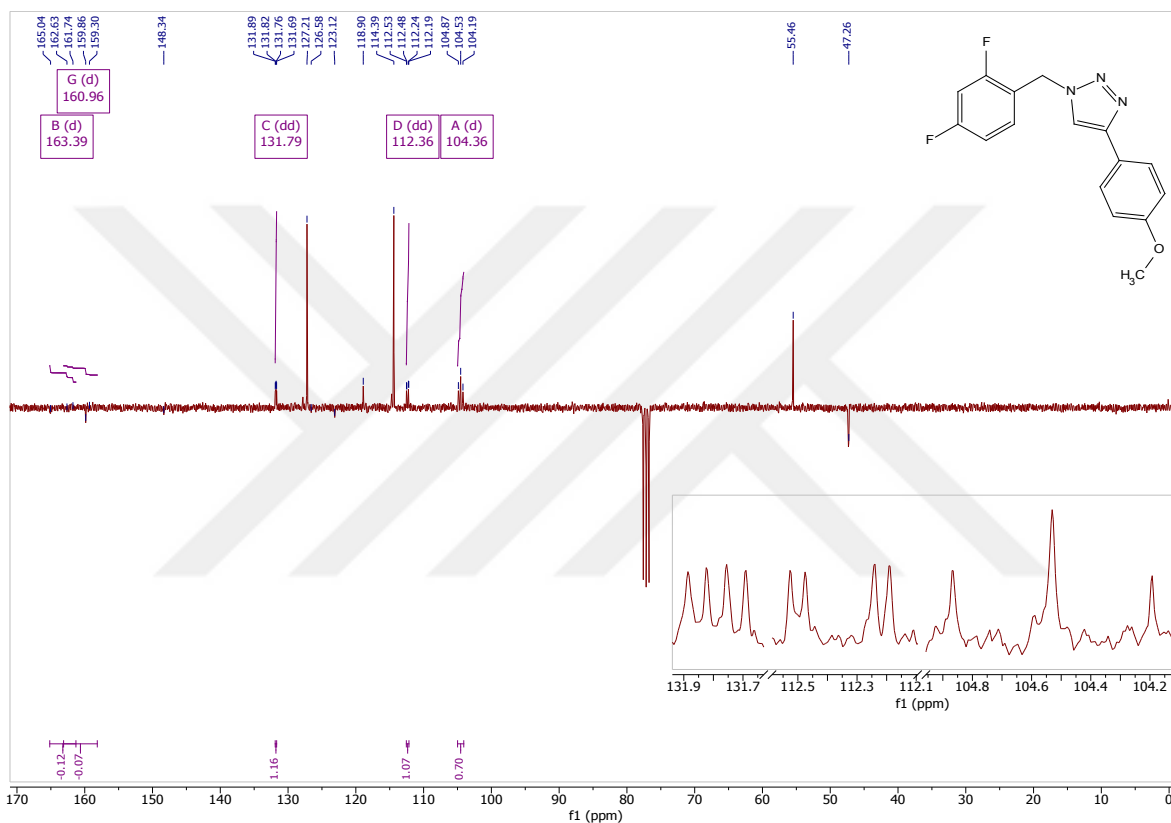


Figure 4.12. APT-NMR spectrum of compound 24

4.1.5. FT-IR, $^1\text{H-NMR}$, $^{13}\text{C-APT-NMR}$ spectroscopy analysis results of 1-(3,4-difluorobenzyl)-4-(4-methoxyphenyl)-1*H*-1,2,3-triazole (25)

FT-IR spectrum data of compound 25

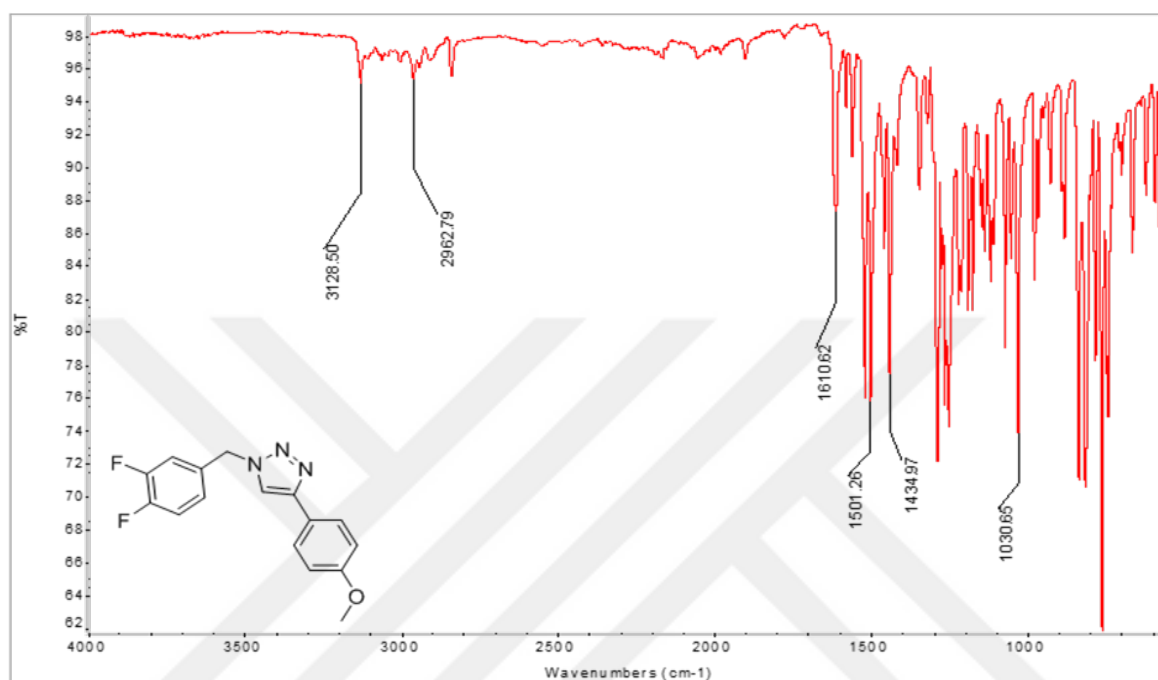


Figure 4.13. FT-IR spectrum of compound 25

Table 4.5. Selected FT-IR spectrum data of compound 25

$\bar{\nu}$ (cm^{-1})	Bonds
3128	Aromatic C-H bond's band
2962	Methyl C-H bond's band
1610-1501-1434	Aromatic C=C, N=N, C=N bond's band
1030	C-O-C bond's band

$^1\text{H-NMR}$ spectrum of compound 25

The target compound 25 was dissolved in CDCl_3 . From $^1\text{H-NMR}$ of analyzed compound, as seen in figure 4.14, one can see the following δ of 3.82 ppm (s, 3H) of $-\text{OCH}_3$ and of 5.65 ppm (s, 2H) of $-\text{CH}_2$. The $\text{AA}'\text{XX}'$ system of hydrogen atoms of para-methoxy benzene ring can be seen at δ of 6.93 (d, $J = 8.6$ Hz, 1H) for the AA' part, while the XX' part appear at δ

of 7.73 (d, $J = 8.6$ Hz, 1H). Hydrogen atoms of 3,4-difluoro phenyl ring resonate at 7.22-7.00 ppm and appear as (m, 3H). Lastly, the hydrogen atom of triazole ring appears at δ of 7.61 ppm (s, 1H).

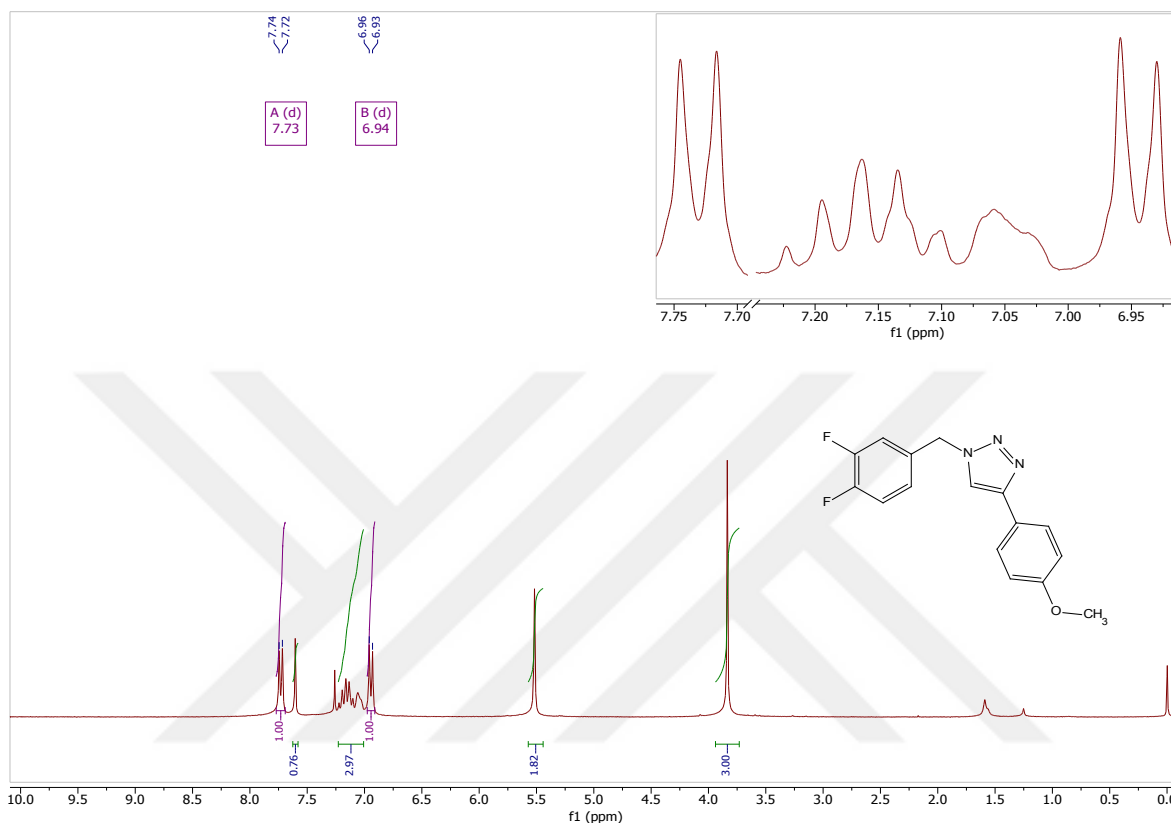


Figure 4.14. $^1\text{H-NMR}$ spectrum of compound 25

$^{13}\text{C-NMR}$ spectrum of compound 25

The target compound 25 was dissolved in CDCl_3 . From APT-NMR of an analyzed compound, as seen in figure 4.15, one can see the following δ of 53.2 ppm belongs to $-\text{OCH}_3$ and of 55.5 ppm belongs to methylene linker. The C-H carbon atoms near para-methoxy group can be seen at δ of 114.4 ppm, while the furthest two C-H atoms appear at δ of 127.2 ppm. Quaternary carbon atoms of para-methoxy benzene at 1-position appears at δ of 123.1 ppm, while carbon at 4-position appears at 159.9 ppm. Carbon atoms of fluorine phenyl ring resonate at δ of 157.3 - 117.3 ppm as following: quaternary carbon atoms at 1-, 3- and 4-positions appear at δ of 132.7 ppm, of 157.3 (d, $J = 247.5$ Hz) ppm, and of 150.8 (d, $J = 247.9$ Hz) ppm. Carbon atom at 5-position appears at δ of 117.3 (d, $J = 18.5$ Hz) ppm, carbon atom at 2-position appears at δ of 124.3 (dd, $J = 6.5, 3.8$ Hz) ppm. Lastly, carbon atom at 5-

position of triazole ring appears at δ of 126.3 ppm, while the quaternary carbon atom at 4-position of triazole ring appears at δ of 146.6 ppm.

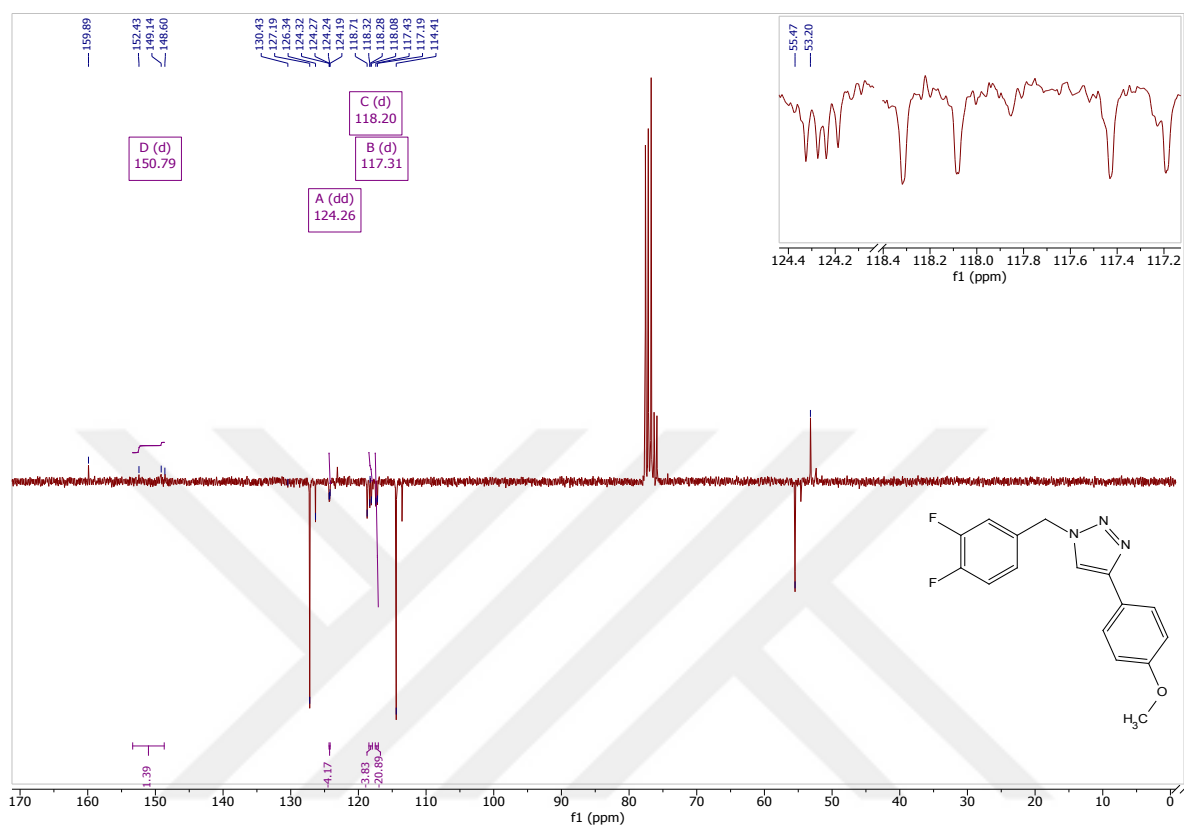


Figure 4.15. APT-NMR spectrum of compound 25

4.1.6. FT-IR, $^1\text{H-NMR}$, $^{13}\text{C-APT-NMR}$ spectroscopy analysis results of 1-(2,5-difluorobenzyl)-4-(4-methoxyphenyl)-1*H*-1,2,3-triazole (26)

FT-IR spectrum data of compound 26

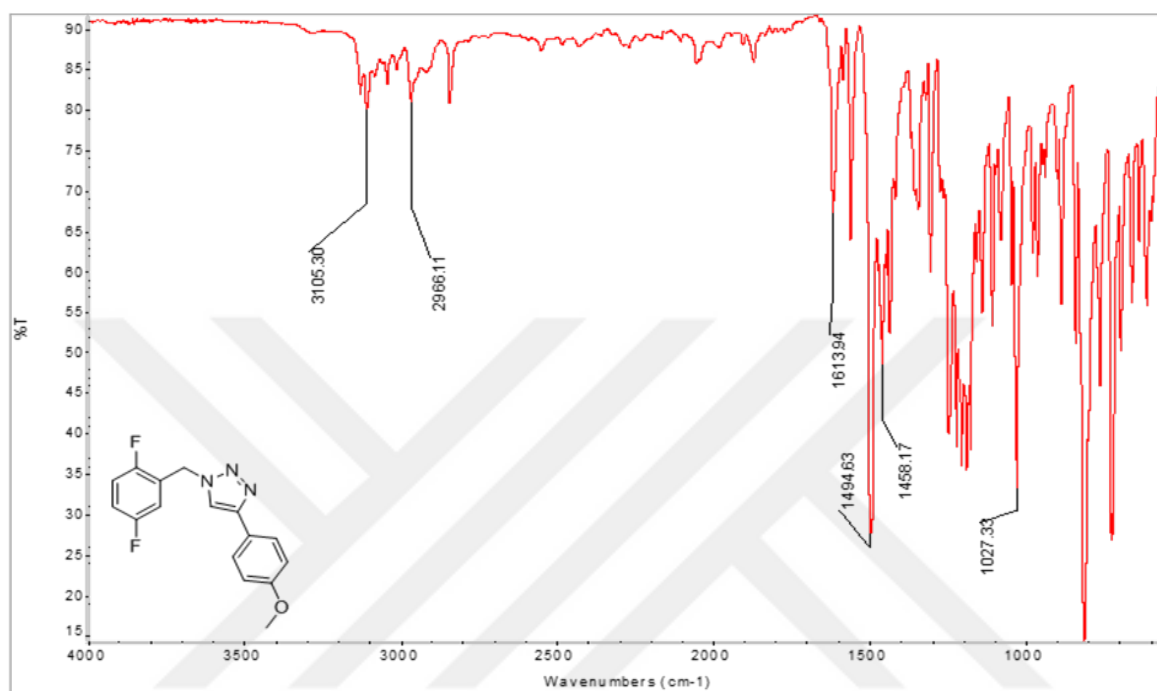


Figure 4.16. FT-IR spectrum of compound 26

Table 4.6. Selected FT-IR spectrum data of compound 26

$\bar{\nu}$ (cm^{-1})	Bonds
3105	Aromatic C-H bond's band
2966	Methyl C-H bond's band
1613-1494-1458	Aromatic C=C, N=N, C=N bond's band
1027	C-O-C bond's band

$^1\text{H-NMR}$ spectrum of compound 26

The target compound 26 was dissolved in CDCl_3 . From $^1\text{H-NMR}$ of an analyzed compound, as seen in figure 4.17, one can see the following δ of 3.82 ppm (s, 3H) of $-\text{OCH}_3$ and of 5.65 ppm (s, 2H) of CH_2 . The AA'XX' system of hydrogen atoms of para-methoxy benzene ring can be seen at δ of 6.80 (quasi d, $J = 8.8$ Hz, 2H) ppm for the AA' part, while the XX' part

appear at δ of 7.42 (quasi d, $J = 8.8$ Hz, 2H) ppm. Hydrogen atoms of 2,5-difluoro phenyl ring resonate at δ of 7.13 – 6.83 ppm: the 6-positioned hydrogen atom appears at δ of 6.83 ppm (m, 1H), hydrogen atom at 4-position appears at δ of 7.05 ppm (m, 1H), followed by the third hydrogen atom, at 3-position, at δ of 7.13 ppm (m, 1H). Lastly, the hydrogen atom of triazole ring appears at δ of 7.83 ppm (s, 1H).

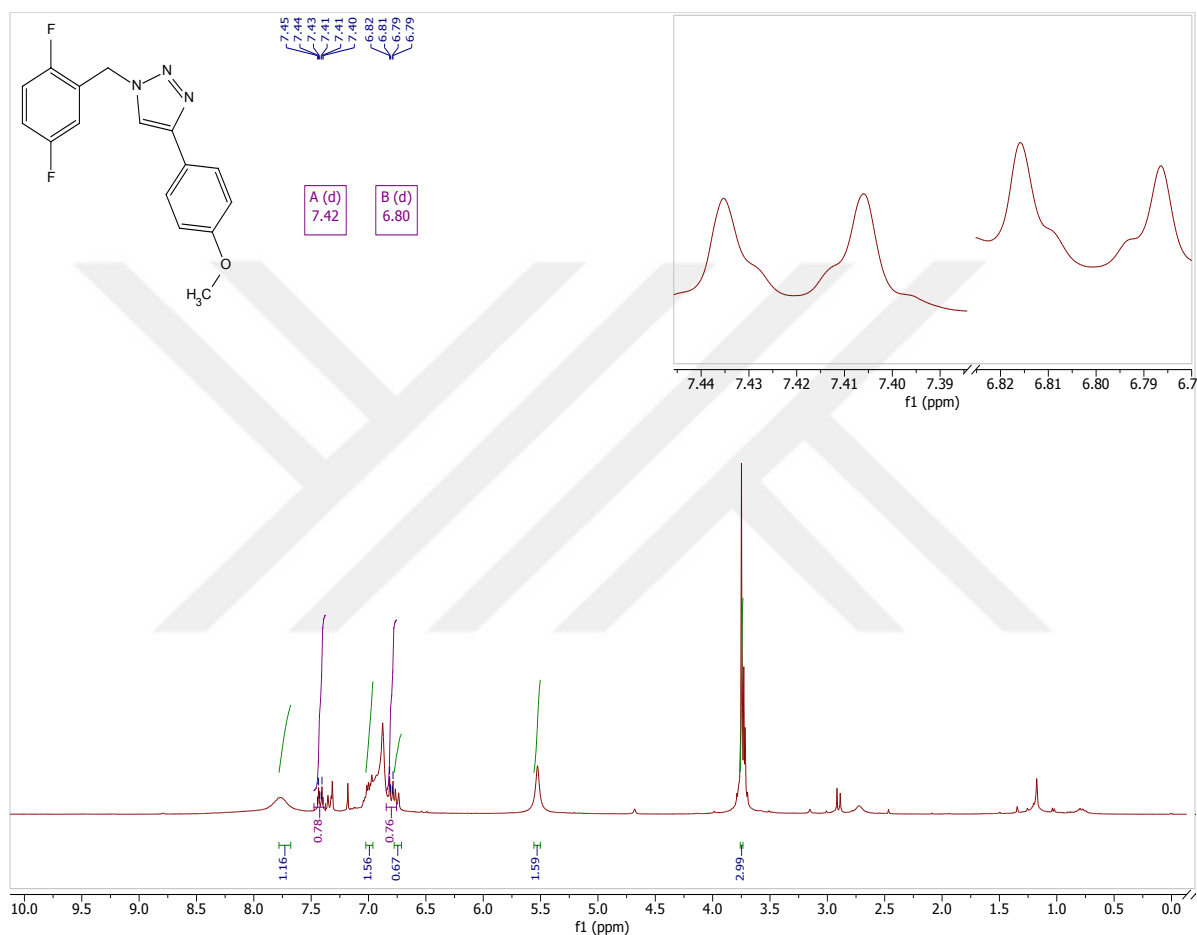


Figure 4.17. ^1H -NMR spectrum of compound 26

^{13}C -NMR spectrum of compound 26

The target compound 26 was dissolved in CDCl_3 . From ^{13}C -NMR of the analyzed compound, as seen in figure 4.18, one can see the following δ of 47.7 ppm belongs to methylene linker and of 55.3 ppm belongs to $-\text{OCH}_3$. The C-H carbon atoms near para-methoxy group can be seen at δ of 114.4 ppm, while the furthest two C-H atoms can be seen at δ 127.1 ppm. Quaternary carbon atoms of para-methoxy benzene at 1-position appears at δ of 123.1 ppm, while carbon at 4-position appears at δ of 159.8 ppm. Carbon atoms of

fluorine phenyl ring resonate at δ of 160.4 – 113.9 ppm as following: quaternary carbon atoms at 1-, 2-, and 5-positions appear at δ of 123.5 (dd, $J = 25.0$ Hz) ppm, of 156.4 (d, $J = 243.6$ Hz) ppm, and of 158.8 (d, $J = 244.6$ Hz) ppm, respectively. Carbon atom at 4-position appears at δ of 116.9 (m, $J = 24.9, 3.5$ Hz) ppm. Carbon atom at 3-position appears at δ of 117.3 (d, $J = 23.6$ Hz) ppm, while carbon atom at 6-position appears at δ of 117.4 (d, $J = 23.6$ Hz). Lastly, carbon atom at 5-position of triazole ring appears at δ of 136.4 ppm, while the quaternary carbon atom at 4-position of triazole ring appears at δ of 129.9 ppm.

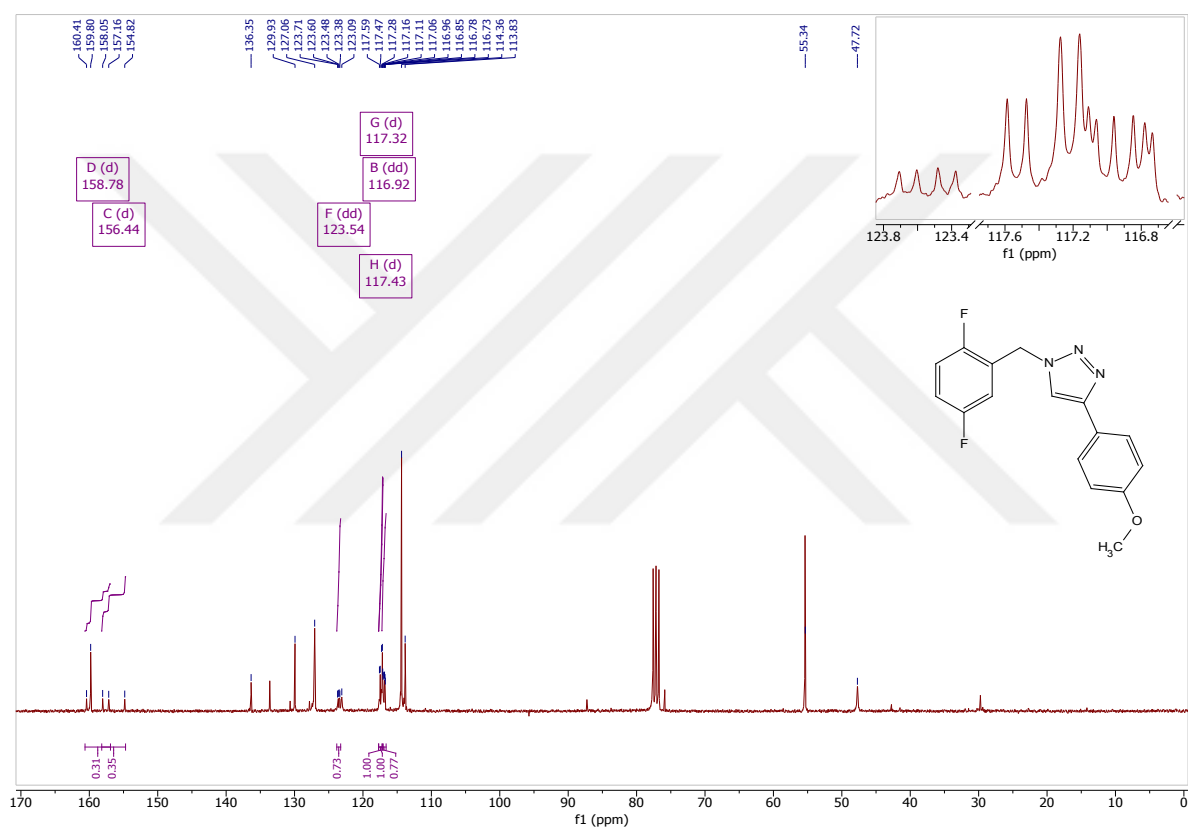


Figure 4.18. ^{13}C -NMR spectrum of compound 26

4.1.7. FT-IR, $^1\text{H-NMR}$, $^{13}\text{C-APT-NMR}$ spectroscopy analysis results of 4-(4-methoxyphenyl)-1-(4-nitrobenzyl)-1*H*-1,2,3-triazole (27)

FT-IR spectrum data of compound 27

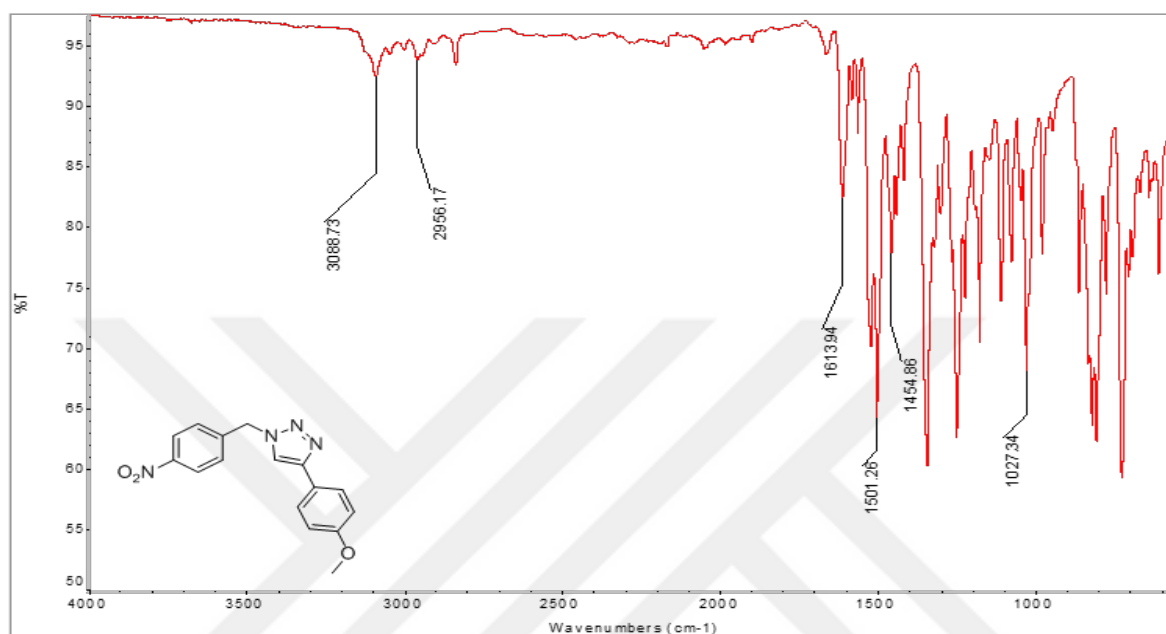


Figure 4.19. FT-IR spectrum of compound 27

Table 4.7. Selected FT-IR spectrum data of compound 27

$\bar{\nu}$ (cm ⁻¹)	Bonds
3088	Aromatic C-H bond's band
2956	Methyl C-H bond's band
1613-1501-1454	Aromatic C=C, N=N, C=N bond's band
1027	C-O-C bond's band

$^1\text{H-NMR}$ spectrum of compound 27

The target compound 27 was dissolved in CDCl_3 . From $^1\text{H-NMR}$ of an analyzed compound, as seen in figure 4.20, one can see the following δ of 3.8 ppm (s, 3H) of $-\text{OCH}_3$ and of 5.6 ppm (s, 2H) of $-\text{CH}_2$. The AA'XX' system of hydrogen atoms of para-methoxy benzene hydrogen ring can be seen at δ of 6.94 (d, $J = 8.5$ Hz, 2H) ppm for hydrogen atoms next to the methoxy group, while the other two appear at δ of 7.73 (d, $J = 8.4$ Hz, 2H) ppm. The

AA'XX' system of hydrogen atoms of para-nitro benzene ring can be seen at δ of 7.43 (d, $J = 8.4$ Hz 2H) ppm for the AA' part, while the XX' part (hydrogen atoms next to the nitro group) appear at δ of 8.22 (d, $J = 8.4$ Hz, 2H) ppm. Lastly, the hydrogen atom of triazole ring appears at δ of 7.67 ppm (s, 1H).

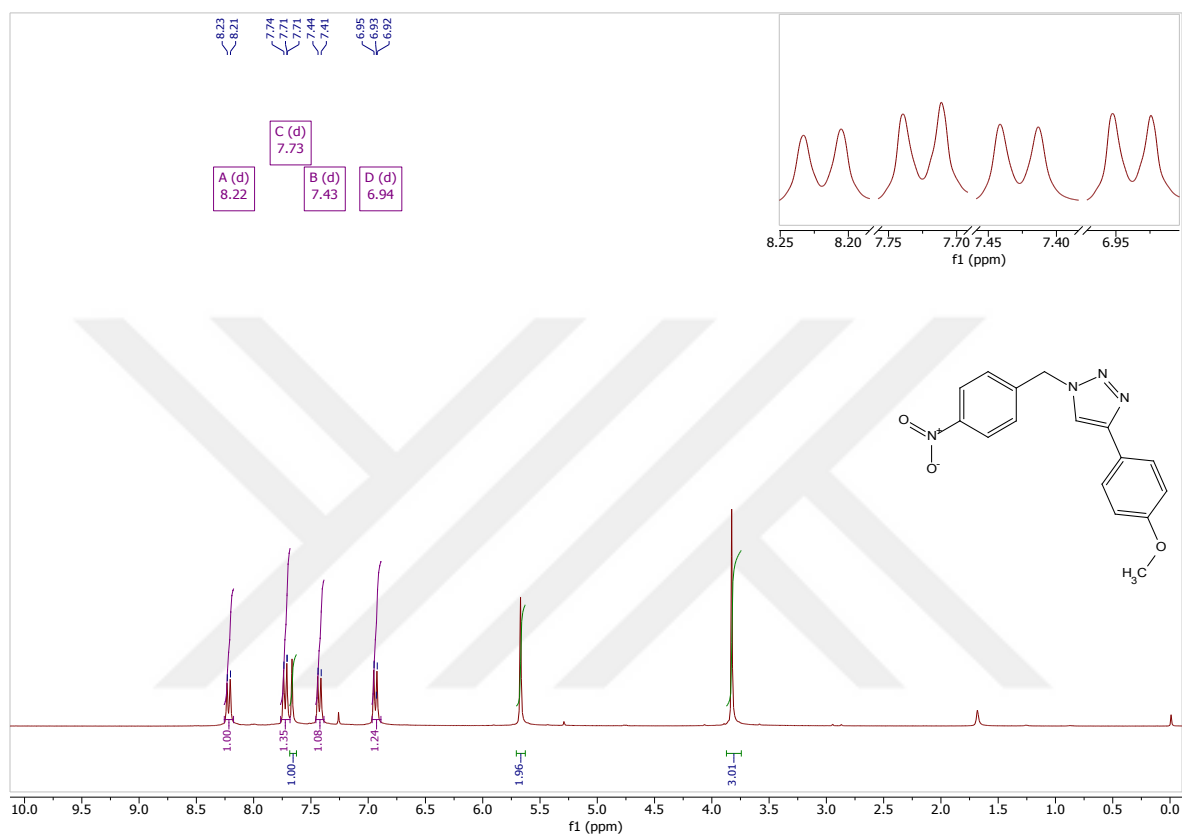


Figure 4.20. $^1\text{H-NMR}$ spectrum of compound 27

$^{13}\text{C-NMR}$ spectrum of compound 27

The target compound 27 was dissolved in CDCl_3 . From APT-NMR of the analyzed compound, as seen in figure 4.21, one can see the following δ of 53.3 ppm belongs to $-\text{OCH}_3$ and of 55.5 ppm belongs to methylene linker. The C-H carbon atoms near para-methoxy group can be seen at δ of 114.4 ppm, while the furthest two C-H atoms can be seen at δ of 127.2 ppm. Quaternary carbon atoms of para-methoxy benzene at 1-position appears at δ of 122.9 ppm, while carbon at 4-position appears at 160.0 ppm. The C-H atoms can be seen at δ of 128.7 ppm. Quaternary carbon atoms of para-nitro phenyl at 1-position appears at δ of 142.0 ppm, while carbon at 4-position appears at δ of 148.2 ppm. Lastly, carbon atom at 5-

position of triazole ring appears at δ of 119.0 ppm, while the quaternary carbon atom at 4-position of triazole ring appears at δ of 148.7 ppm.

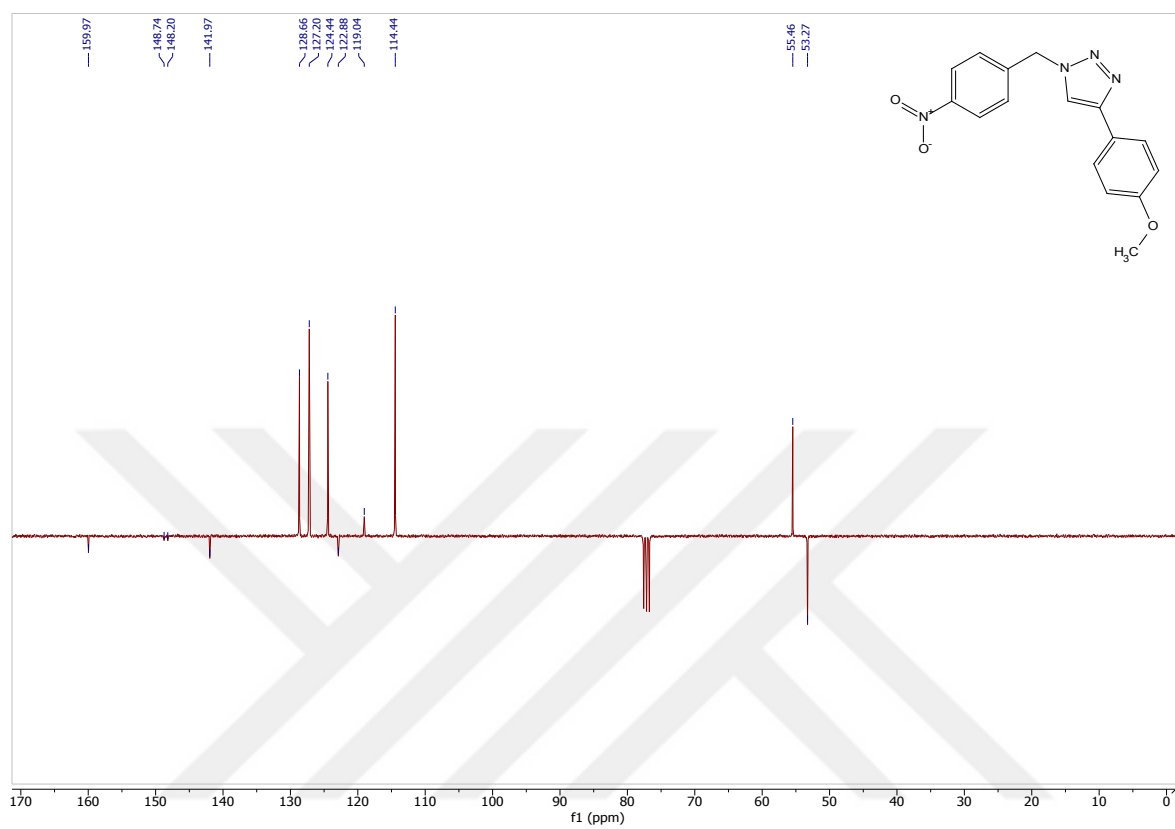


Figure 4.21. APT-NMR spectrum of compound 27

4.1.8. FT-IR, $^1\text{H-NMR}$, $^{13}\text{C-APT-NMR}$ spectroscopy analysis results of 1-(3-fluorobenzyl)-4-(thiophen-2-yl)-1*H*-1,2,3-triazole (28)

FT-IR spectrum data of compound 28

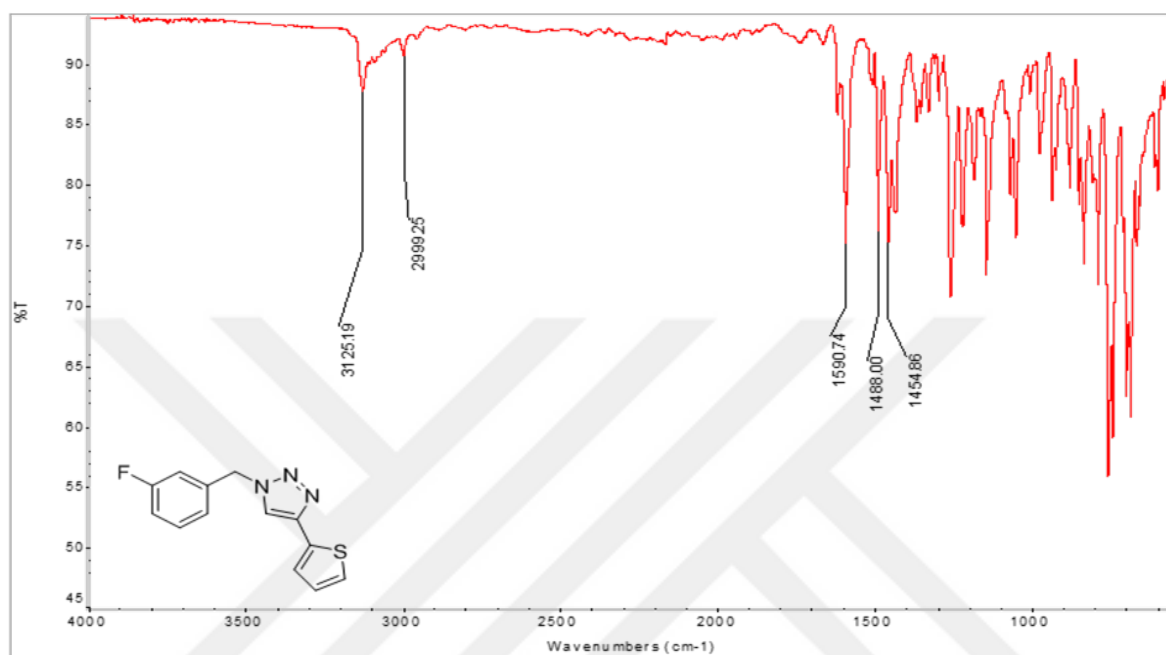


Figure 4.22. FT-IR spectrum of compound 28

Table 4.8. Selected FT-IR spectrum data of compound 28

$\bar{\nu}$ (cm^{-1})	Bonds
3125	Aromatic C-H bond's band
2999	Methyl C-H bond's band
1590-1488-1454	Aromatic C=C, N=N, C=N bond's band

$^1\text{H-NMR}$ spectrum of compound 28

The target compound 28 was dissolved in CDCl_3 . From $^1\text{H-NMR}$ of an analyzed compound, as seen in figure 4.23, one can see the following δ of 5.64 ppm (s, 2H) of $-\text{CH}_2$. Hydrogen atoms of thiophene ring resonate at δ of 7.40 – 7.27 ppm. The hydrogen atom at 4-position appears at δ of 7.22 (dd, 1H) ppm, and hydrogen atoms at 3- and 5-positions appear at δ of 7.33 (d, 2H) ppm. Hydrogen atoms of 3-fluorophenyl ring appear at δ of 7.40 – 6.94 ppm as following: hydrogen atom at 2-position appears at δ of 6.94 (d, 1H) ppm, hydrogen atoms at

4- and 6-positions appear at δ of 7.33 (d, 2H) ppm, hydrogen atom at 5-position appears at δ of 7.40 (dd, 1H) ppm. Lastly, the hydrogen atom of the triazole ring appears at δ of 7.78 ppm (s, 1H).

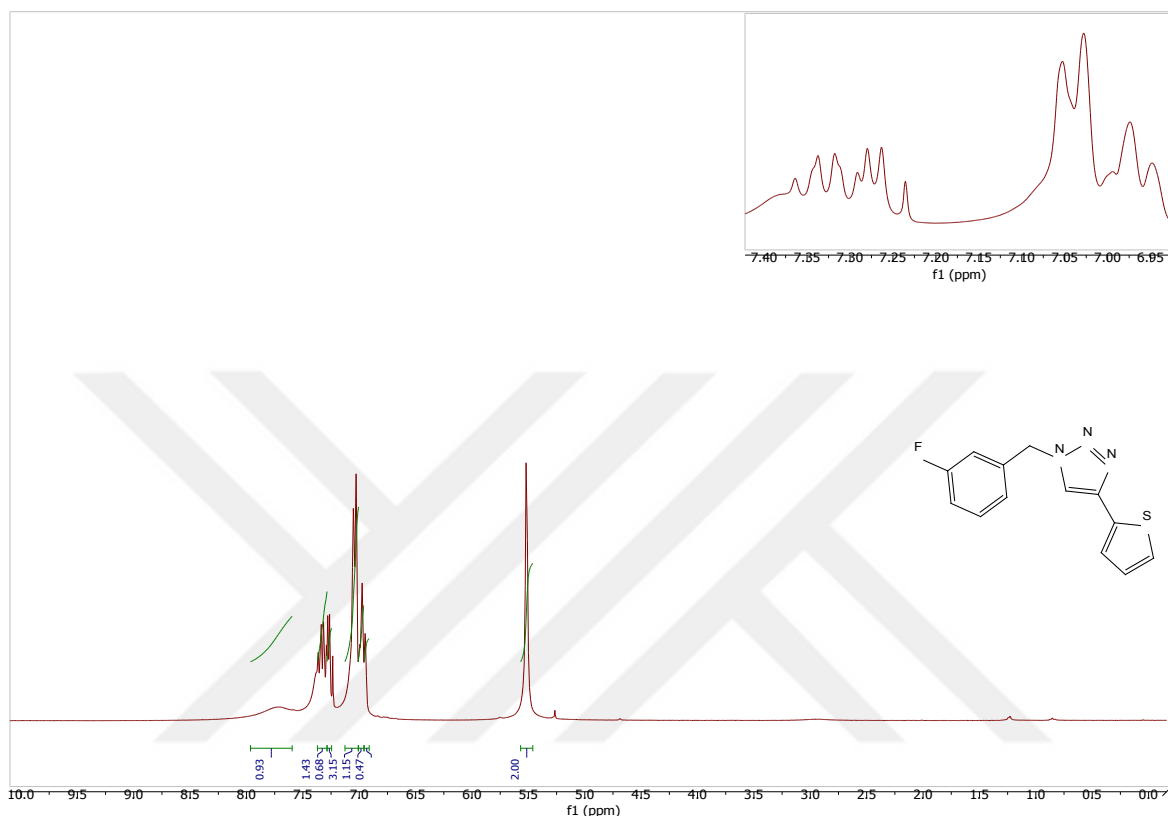


Figure 4.23. $^1\text{H-NMR}$ spectrum of compound 28

$^{13}\text{C-NMR}$ spectrum of compound 28

The target compound 28 was dissolved in CDCl_3 . From APT-NMR of an analyzed compound, as seen in figure 4.24, one can see the following δ of 54.0 ppm belongs to methylene linker. Carbon atoms of thiophene ring resonate at δ of 137.1 -124.5 ppm. The quaternary carbon at 2-position appears at δ of 137.1 ppm, carbon atom at 3-position, on the other hand, appears at δ of 124.5 ppm, carbon atom at 4-position appears at δ of 125.3 ppm, and 5-position appears at δ of 127.8 ppm. Carbon atoms of fluorine phenyl ring resonate at 163.1 – 115.2 ppm as following: quaternary carbon atoms at 1- and 3-positions appear at δ of 136.9 (d, $J = 7.2$ Hz) ppm and of 163.1 (d, $J = 248$ Hz) ppm. Carbon atom at 4-position appears at δ of 115.2 (d, $J = 22.3$ Hz) ppm, carbon atom at 2-position appears at δ of 123.6 (d, $J = 3.0$ Hz). Carbon atom at 6-position appears at δ of 125.6 ppm. Lastly, carbon atom of

5-positioned triazole ring appears at δ of 130.6 ppm, while the quaternary carbon atom of 4-position appears at δ of 131.0 (d, $J = 8.2$ Hz) ppm.

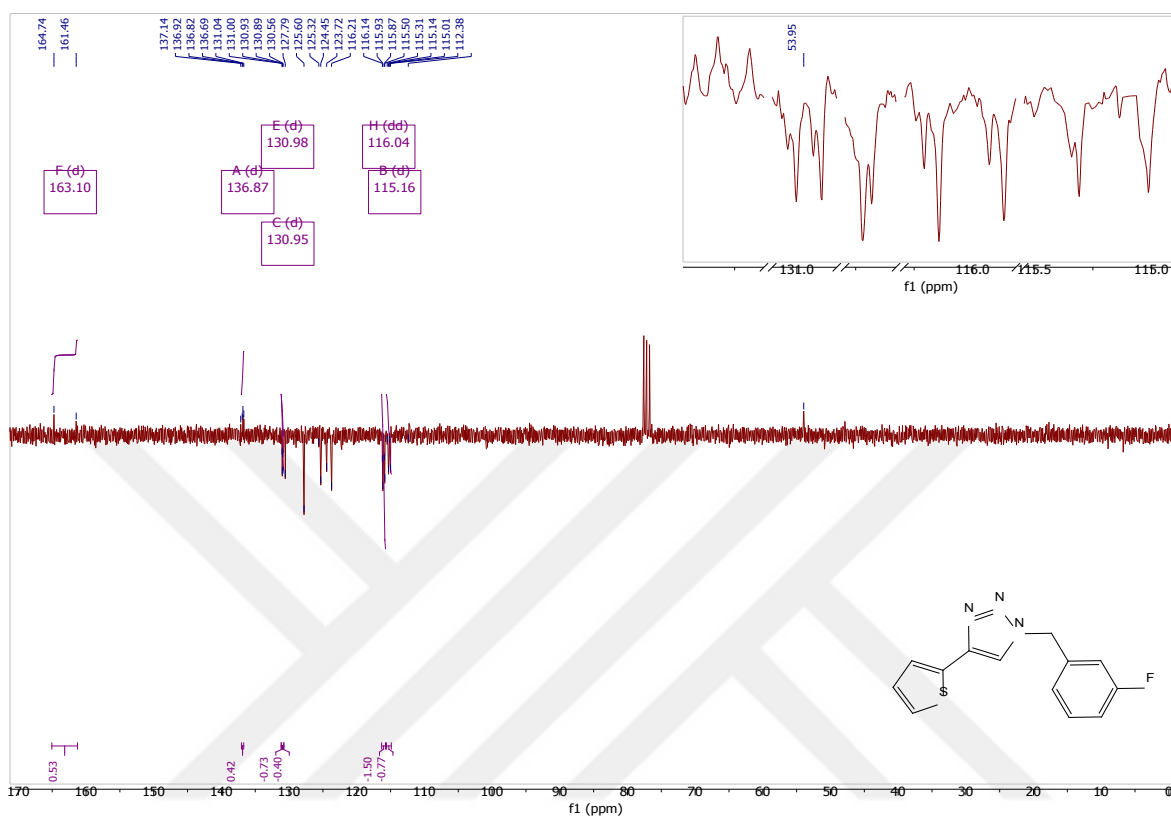


Figure 4.24. APT-NMR spectrum of compound 28

4.1.9. FT-IR, $^1\text{H-NMR}$, $^{13}\text{C-APT-NMR}$ spectroscopy analysis results of 1-(2,5-difluorobenzyl)-4-(thiophen-2-yl)-1*H*-1,2,3-triazole (29)

FT-IR spectrum data of compound 29

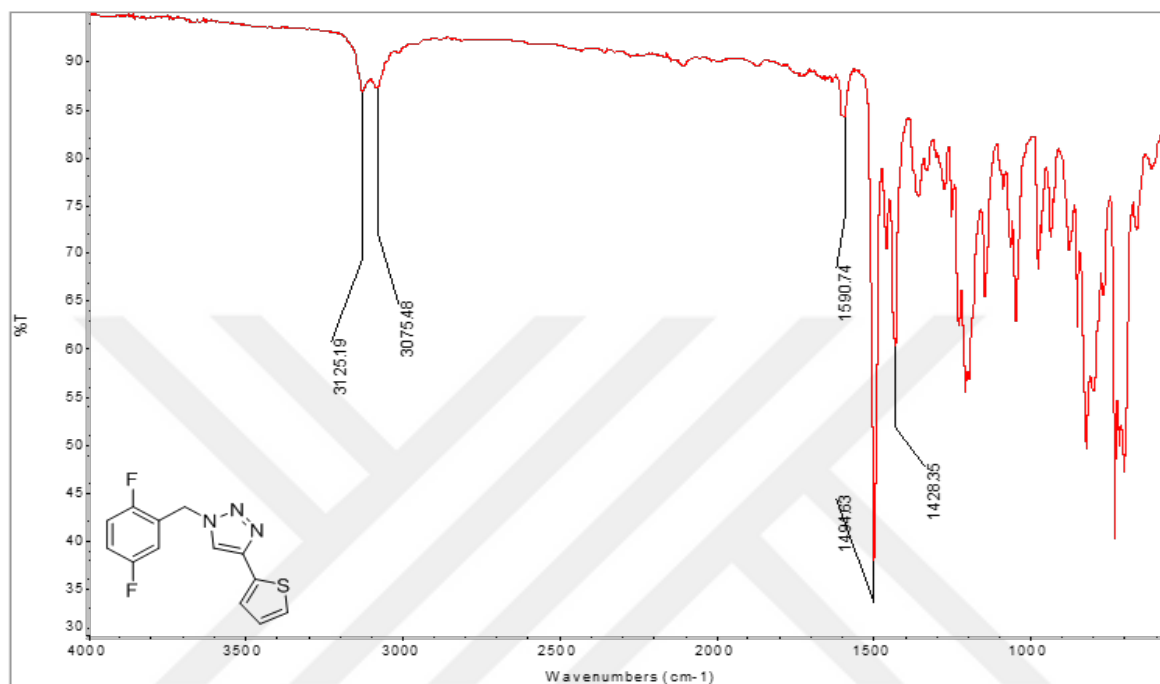


Figure 4.25. FT-IR spectrum of compound 29

Table 4.9. Selected FT-IR spectrum data of compound 29

$\bar{\nu}$ (cm ⁻¹)	Bonds
3125	Aromatic C-H bond's band
3075	Methyl C-H bond's band
1590-1494-1428	Aromatic C=C, N=N, C=N bond's band

$^1\text{H-NMR}$ spectrum of compound 29

The target compound 29 was dissolved in CDCl_3 . From $^1\text{H-NMR}$ of an analyzed compound, as seen in figure 4.26, one can see the following δ of 5.6 ppm (s, 2H) of $-\text{CH}_2-$ hydrogen atoms of thiophene ring resonate at δ of 7.29 – 7.07 ppm. The hydrogen atom at 4-position appears δ of 7.07 (dd, 1H) ppm, and hydrogen atoms at 3- and 5-appear at δ of 7.29 (d, 2H) ppm. Hydrogen atoms of 2,5-difluoro phenyl ring appear at δ of 7.01 – 6.95 ppm as

following: the 6-positioned hydrogen atom appears at δ of 6.95 (t, 1H) ppm, while hydrogen atoms at 3- and 4-positions appear at δ of 7.01 (m, 2H) ppm. Lastly, the hydrogen atom of triazole ring appears at δ of 7.74 (s, 1H) ppm.

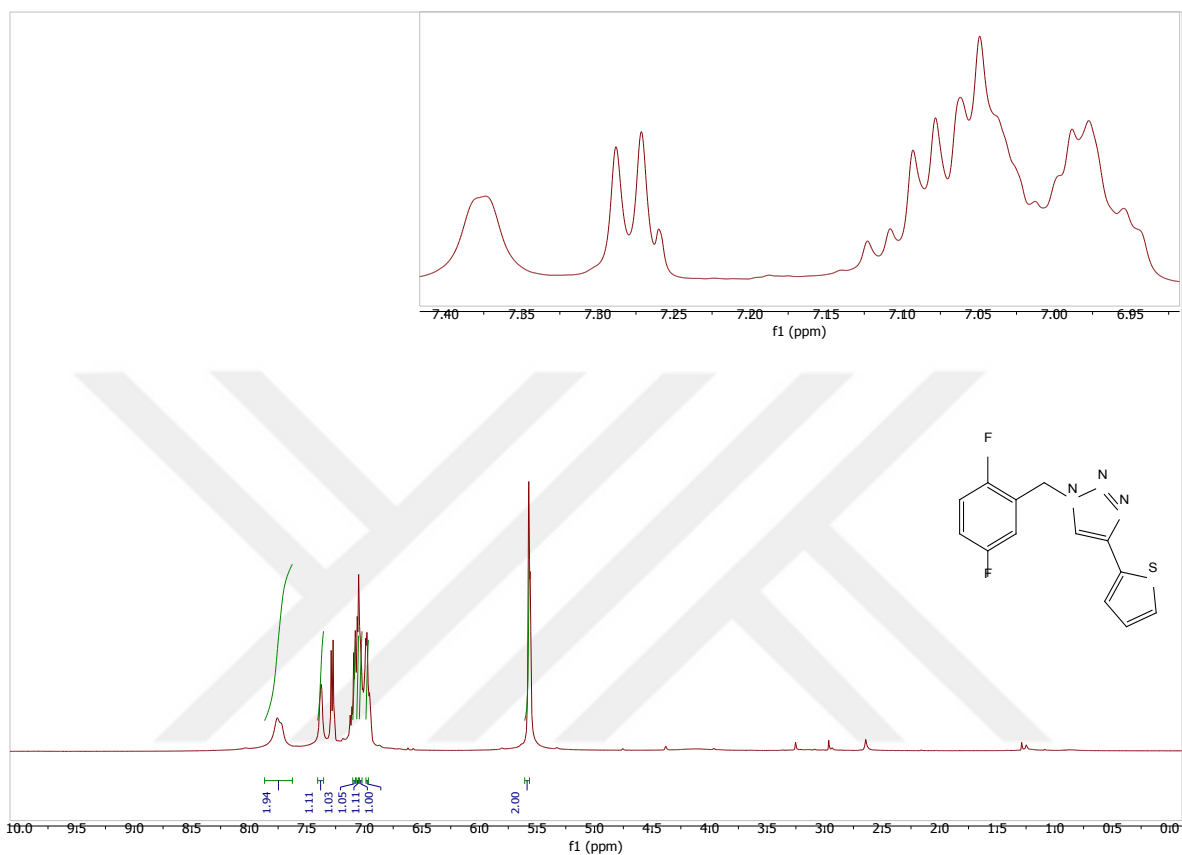


Figure 4.26. ¹H-NMR spectrum of compound 29

¹³C-NMR spectrum of compound 29

The target compound 29 was dissolved in CDCl₃. From APT-NMR of an analyzed compound, as seen in figure 4.27, one can see the following δ of 53.7 ppm belongs to methylene linker. Carbon atoms of thiophene ring resonate at δ of 134.3 – 124.5 ppm. The quaternary carbon at 2-position appears at δ of 134.3 ppm, carbon atom at 3-position, on the other hand, appears at δ of 124.5 ppm, carbon atom at 4-position appears at δ of 125.4 ppm, and 5-position appears at δ of 127.7 ppm. Carbon atoms of fluorine phenyl ring resonate at δ of 161.5 – 115.2 ppm as following: quaternary carbon atoms at 1-, 2-, and 5-positions appear at δ of 123.3 (dd, $J = 25.5$ Hz) ppm, of 156.4 (d, $J = 22.1$ Hz) ppm, and of 158.8 (d, $J = 242.4$) ppm, respectively. Carbon atom at 3-position appears at δ of 116.9 (dd, $J = 21.0$ Hz) ppm, carbon atoms at 4-position appears at δ of 117.3 (dd, $J = 22.1$ Hz) ppm, and carbon

atom at 6-position appears at δ of 117.6 (d, $J = 24.2$ Hz) ppm. Lastly, carbon atom of 5-position appears at δ of 132.5 ppm.

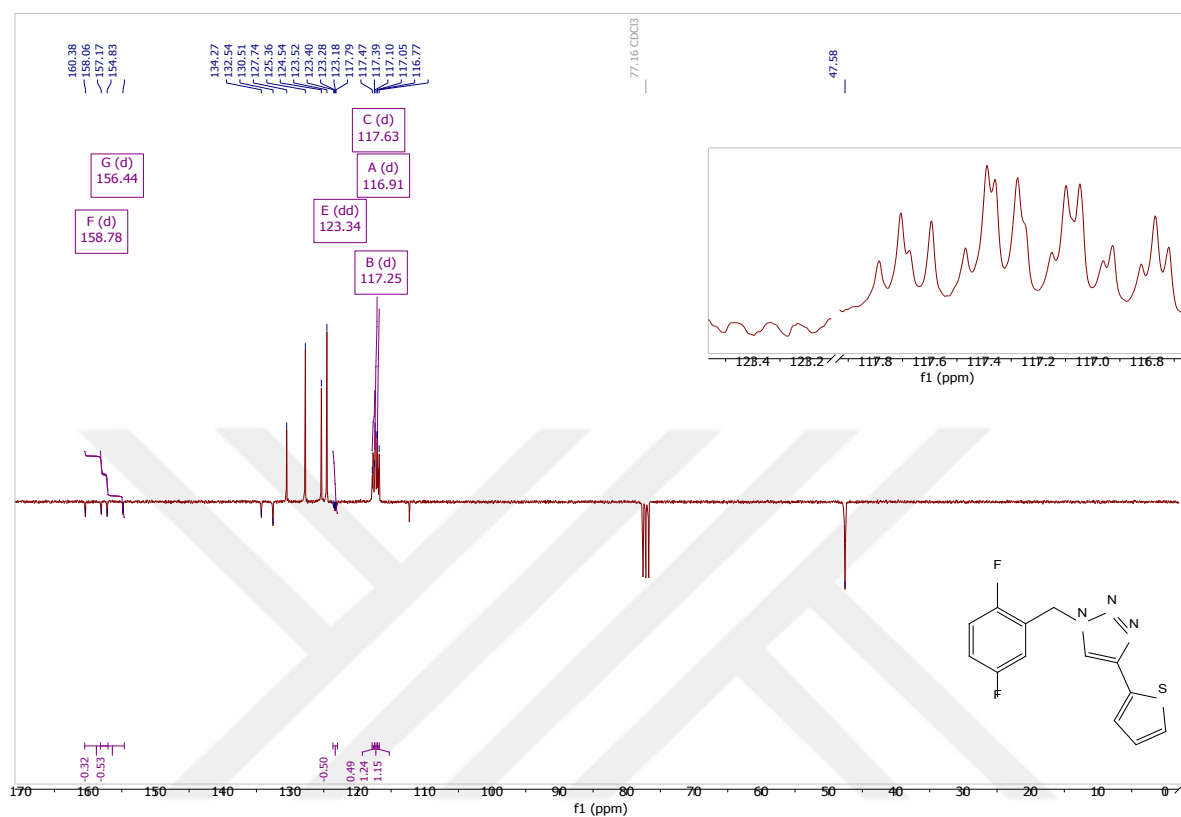


Figure 4.27. APT-NMR spectrum of compound 29

4.1.10. FT-IR, $^1\text{H-NMR}$, $^{13}\text{C-APT-NMR}$ spectroscopy analysis results of 1-(3,5-difluorobenzyl)-4-(thiophen-2-yl)-1*H*-1,2,3-triazole (30)

FT-IR spectrum data of compound 30

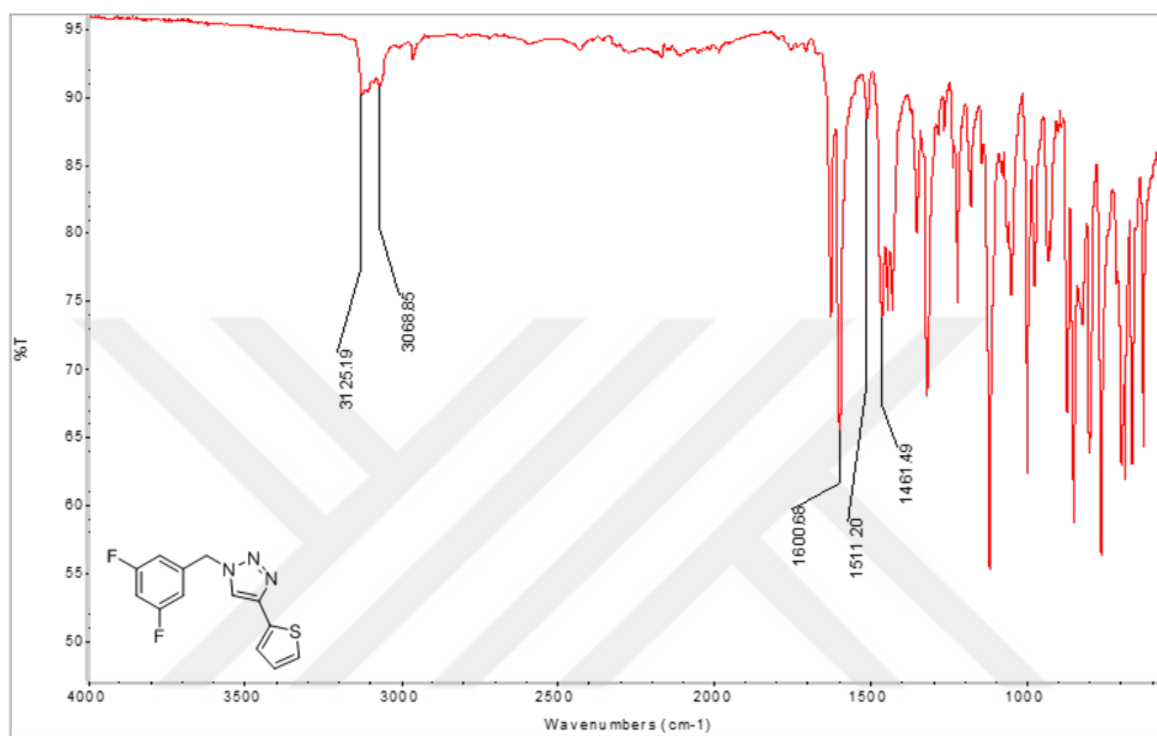


Figure 4.28. FT-IR spectrum of compound 30

Table 4.10. Selected FT-IR spectrum data of compound 30

$\bar{\nu}$ (cm^{-1})	Bonds
3125	Aromatic C-H bond's band
3068	Methyl C-H bond's band
1600-1511-1461	Aromatic C=C, N=N, C=N bond's band

$^1\text{H-NMR}$ spectrum of compound 30

The target compound 30 was dissolved in CDCl_3 . From $^1\text{H-NMR}$ of an analyzed compound, as seen in figure 4.29, one can see the following δ of 5.6 ppm (s, 2H) of $-\text{CH}_2$. Hydrogen atoms of thiophene ring resonate at δ of 7.33 – 7.08 ppm. The hydrogen atom at 4-position appears at δ of 7.08 (dd, 1H) ppm, and hydrogen atoms at 3- and 5-positions appear at δ of

7.33 (d, 2H) ppm. Hydrogen atoms of 3,5-difluoro phenyl ring appear at δ of 6.80 ppm as a conjugate of doublet and singlet of 3H. Lastly, the hydrogen atom of triazole ring appears at δ of 7.67 ppm (s, 1H).

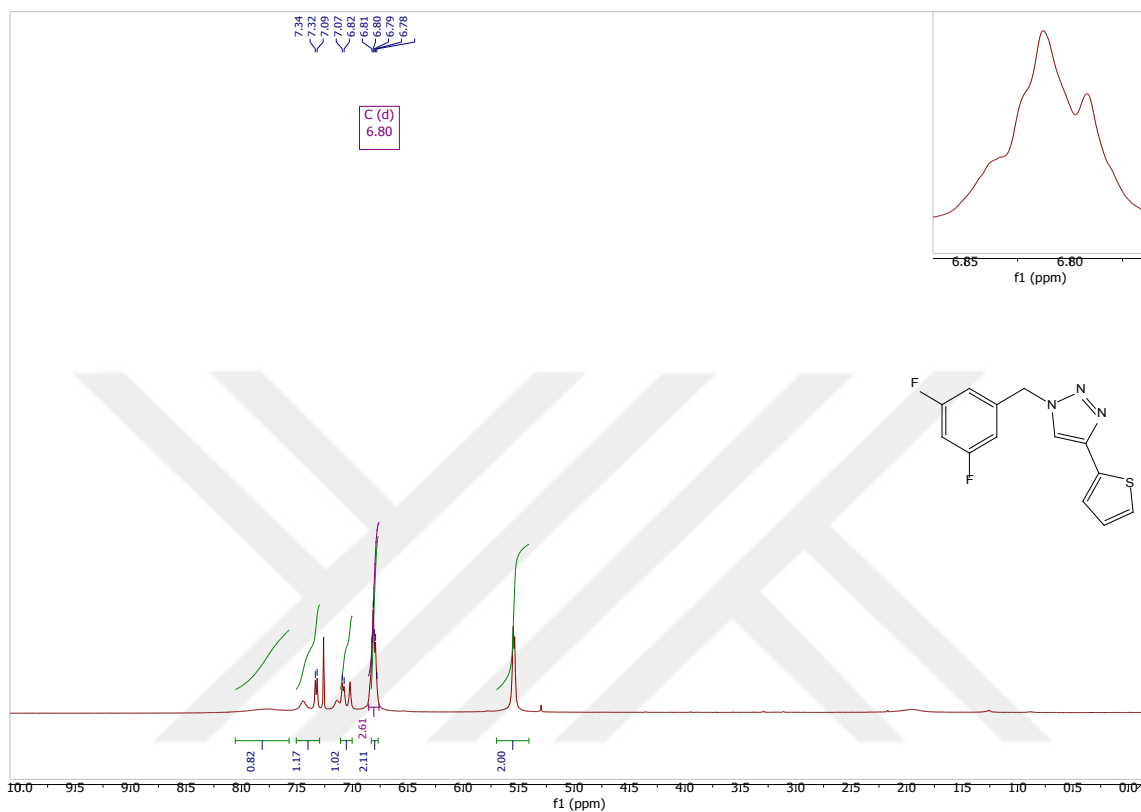


Figure 4.29. ^1H -NMR spectrum of compound 30

^{13}C -NMR spectrum of compound 30

The target compound 30 was dissolved in CDCl_3 . From APT-NMR of an analyzed compound, as seen in figure 4.30, one can see the following δ of 53.7 ppm belongs to methylene linker. Carbon atoms of thiophene ring resonate at δ of 149.7 – 124.6 ppm. The quaternary carbon atom at 2-position appears at δ of 138.3 ppm. Carbon atom at 3-position, on the other hand, appears at δ of 124.6 ppm, carbon atom at 4-position appears at δ of 125.5 ppm, while carbon atom at 5-position appears at δ of 127.9 ppm. Carbon atoms of fluorine phenyl ring resonate at δ of 163.5 – 104.6 ppm as following: quaternary carbon atoms at 1-, 3-, and 5-positions appear at δ of 138.2 ppm, of 163.4 (d, $J = 250.8$ Hz) ppm, and of 163.5 (d, $J = 250.9$ Hz) ppm, respectively. Carbon atom at 4-position appears at δ of 104.6 (td, $J = 25.0, 4.4$ Hz) ppm, carbon atoms at 2- and 6-positions appear at δ of 111.1 (dd, $J = 25.9, 2.4$

Hz) ppm. Lastly, carbon atom of 5-positioned triazole ring appears at δ of 130.6 ppm, while carbon atom at 4-position appears at δ of 138.1 ppm.

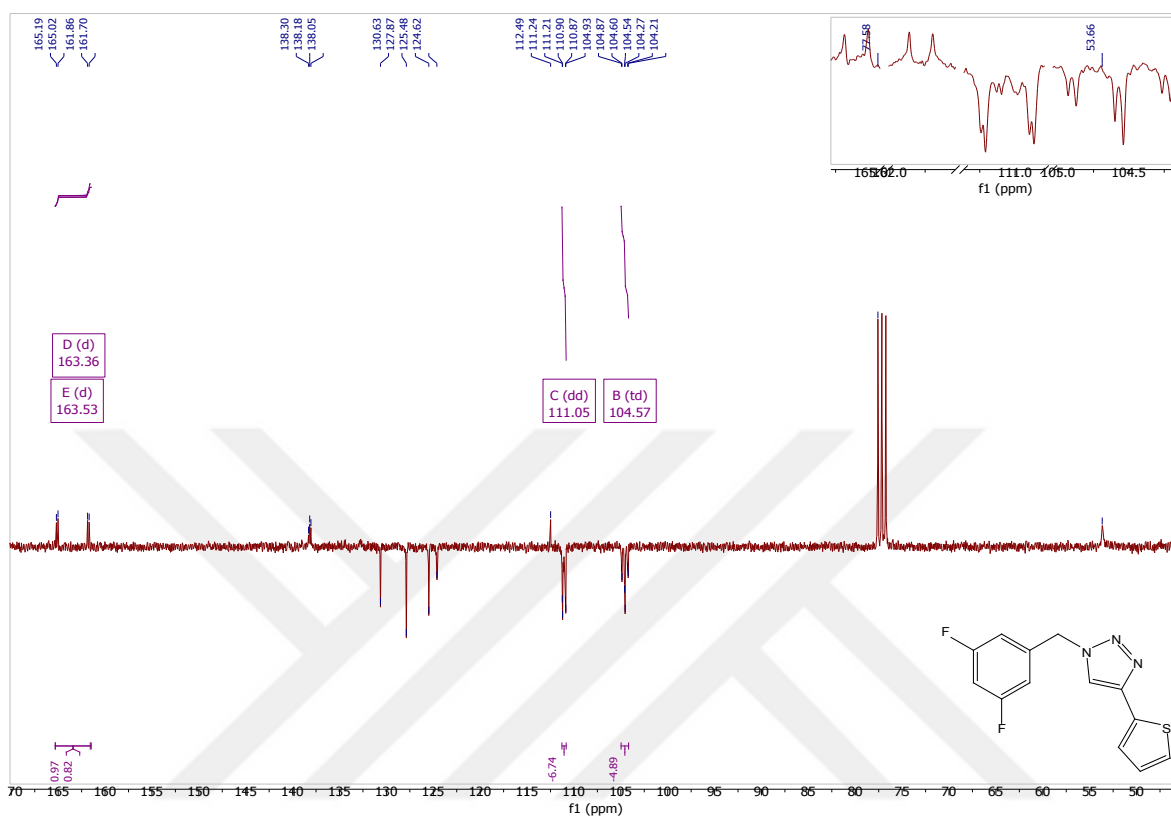


Figure 4.30. APT-NMR spectrum of compound 30

4.1.11. FT-IR, $^1\text{H-NMR}$, $^{13}\text{C-APT-NMR}$ spectroscopy analysis results of 1-(4-nitrobenzyl)-4-(thiophen-2-yl)-1*H*-1,2,3-triazole (31)

FT-IR spectrum data of compound 31

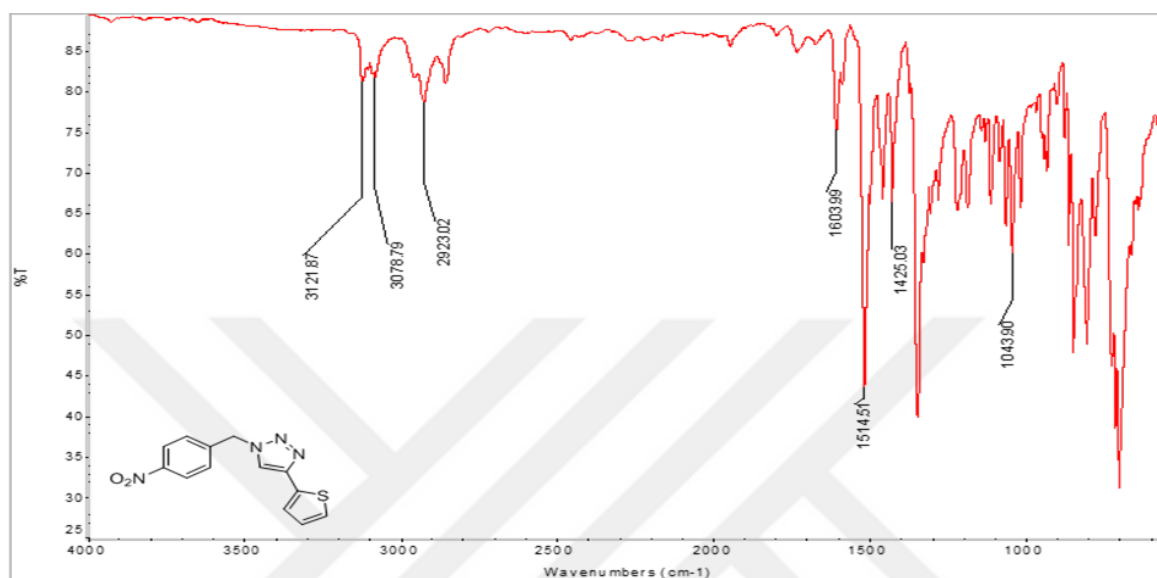


Figure 4.31. FT-IR spectrum of compound 31

Table 4.11. Selected FT-IR spectrum data of compound 31

$\bar{\nu}$ (cm ⁻¹)	Bonds
3121	Aromatic C-H bond's band
3078, 2923	Methyl C-H bond's band
1603-1514-1424	Aromatic C=C, N=N, C=N bond's band
1043	C-N-O bond's band

$^1\text{H-NMR}$ spectrum of compound 31

The target compound 31 was dissolved in CDCl_3 . From $^1\text{H-NMR}$ of an analyzed compound, as seen in figure 4.32, one can see the following δ of 5.64 ppm (s, 2H) of -CH₂. Hydrogen atoms of thiophene ring resonate at δ of 7.37 – 7.07 ppm. The hydrogen atom at 4-position appears at δ of 7.07 ppm (dd, 1H), and hydrogen atom at 3-position appears at δ of 7.30 ppm (d, 1H) ppm, while atom 5-position appears at δ of 7.33 ppm (d, 1H). The para-nitro benzene ring forms AA'XX' system in which hydrogen atoms for the AA' part appear at δ of 7.44

(d, $J = 8.6$ Hz, 2H) ppm, while the XX' part (hydrogen atoms next to the nitro group) appear at δ of 8.23 (d, $J = 8.6$ Hz, 2H) ppm. Lastly, the hydrogen atom of triazole ring appears at δ of 7.67 ppm (s, 1H).

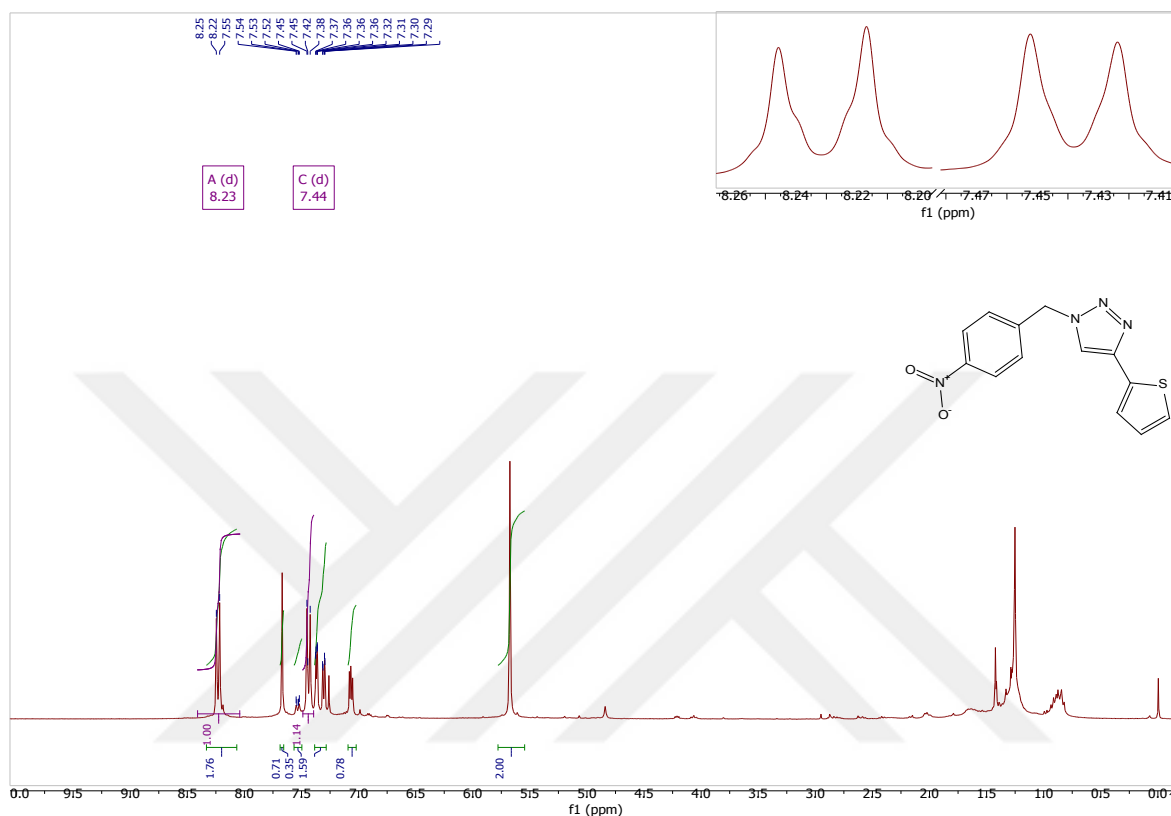


Figure 4.32. ^1H -NMR spectrum of compound 31

^{13}C -NMR spectrum of compound 31

The target compound 31 was dissolved in CDCl_3 . From APT-NMR of an analyzed compound, as seen in figure 4.33, one can see the following δ of 53.3 ppm belongs to methylene linker. Carbon atoms of thiophene ring resonate at δ of 141.7 – 124.6 ppm. The quaternary carbon atoms at 2-position appears at δ of 141.7 ppm. Carbon atom at 3-position appears at δ of 124.6 ppm, carbon atom at 4-position, on the other hand, appears at δ of 125.5 ppm, while carbon atom at 5-position appears at δ of 127.8 ppm. The C-H carbon atoms near para-nitro phenyl group can be seen at δ of 124.4 ppm, while the furthest two C-H atoms can be seen at δ of 128.7 ppm. Quaternary carbon atoms of para-nitro phenyl at 1-position appears at 143.9 ppm, while carbon at 4-position appears at 148.2 ppm. Lastly, carbon atom

of 5-positioned triazole ring appears at δ of 119.3 ppm, while the quaternary carbon atom at 4-position appears at δ of 132.5 ppm.

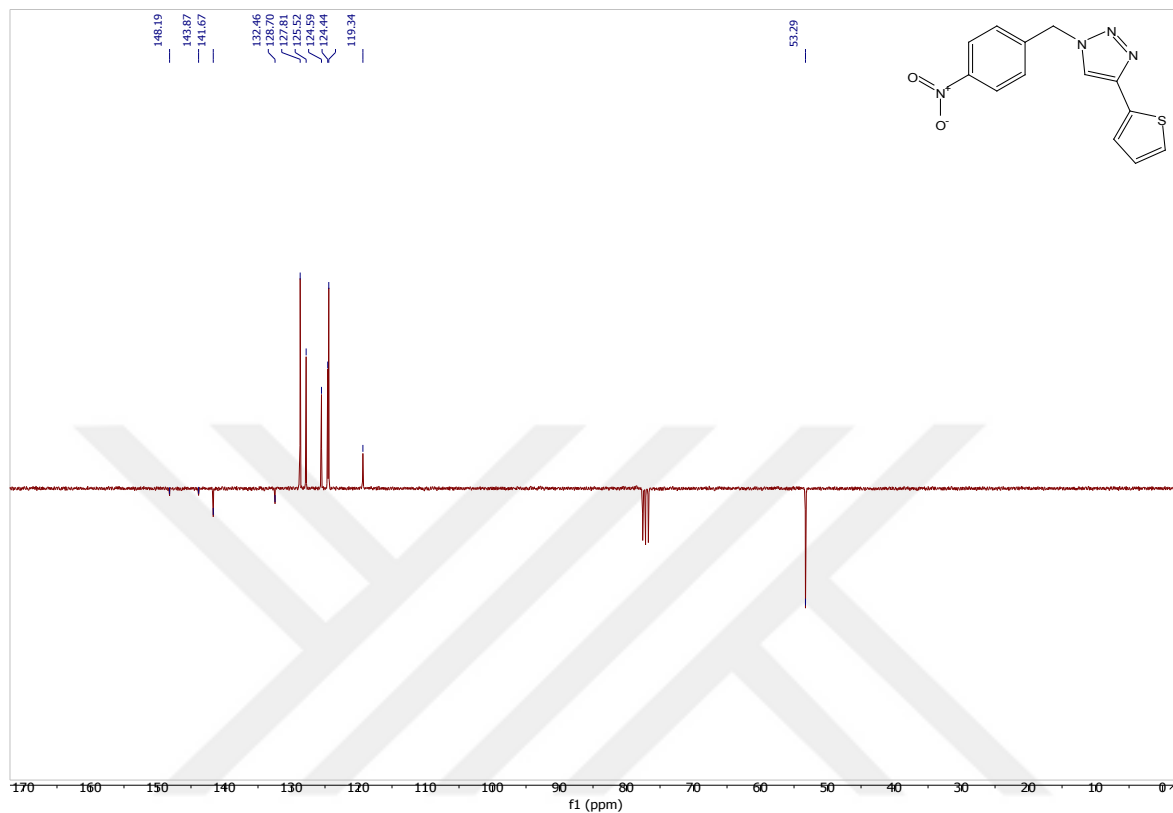


Figure 4.33. APT-NMR spectrum of compound 31

4.1.12. FT-IR, ¹H-NMR, ¹³C-APT-NMR spectroscopy analysis results of (1-(3-fluorobenzyl)-1*H*-1,2,3-triazol-4-yl)(5-methylthiophen-2-yl)methanone (32)

FT-IR spectrum data of compound 32

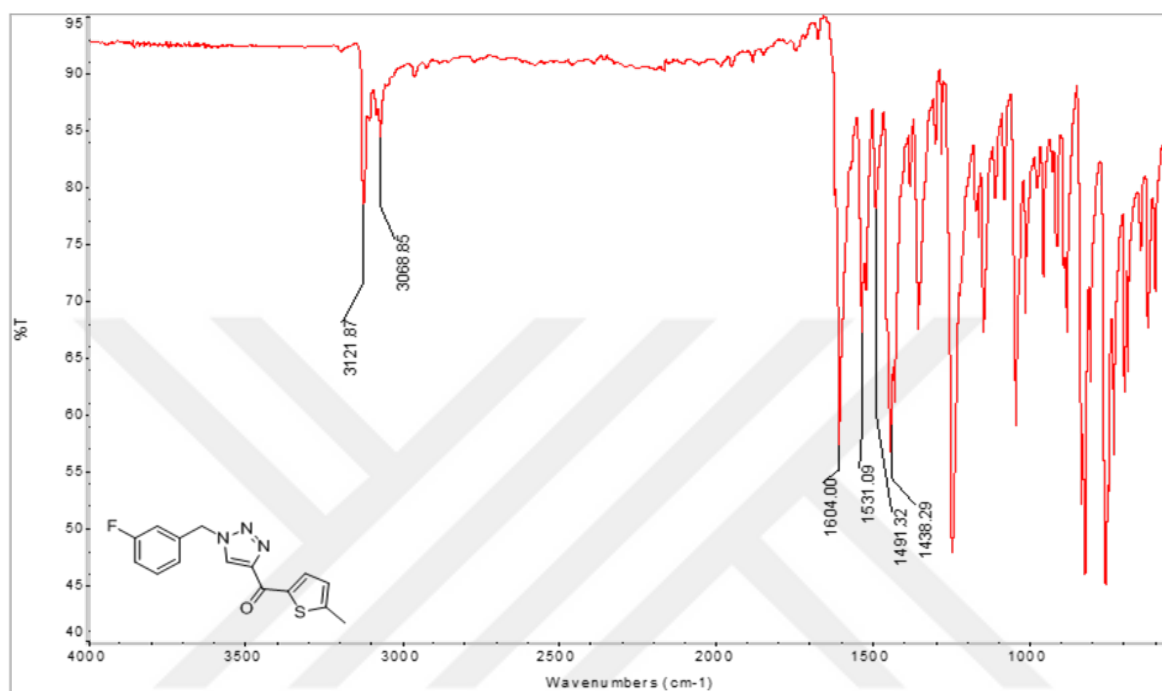


Figure 4.34. FT-IR spectrum of compound 32

Table 4.12. Selected FT-IR spectrum data of compound 32

$\bar{\nu}$ (cm ⁻¹)	Bonds
3121	Aromatic C-H bond's band
3068	Methyl C-H bond's band
1604	C=O bond's band
1531-1491-1438	Aromatic C=C, N=N, C=N bond's band

¹H-NMR spectrum of compound 32

The target compound 32 was dissolved in CDCl₃. From ¹H-NMR of an analyzed compound, as seen in figure 4.35, one can see the following δ of 2.37 ppm (s, 3H) of -CH₃ and of 5.6 ppm (s, 2H) of -CH₂. Hydrogen atoms of thiophene ring resonate at δ of 8.56 – 7.09 ppm. The hydrogen atom at 4-position appears at δ of 7.09 (dd, 1H) ppm, and hydrogen atom at

3-position appears at δ of 8.56 (d, 1H) ppm. Hydrogen atoms of 3-fluorophenyl ring appear at δ of 7.37 – 6.89 as following: hydrogen atom at 2-position appears at δ of 6.89 (d, 1H) ppm, hydrogen atoms at 4- and 6-positions appear at δ of 7.02 (dt, 2H) ppm, hydrogen atom at 5-position appears at δ of 7.37 (td, 1H) ppm. Lastly, the hydrogen atom of the triazole ring appears at δ of 8.17 (s, 1H) ppm.

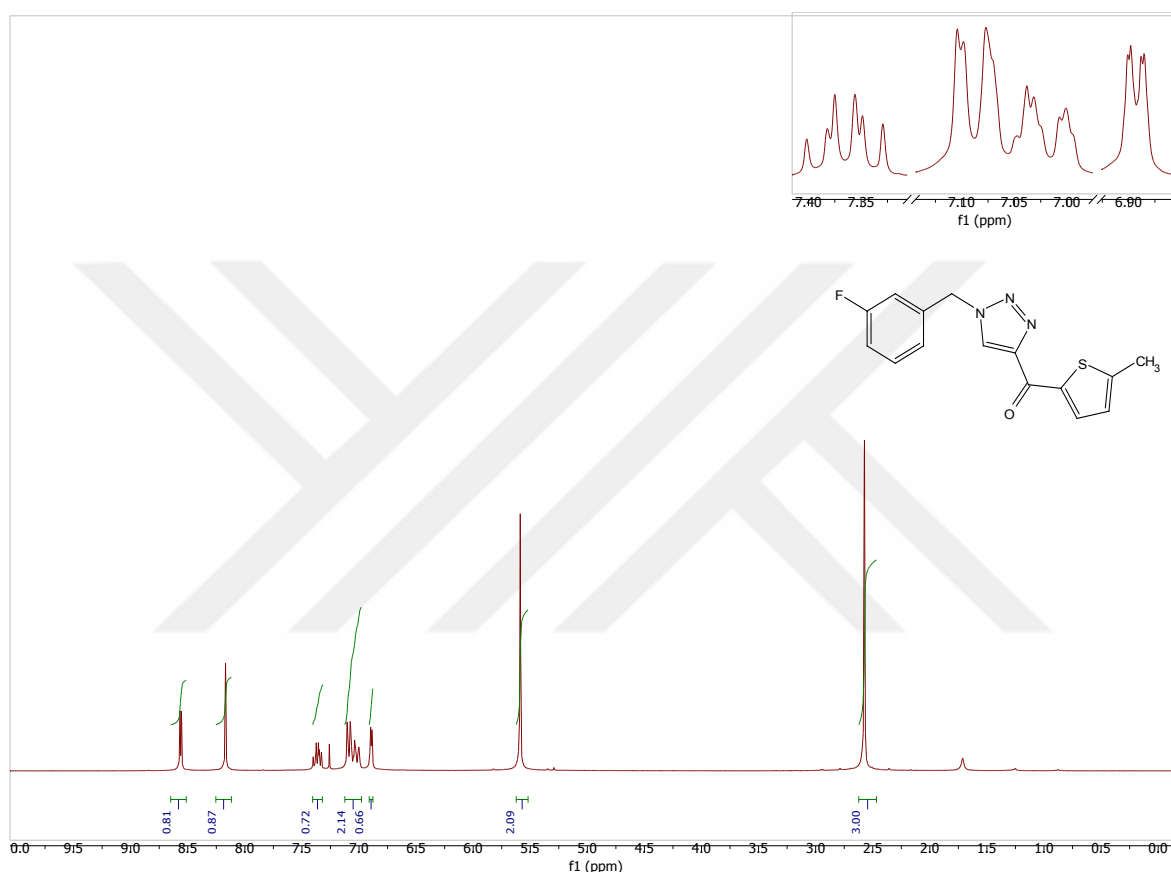


Figure 4.35. ¹H-NMR spectrum of compound 32

¹³C-NMR spectrum of compound 32

The target compound 32 was dissolved in CDCl₃. From APT-NMR of an analyzed compound, as seen in figure 4.36, one can see the following δ of 14.6 ppm belongs to -CH₃ and of 53.9 ppm belongs to methylene linker. Carbon atoms of thiophene ring resonate at δ of 151.6 – 127.6 ppm. The quaternary carbon atoms at 2- and 5-positions appear at δ of 140.1 ppm, of 151.6 ppm, and of 151.6 ppm. Carbon atom at 3-position, on the other hand, appears at δ of 137.3 ppm, carbon atom at 4-position appears at δ of 127.6 ppm. Carbon atoms of fluorine phenyl ring resonate at δ of 163.2 – 115.4 ppm as following: quaternary carbon

atoms at 1- and 3-positions appear at δ of 136.2 (d, $J = 7.4$ Hz) ppm and of 163.2 (d, $J = 248.5$ Hz) ppm. Carbon atom at 4-position appears at δ of 115.4 (d, $J = 22.5$ Hz) ppm, carbon atom at 2-position appears at δ of 116.3 (d, $J = 21.0$ Hz), and carbon at 5-position appears at δ of 123.9 (d, $J = 3.2$ Hz) ppm. Carbon atom 6-position appears at δ of 127.5 ppm. The carbon atom of 5-positioned triazole ring appears at δ of 131.1 (d, $J = 8.2$ Hz) ppm, while the quaternary carbon atom at 4-position appears at δ of 148.4 ppm. Lastly, the quaternary carbon atom of ketone moiety appears at δ of 176.7 ppm.

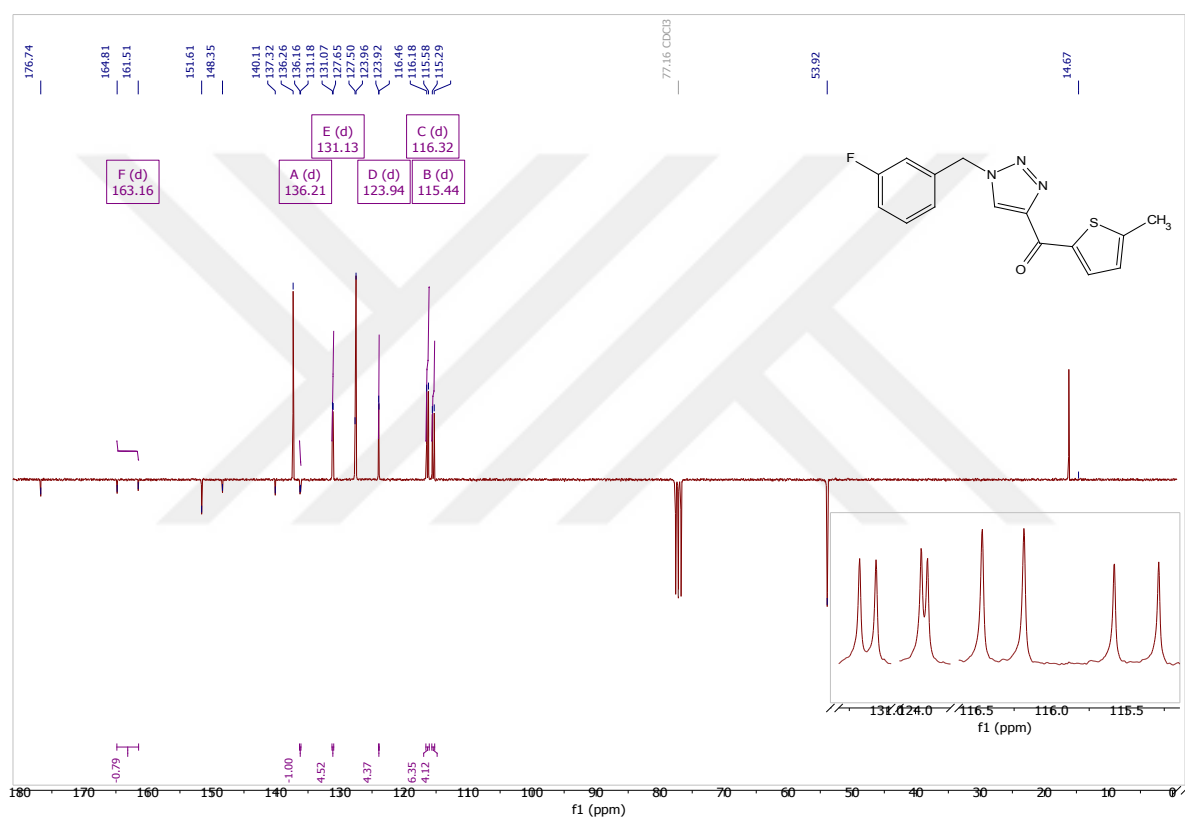


Figure 4.36. APT-NMR spectrum of compound 32

4.1.13. FT-IR, $^1\text{H-NMR}$, $^{13}\text{C-APT-NMR}$ spectroscopy analysis results of (1-(3-fluorobenzyl)-1*H*-1,2,3-triazol-4-yl)(5-methylthiophen-2-yl)methanone (33)

FT-IR spectrum data of compound 33

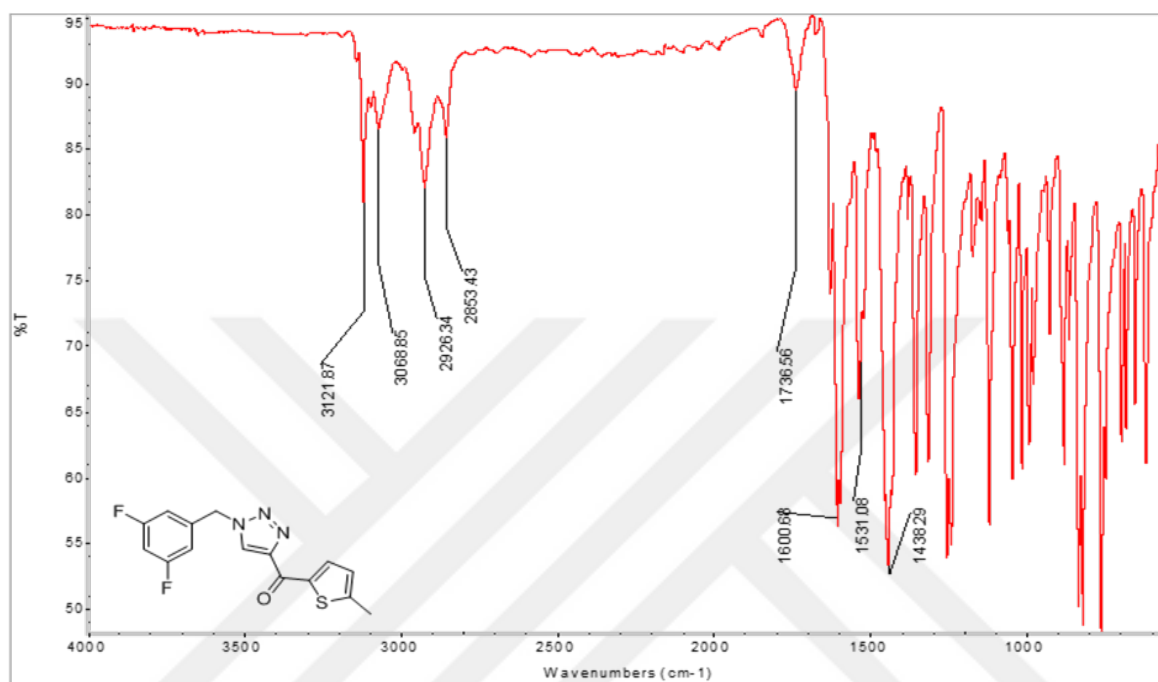


Figure 4.37. FT-IR spectrum of compound 33

Table 4.13. Selected FT-IR spectrum data of compound 33

$\bar{\nu}$ (cm ⁻¹)	Bonds
3121, 3068	Aromatic C-H bond's band
2926, 2853	Methyl C-H bond's band
1736	C=O bond's band
1600-1531-1438	Aromatic C=C, N=N, C=N bond's band

$^1\text{H-NMR}$ spectrum of compound 33

The target compound 33 was dissolved in CDCl_3 . From $^1\text{H-NMR}$ of an analyzed compound, as seen in figure 4.38, one can see the following δ of 2.37 ppm (s, 3H) of $-\text{CH}_3$ and of 5.6 ppm (s, 2H) of $-\text{CH}_2$. Hydrogen atoms of thiophene ring resonate at δ of 8.48 – 7.17 ppm the hydrogen atom at 4-position appears at δ of 7.17 ppm (s, 1H), and hydrogen atom at 3-

position appears at δ of 8.48 ppm (s, 1H). hydrogen atoms of 3,5-difluoro phenyl ring appear at δ of 6.77 ppm as a conjugate of doublet and singlet of 3H. Lastly, the hydrogen atom of triazole ring appears at δ of 8.11 ppm (s, 1H).

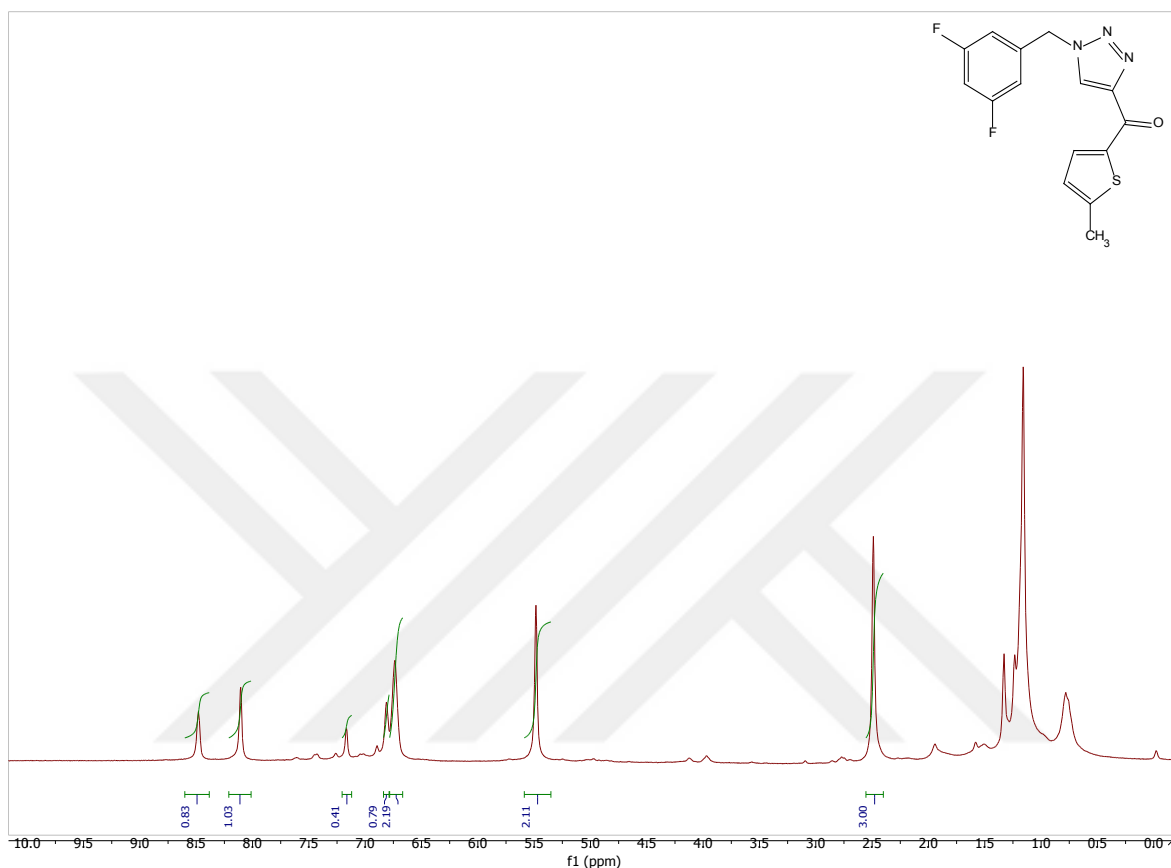


Figure 4.38. ^1H -NMR spectrum of compound 33

^{13}C -NMR spectrum of compound 33

The target compound 33 was dissolved in CDCl_3 . From ^{13}C -NMR of an analyzed compound, as seen in figure 4.39, one can see the following δ of 16.4 ppm belongs to $-\text{CH}_3$ and of 53.5 ppm belongs to methylene linker. Carbon atoms of thiophene ring resonate at δ of 151.8 – 127.6 ppm. The quaternary carbon atoms at 2- and 5-positions appear at δ of 140.1 ppm, and at δ of 151.8 ppm. Carbon atom at 3-position, on the other hand, appears at δ of 137.4 ppm, carbon atom at 4-position appears at δ of 127.6 ppm. Carbon atoms of fluorine phenyl ring resonate at 165.2 – 104.8 ppm as following: quaternary carbon atoms at 1-, 3-, and 5-positions appear at δ of 138.1 ppm; of 163.5 (d, $J = 251.4$ Hz) ppm; and of 163.6 (d, $J = 251.2$ Hz) ppm, respectively. Carbon atom at 4-position appears at δ of 104.8 (dd, $J = 25.1$

Hz) ppm, carbon atoms at 2- and 6-position appear at δ of 111.3 (dd, $J = 26.0, 17.5$ Hz) ppm. The carbon atom of 5-positioned triazole ring appears at δ of 124.9 ppm, while the quaternary carbon atom at 4-position appears at δ of 148.6 ppm. Lastly, the quaternary carbon atom of ketone moiety appears at δ of 176.6 ppm.

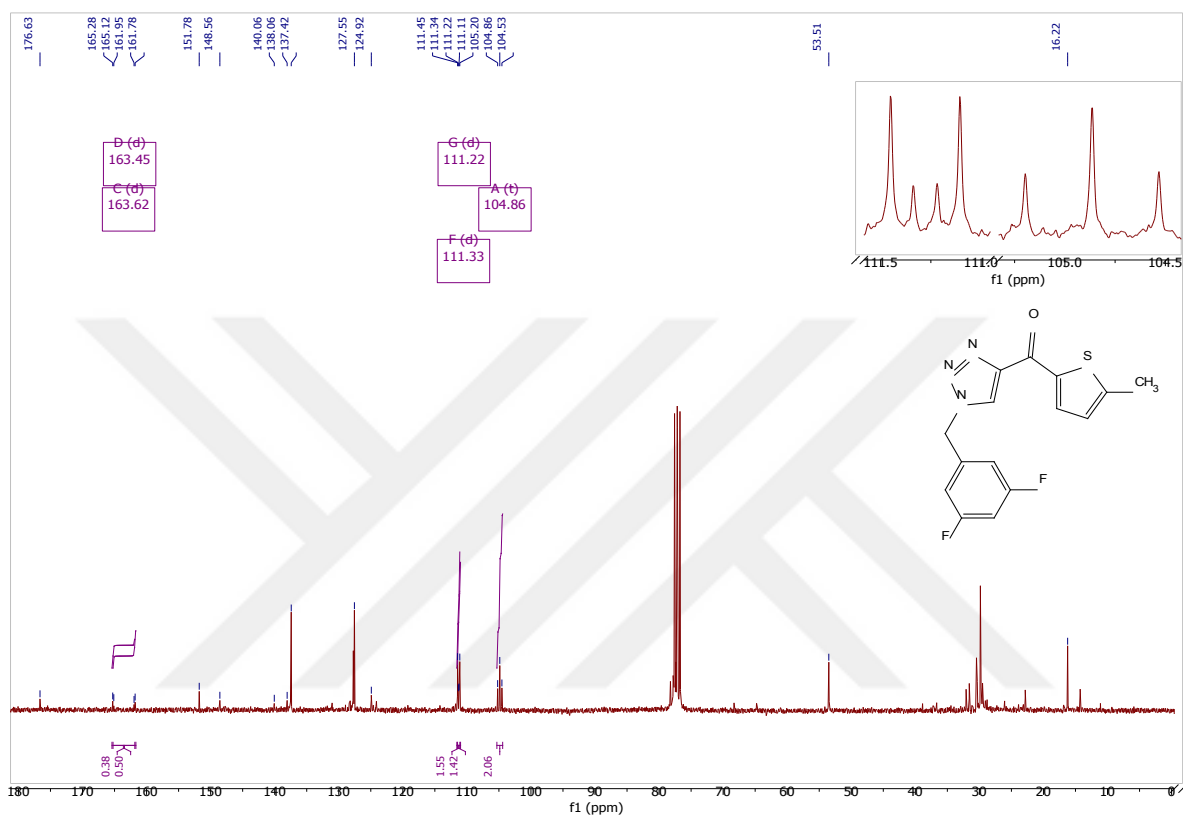


Figure 4.39. ^{13}C -NMR spectrum of compound 33

4.1.14. FT-IR, $^1\text{H-NMR}$, $^{13}\text{C-APT-NMR}$ spectroscopy analysis results of (5-bromothiophen-2-yl)(1-(3-fluorobenzyl)-1*H*-1,2,3-triazol-4-yl)methanone (34)

FT-IR spectrum data of compound 34

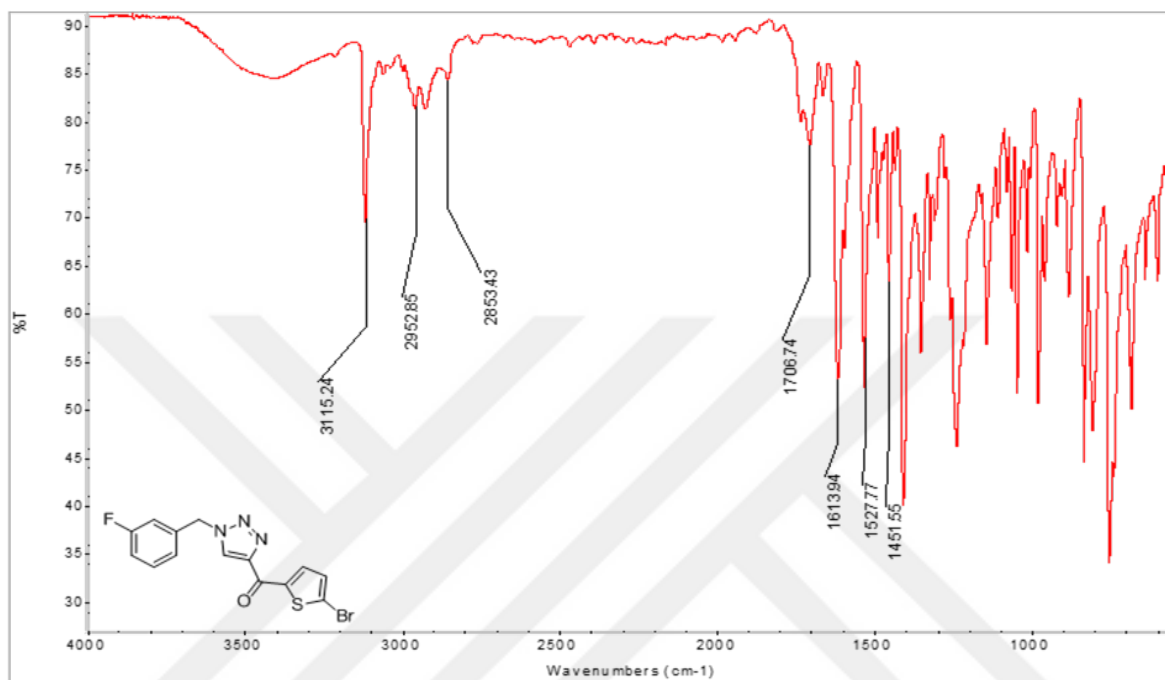


Figure 4.40. FT-IR spectrum of compound 34

Table 4.14. Selected FT-IR spectrum data of compound 34

$\bar{\nu}$ (cm ⁻¹)	Bonds
3111	Aromatic C-H bond's band
2952, 2853	Methyl C-H bond's band
1706	C=O bond's band
1613-1527-1451	Aromatic C=C, N=N, C=N bond's band

$^1\text{H-NMR}$ spectrum of compound 34

The target compound 34 was dissolved in CDCl_3 . From $^1\text{H-NMR}$ of an analyzed compound, as seen in figure 4.41, one can see the following δ of 5.6 ppm (s, 2H) of $-\text{CH}_2$. Hydrogen atoms of thiophene ring resonate at δ of 8.37 – 7.10 ppm. The hydrogen atom at 4-position appears at δ of 7.10 (d, 1H), and hydrogen atom at 3-position appears at δ of 8.37 ppm (d,

1H). Hydrogen atoms of 3-fluorophenyl ring appears at δ of 7.37 – 6.93 ppm as following: hydrogen atom at 2-position appears at δ of 6.93 ppm as (d, 1H), hydrogen atoms at 4- and 6-positions appear at δ of 7.01 ppm as (dd, 2H), hydrogen atom at 5-position appears at δ of 7.37 ppm (td, 1H). Lastly, the hydrogen atom of the triazole ring appears at δ of 8.09 ppm (s, 1H).

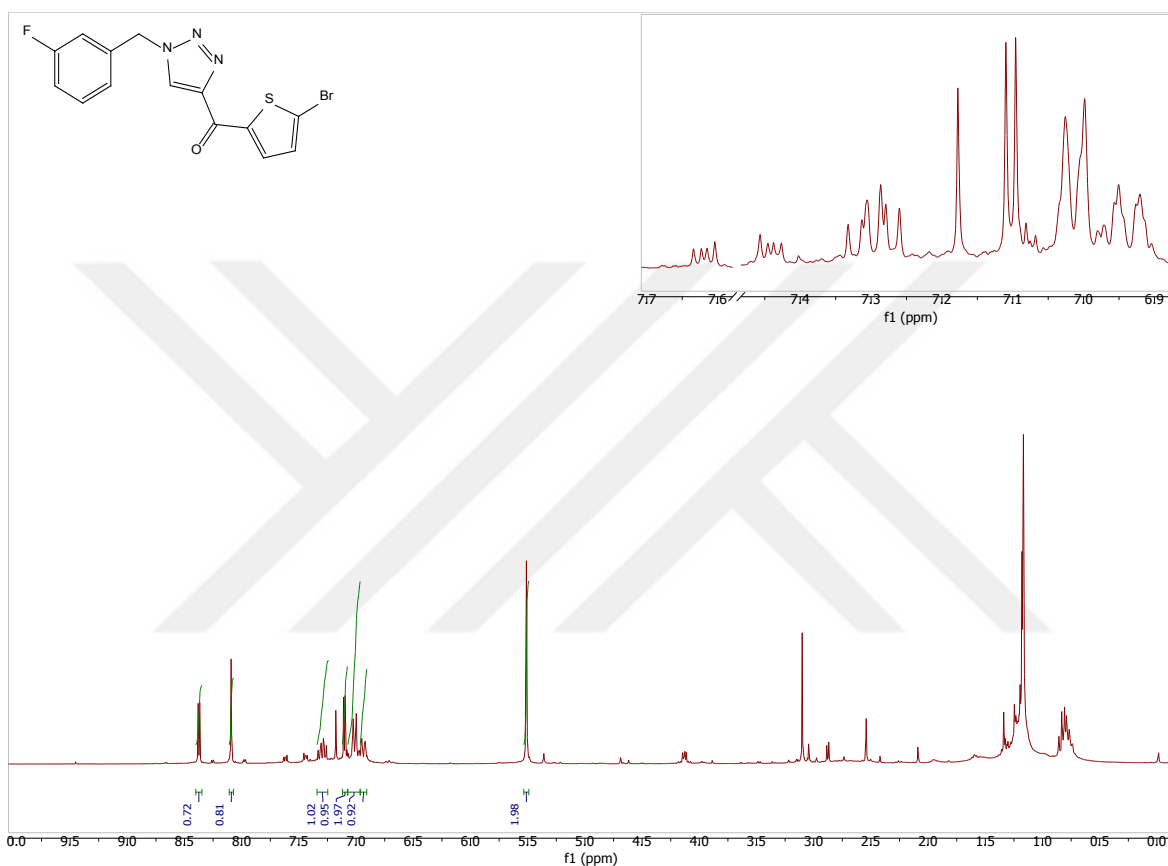


Figure 4.41. ^1H -NMR spectrum of compound 34

^{13}C -NMR spectrum of compound 34

The target compound 34 was dissolved in CDCl_3 . From APT-NMR of an analyzed compound, as seen in figure 4.42, one can see the following δ of 54.0 ppm belongs to methylene linker. Carbon atoms of thiophene ring resonate at δ of 145.0 – 124.8 ppm. The quaternary carbon atoms at 2- and 5-positions appear at δ of 145.0 ppm, and of 124.8 ppm. Carbon atom at 3-position, on the other hand, appears at δ of 136.7 ppm, carbon atom at 4-position appears at 4-position appears at δ of 131.7 ppm. Carbon atoms of fluorine phenyl ring resonate at δ of 163.2 – 115.5 ppm as following: quaternary carbon atom at 1- and 3-

positions appear at δ of 136.0 ppm and of 163.2 (d, $J = 248.6$ Hz) ppm. Carbon atom at 4-position appears at δ of 115.5 (d, $J = 22.4$ Hz) ppm, carbon atoms at 2-position appears at δ of 116.5 (d, $J = 21.0$ Hz) ppm, and carbon atom at 5-position appears at δ of 124.0 (d, $J = 3.1$ Hz) ppm. Carbon atom 6-position appears at δ of 127.8 ppm. Quaternary carbon atom of 4-positioned triazole ring appear at δ of 147.8 ppm, while carbon atom at 5-position appears at δ of 131.3 (d, $J = 8.3$ Hz) ppm. Lastly, the quaternary carbon atom of ketone appears at δ of 175.8 ppm.

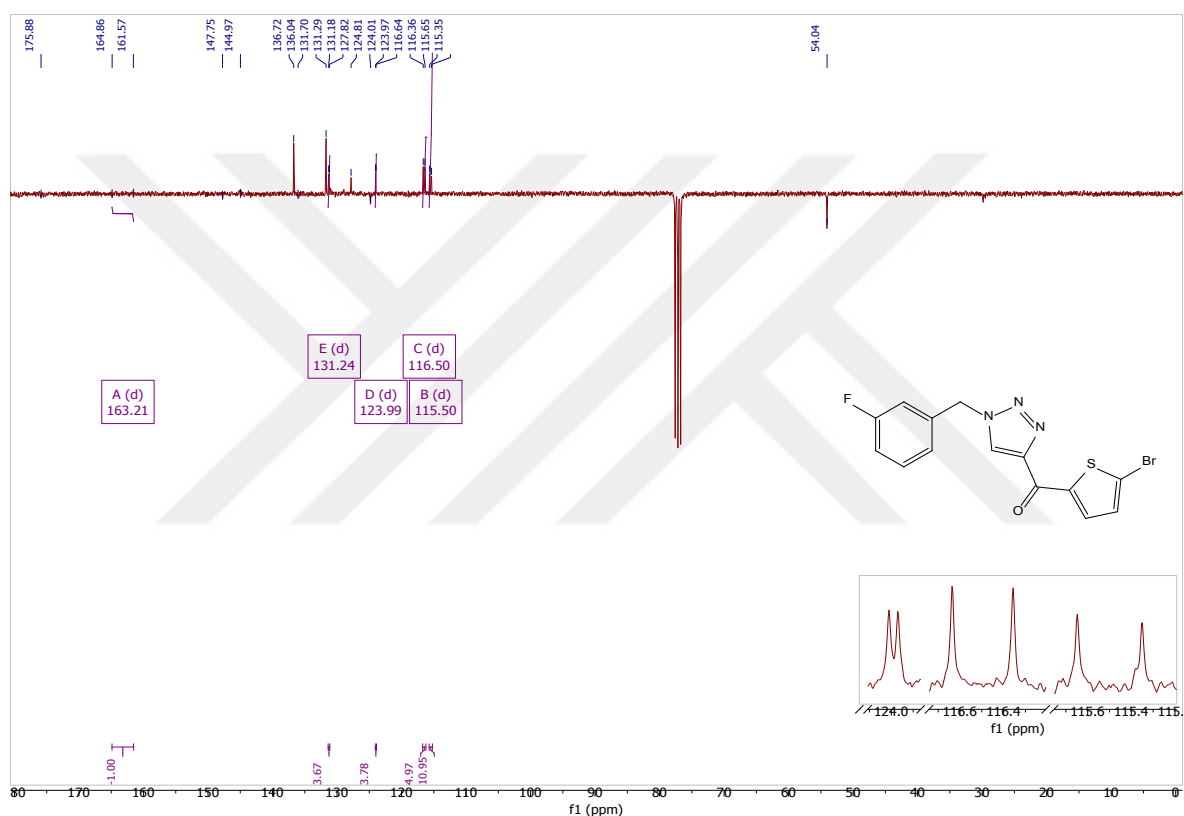


Figure 4.42. APT-NMR spectrum of compound 34

4.1.15. FT-IR, $^1\text{H-NMR}$, $^{13}\text{C-APT-NMR}$ spectroscopy analysis results of (5-bromothiophen-2-yl)(1-(4-methoxybenzyl)-1*H*-1,2,3-triazol-4-yl)methanone (35)

FT-IR spectrum data of compound 35

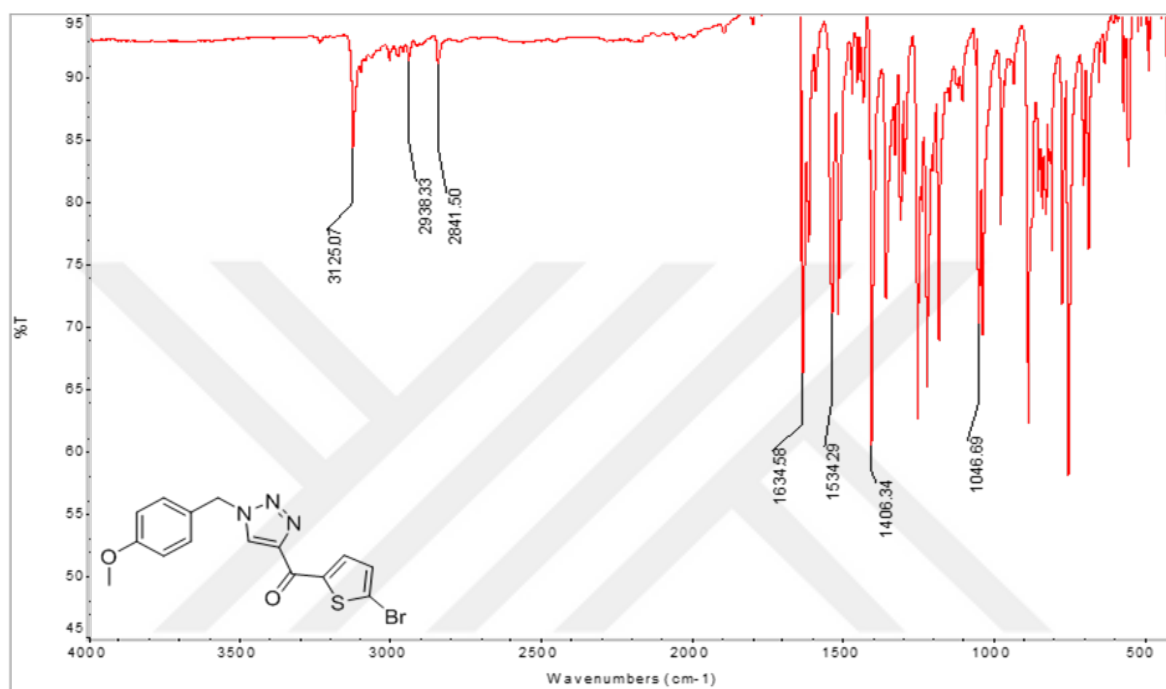


Figure 4.43. FT-IR spectrum of compound 35

Table 4.15. Selected FT-IR spectrum data of compound 35

$\bar{\nu}$ (cm ⁻¹)	Bonds
3125	Aromatic C-H bond's band
2938, 2841	Methyl C-H bond's band
1700	C=O bond's band
1634-1534-1406	Aromatic C=C, N=N, C=N bond's band
1046	C-O-C bond's band

$^1\text{H-NMR}$ spectrum of compound 35

The target compound 35 was dissolved in CDCl_3 . From $^1\text{H-NMR}$ of an analyzed compound, as seen in figure 4.44, one can see the following δ of 5.6 ppm (s, 2H) of $-\text{CH}_2$. Hydrogen

atoms of thiophene ring resonate at δ of 8.45 – 7.18 ppm. The quaternary atom at 4-position appears at δ of 7.18 ppm (d, 1H), and hydrogen atom at 3-position appears at δ of 8.45 ppm (d, 1H). the para-methoxy benzene ring forms AA'XX' system in which hydrogen atoms for the AA' part appear at δ of 6.92 (quasi d, $J = 8.7$ Hz, 2H) ppm, while the XX' part appear at δ of 7.28 (quasi d, $J = 8.7$ Hz, 2H) ppm. Lastly, there is δ of 8.08 ppm (s, 1H) belongs to the hydrogen atom of the triazole ring.

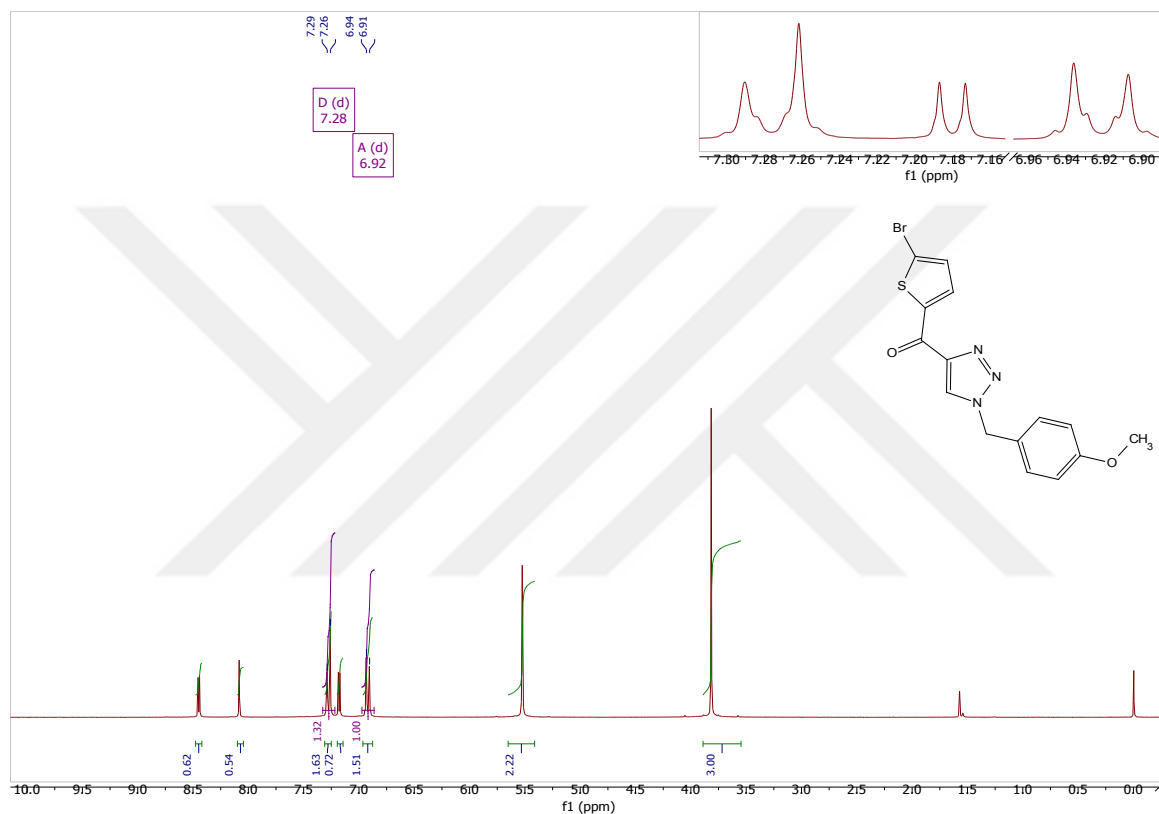


Figure 4.44. ^1H -NMR spectrum of compound 35

^{13}C -NMR spectrum of compound 35

The target compound 35 was dissolved in CDCl_3 . From APT-NMR of an analyzed compound, as seen in figure 4.45, one can see the following δ of 54.3 ppm belongs to $-\text{OCH}_3$ and of 55.5 ppm belongs to methylene linker. Carbon atoms of thiophene ring resonate at δ of 149 – 124.6 ppm. The quaternary carbon atoms at 2- and 5- positions appear at δ of 149.7 ppm, and of 124.6 ppm. Carbon atom at 3-position, on the other hand, appears at δ of 136.6 ppm, carbon atom at 4-position appears at δ of 131.6 ppm. The C-H carbon atoms near para-methoxy group can be seen at δ of 114.9 ppm, while the furthest two C-H atoms can be seen

at δ of 130.2 ppm. Quaternary carbon atoms of para-methoxy benzene at 1-position appears at δ of 125.6 ppm, while carbon at 4-position appears at 160.4 ppm. Quaternary carbon atom of 4-positioned triazole ring appear at δ of 147.5 ppm, while carbon atom at 5-position appears at δ of 127.5 ppm. Lastly, the quaternary carbon atom of ketone appears at δ of 176.0 ppm.

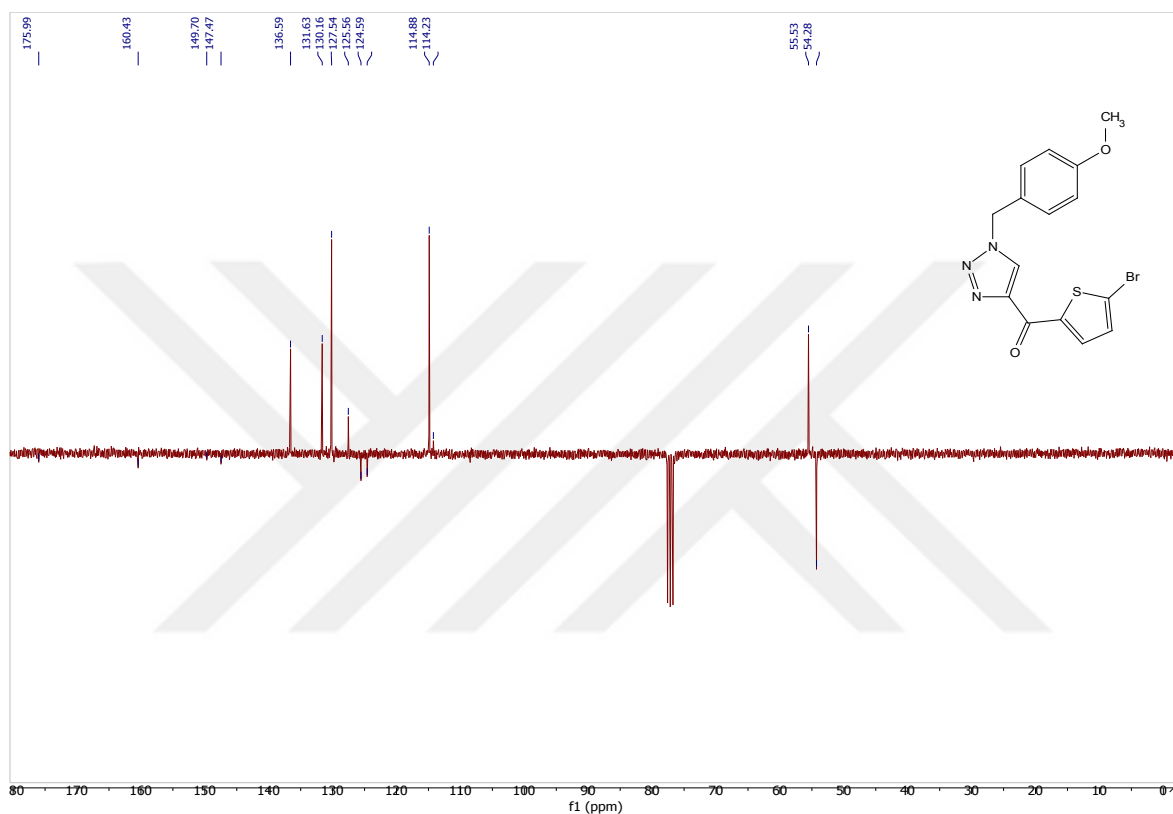


Figure 4.45. APT-NMR spectrum of compound 35

4.2. Biological analysis of triazole compounds

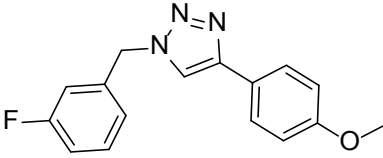
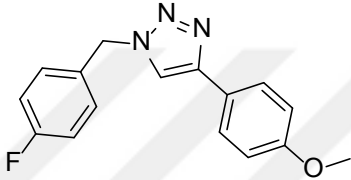
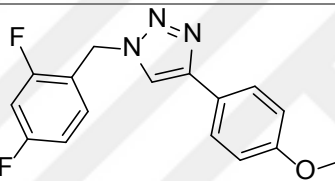
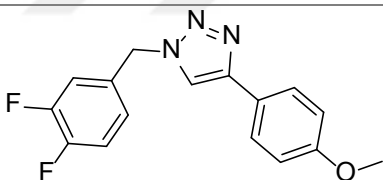
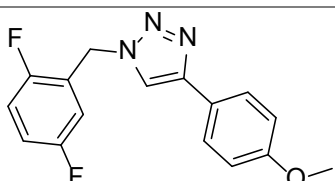
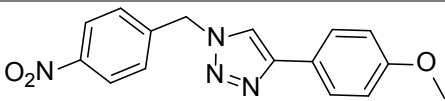
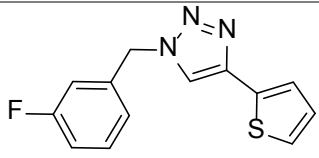
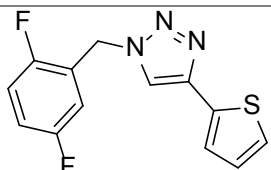
In this thesis, we set two targets to attain: first one, replacing purine ring fo allopurinol with triazole ring so that this replacement leads to lower uric acid accumulation level in patient's veins level compared to the level reached with allopurinol (namely; 20 – 40%) as mentioned in Becker, et al. [34]; second, understanding the influence of alternative substituents influence (namely; fluorine, nitro substituted azido phenyl rings) on triazole ring, in bioassay sense, compared to allopurinol.

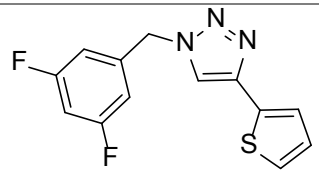
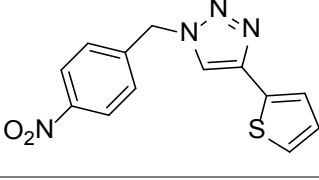
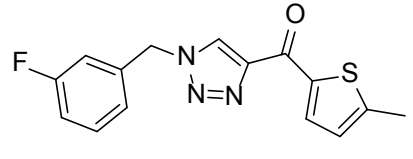
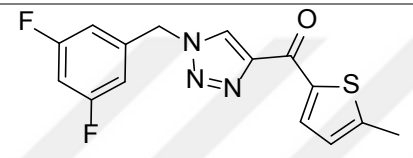
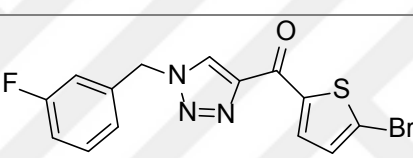
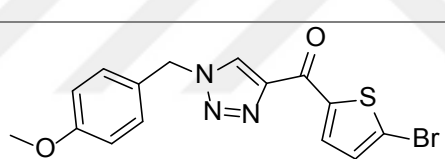
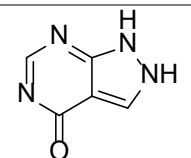
We followed two different methods to acquire triazole surrogate of purine ring as mentioned extensively. Using fluorine and nitro substituted benzyl groups, we synthesized fifteen target compounds. Thirteen of these compounds are fluorine substituted triazole derivatives, and the rest are nitro substituted triazoles.

When in vitro activity test was run on these compounds, all showed superior behavior as an inhibitor to xanthine oxidase compared to that of allopurinol. Through biochemical investigation one can notice, form table 4.16 down below, that compounds 34 and 35 have higher IC_{50} values compared to that of compound 32 (which has a very similar chemical structure to 34) and 33. Compounds 21-27, on the other hand, possessed high to moderate IC_{50} values. Compounds 27, 24, and 23, which are ortho-para, and para substituted functional groups, are preferred more in vitro over compounds 26, 21, 22, and 25, which have the lowest IC_{50} values among para-methoxy substituted triazole rings. Lastly, compounds 28-31 reported the worst IC_{50} values compared to the other three groups, except for compound 30, which is meta substituted functional group.

Unfortunately, our target molecules are less effective in vitro activity compared to febuxostat. We propose two reasons for this observation. First, fluorine atoms are among the worst lone pair donors due to their higher electro negativity compared to the cyanides group. Moreover, nitrogen atom presence at 3 position raises triazole ring hydrophilicity and polarity at that position, which may contribute to weak in vitro potency compared to febuxostat as deduced by Zhang, et al. [39].

Table 4.16. Xanthine oxidase inhibition values

Compound	formula	IC ₅₀ (μ M)
21		1.68 \pm 0.053
22		1.95 \pm 0.013
23		1.58 \pm 0.030
24		1.47 \pm 0.043
25		2.07 \pm 0.075
26		1.59 \pm 0.057
27		1.41 \pm 0.042
28		1.93 \pm 0.085
29		1.99 \pm 0.037

30		1.57 ± 0.014
31		2.11 ± 0.065
32		1.51 ± 0.027
33		1.98 ± 0.073
34		0.93 ± 0.020
35		0.99 ± 0.043
Allopurinol		3.32 ± 0.029

4.3. Conclusion

- 1 First, we followed two different methods to synthesize 1,4-disubstituted-1,2,3-triazole surrogate. Throughout reaction course, we synthesized fifteen compounds in total; eleven of these compounds followed Sharpless synthetic pathway, and four of these compounds followed cross-dehydrogenative coupling synthetic pathway.
- 2 In vitro activity analysis of these compounds all provides to be biochemically superior, as an inhibitor to xanthine oxidase, to allopurinol. By mere discern one can notice, from earlier table, that compound 34 has a higher IC_{50} value, then compound 35 has approximately the same IC_{50} value. And among para-methoxy substituted triazole ring derivatives compound 27 and 24 have the highest IC_{50} value within that group. Lastly, in the class of thiophen-2-yl substituted triazole group compound 30 has the highest IC_{50} value.
- 3 In conclusion, when compared substituted effect on IC_{50} value, specific preference of electron donating group as xanthine oxidase inhibition is noticeable. The clear example of that effect is seen when thiophene moiety is replaced with para-methoxy moiety. While comparing N-arylmethanone-1,2,3-triazole inhibition effect: bromine attached thiophene ring triazole displays an enhanced inhibition ability; methyl attached thiophene ring triazole, on the other hand, has as equal inhibition efficacy to that unattached normal thiophene ring as can be seen from the table above.



REFERENCES

1. Huisgen, R. (1963). 1, 3-dipolar cycloadditions. Past and future. *Angewandte Chemie International Edition in English*, 2(10), 565-598.
2. Michael, A. (1893). Ueber die einwirkung von diazobenzolimid auf acetylendicarbonsäuremethylester. *Journal für Praktische Chemie*, 48(1), 94-95.
3. Sharpless, K. B., Lovell, T., Hilgraf, R., Rostovtsev, V. V., Noodleman, L., Himo, F. *et al.* (2005). Copper (I)-catalyzed synthesis of azoles. DFT study predicts unprecedented reactivity and intermediates. *Journal of the American Chemical Society*, 127(1), 210-216.
4. Rostovtsev, V. V., Green, L. G., Fokin, V. V. and Sharpless, K. B. (2002). A stepwise huisgen cycloaddition process: copper (I)-catalyzed regioselective "ligation" of azides and terminal alkynes. *Angewandte Chemie International Edition*, 41(14), 2596-2599.
5. Meldal, M., Christensen, C. and Tornøe, C. W. (2002). Peptidotriazoles on solid phase:[1, 2, 3]-triazoles by regiospecific copper (I)-catalyzed 1, 3-dipolar cycloadditions of terminal alkynes to azides. *The Journal of Organic Chemistry*, 67(9), 3057-3064.
6. Boren, B. C., Narayan, S., Rasmussen, L. K., Zhang, L., Zhao, H., Lin, Z. *et al.* (2008). Ruthenium-catalyzed azide-alkyne cycloaddition: Scope and mechanism. *Journal of the American Chemical Society*, 130(28), 8923-8930.
7. Worrell, B., Malik, J. and Fokin, V. V. (2013). Direct evidence of a dinuclear copper intermediate in Cu (I)-catalyzed azide-alkyne cycloadditions. *Science*, 340(6131), 457-460.
8. Speers, A. E., Adam, G. C. and Cravatt, B. F. (2003). Activity-based protein profiling in vivo using a copper (I)-catalyzed azide-alkyne [3+ 2] cycloaddition. *Journal of the American Chemical Society*, 125(16), 4686-4687.
9. Agard, N. J., Baskin, J. M., Prescher, J. A., Lo, A. and Bertozzi, C. R. (2006). A comparative study of bioorthogonal reactions with azides. *ACS Chemical Biology*, 1(10), 644-648.
10. Baskin, J. M. and Bertozzi, C. R. (2007). Bioorthogonal click chemistry: Covalent labeling in living systems. *QSAR & Combinatorial Science*, 26(11-12), 1211-1219.
11. Wang, X., Huang, B., Liu, X. and Zhan, P. (2016). Discovery of bioactive molecules from CuAAC click-chemistry-based combinatorial libraries. *Drug Discovery Today*, 21(1), 118-132.
12. Li, W., Jia, Q., Du, Z. and Wang, J. (2013). Direct access to triazole-olefins through catalytic cycloaddition of azides to unsaturated aldehydes. *Chemical Communications*, 49(86), 10187-10189.

13. Ramachary, D. B., Shashank, A. B. and Karthik, S. (2014). An Organocatalytic Azide–Aldehyde [3+ 2] Cycloaddition: High-Yielding Regioselective Synthesis of 1, 4-Disubstituted 1, 2, 3-Triazoles. *Angewandte Chemie International Edition*, 53(39), 10420-10424.
14. Ali, A., Corrêa, A. G., Alves, D., Zukerman-Schpector, J., Westermann, B., Ferreira, M. A. *et al.* (2014). An efficient one-pot strategy for the highly regioselective metal-free synthesis of 1, 4-disubstituted-1, 2, 3-triazoles. *Chemical Communications*, 50(80), 11926-11929.
15. Rozin, Y. A., Leban, J., Dehaen, W., Nenajdenko, V. G., Muzalevskiy, V. M., Eltsov, O. S. *et al.* (2012). Regioselective synthesis of 5-trifluoromethyl-1,2,3-triazoles via CF₃-directed cyclization of 1-trifluoromethyl-1,3-dicarbonyl compounds with azides. *Tetrahedron*, 68(2), 614-618.
16. Ahsanullah, Schmieder, P., Kühne, R. and Rademann, J. (2009). Metal-Free, Regioselective Triazole Ligations that Deliver Locked cis Peptide Mimetics. *Angewandte Chemie International Edition*, 48(27), 5042-5045.
17. Ahsanullah and Rademann, J. (2010). Cyclative Cleavage through Dipolar Cycloaddition: Polymer-Bound Azidopeptidylphosphoranes Deliver Locked cis-Triazolylcyclopeptides as Privileged Protein Binders. *Angewandte Chemie International Edition*, 49(31), 5378-5382.
18. Kwok, S. W., Fotsing, J. R., Fraser, R. J., Rodionov, V. O. and Fokin, V. V. (2010). Transition-Metal-Free Catalytic Synthesis of 1,5-Diaryl-1,2,3-triazoles. *Organic Letters*, 12(19), 4217-4219.
19. Letschert, S., Göhler, A., Franke, C., Bertleff-Zieschang, N., Memmel, E., Doose, S. *et al.* (2014). Super-resolution imaging of plasma membrane glycans. *Angewandte Chemie International Edition*, 53(41), 10921-10924.
20. van Berkel, S. S., Dirks, A. J., Debets, M. F., van Delft, F. L., Cornelissen, J. J. L. M., Nolte, R. J. M. *et al.* (2007). Metal-Free Triazole Formation as a Tool for Bioconjugation. *ChemBioChem*, 8(13), 1504-1508.
21. Brik, A., Alexandratos, J., Lin, Y.-C., Elder, J. H., Olson, A. J., Wlodawer, A. *et al.* (2005). 1,2,3-Triazole as a Peptide Surrogate in the Rapid Synthesis of HIV-1 Protease Inhibitors. *ChemBioChem*, 6(7), 1167-1169.
22. Monceaux, C. J., Hirata-Fukae, C., Lam, P. C.-H., Totrov, M. M., Matsuoka, Y. and Carlier, P. R. (2011). Triazole-linked reduced amide isosteres: An approach for the fragment-based drug discovery of anti-Alzheimer's BACE1 inhibitors. *Bioorganic & Medicinal Chemistry Letters*, 21(13), 3992-3996.
23. Imperio, D., Pirali, T., Galli, U., Pagliai, F., Cafici, L., Canonico, P. L. *et al.* (2007). Replacement of the lactone moiety on podophyllotoxin and steganacin analogues with a 1, 5-disubstituted 1, 2, 3-triazole via ruthenium-catalyzed click chemistry. *Bioorganic & Medicinal Chemistry*, 15(21), 6748-6757.

24. Li, L., Chang, K.-C., Zhou, Y., Shieh, B., Ponder, J., Abraham, A. D. *et al.* (2013). Design of an amide N-glycoside derivative of β -glucogallin: a stable, potent, and specific inhibitor of aldose reductase. *Journal of Medicinal Chemistry*, 57(1), 71-77.
25. Pippione, A. C., Dosio, F., Ducime, A., Federico, A., Martina, K., Sainas, S. *et al.* (2015). Substituted 4-hydroxy-1, 2, 3-triazoles: synthesis, characterization and first drug design applications through bioisosteric modulation and scaffold hopping approaches. *MedChemComm*, 6(7), 1285-1292.
26. Beale, T. M., Bond, P. J., Brenton, J. D., Charnock-Jones, D. S., Ley, S. V. and Myers, R. M. (2012). Increased endothelial cell selectivity of triazole-bridged dihalogenated A-ring analogues of combretastatin A-1. *Bioorganic & Medicinal Chemistry*, 20(5), 1749-1759.
27. Mesenzani, O., Massarotti, A., Giustiniano, M., Pirali, T., Bevilacqua, V., Caldarelli, A. *et al.* (2011). Replacement of the double bond of antitubulin chalcones with triazoles and tetrazoles: Synthesis and biological evaluation. *Bioorganic & Medicinal Chemistry Letters*, 21(2), 764-768.
28. Suzuki, T., Ota, Y., Ri, M., Bando, M., Gotoh, A., Itoh, Y. *et al.* (2012). Rapid Discovery of Highly Potent and Selective Inhibitors of Histone Deacetylase 8 Using Click Chemistry to Generate Candidate Libraries. *Journal of Medicinal Chemistry*, 55(22), 9562-9575.
29. Suzuki, T., Muto, N., Bando, M., Itoh, Y., Masaki, A., Ri, M. *et al.* (2014). Design, Synthesis, and Biological Activity of NCC149 Derivatives as Histone Deacetylase 8-Selective Inhibitors. *ChemMedChem*, 9(3), 657-664.
30. Massarotti, A., Aprile, S., Mercalli, V., Del Grosso, E., Grosa, G., Sorba, G. *et al.* (2014). Are 1,4- and 1,5-Disubstituted 1,2,3-Triazoles Good Pharmacophoric Groups? *ChemMedChem*, 9(11), 2497-2508.
31. Bonandi, E., Christodoulou, M. S., Fumagalli, G., Perdicchia, D., Rastelli, G. and Passarella, D. (2017). The 1, 2, 3-triazole ring as a bioisostere in medicinal chemistry. *Drug Discovery Today*, 22(10), 1572-1581.
32. Gliozzi, M., Malara, N., Muscoli, S. and Mollace, V. (2016). The treatment of hyperuricemia. *International Journal of Cardiology*, 213(23-27).
33. Evenäs, J., Edfeldt, F., Lepistö, M., Svitacheva, N., Synnergren, A., Lundquist, B. *et al.* (2014). HTS followed by NMR based counterscreening. Discovery and optimization of pyrimidones as reversible and competitive inhibitors of xanthine oxidase. *Bioorganic & Medicinal Chemistry Letters*, 24(5), 1315-1321.
34. Becker, M. A., Schumacher, H. R., Espinoza, L. R., Wells, A. F., MacDonald, P., Lloyd, E. *et al.* (2010). The urate-lowering efficacy and safety of febuxostat in the treatment of the hyperuricemia of gout: the CONFIRMS trial. *Arthritis Research & Therapy*, 12(2), R63.
35. Suresh, E. and Das, P. (2011). Recent advances in management of gout. *QJM: An International Journal of Medicine*, 105(5), 407-417.

36. Matsumoto, K., Okamoto, K., Ashizawa, N. and Nishino, T. (2011). FYX-051: a novel and potent hybrid-type inhibitor of xanthine oxidoreductase. *Journal of Pharmacology and Experimental Therapeutics*, 336(1), 95-103.
37. Shi, A., Wang, D., Wang, H., Wu, Y., Tian, H., Guan, Q. *et al.* (2016). Synthesis and bioevaluation of 2-phenyl-5-methyl-2 H-1, 2, 3-triazole-4-carboxylic acid/carbohydrazide derivatives as potent xanthine oxidase inhibitors. *RSC Advances*, 6(115), 114879-114888.
38. Sahu, B., Muruganantham, R. and Namboothiri, I. N. N. (2007). Synthetic and Mechanistic Investigations on the Rearrangement of 2,3-Unsaturated 1,4-Bis(alkylidene)carbenes to Eneidyne. *European Journal of Organic Chemistry*, 2007(15), 2477-2489.
39. Zhang, T.-j., Wu, Q.-x., Li, S.-y., Wang, L., Sun, Q., Zhang, Y. *et al.* (2017). Synthesis and evaluation of 1-phenyl-1H-1, 2, 3-triazole-4-carboxylic acid derivatives as xanthine oxidase inhibitors. *Bioorganic & Medicinal chemistry letters*, 27(16), 3812-3816.

CURRICULUM VITAE

Personal Information

Surname, Name : MIRDAN, Mustafa Nabeel Mirdan
 Nationality : Iraqi
 Date and Place of Birth : 19.10.1990, Kirkuk
 Marital status : Single
 Phone number : 05353090962
 e-mail : mustafa.mirdan@gazi.edu.tr



Education

Degree	School/ Program	Graduation Date
MSc	Gazi University / Chemistry department	On going
Undergraduate	Kirkuk University / Chemistry department	2013
High School	Kirkuk High School	2009

Professional Experience

-

Foreign Language

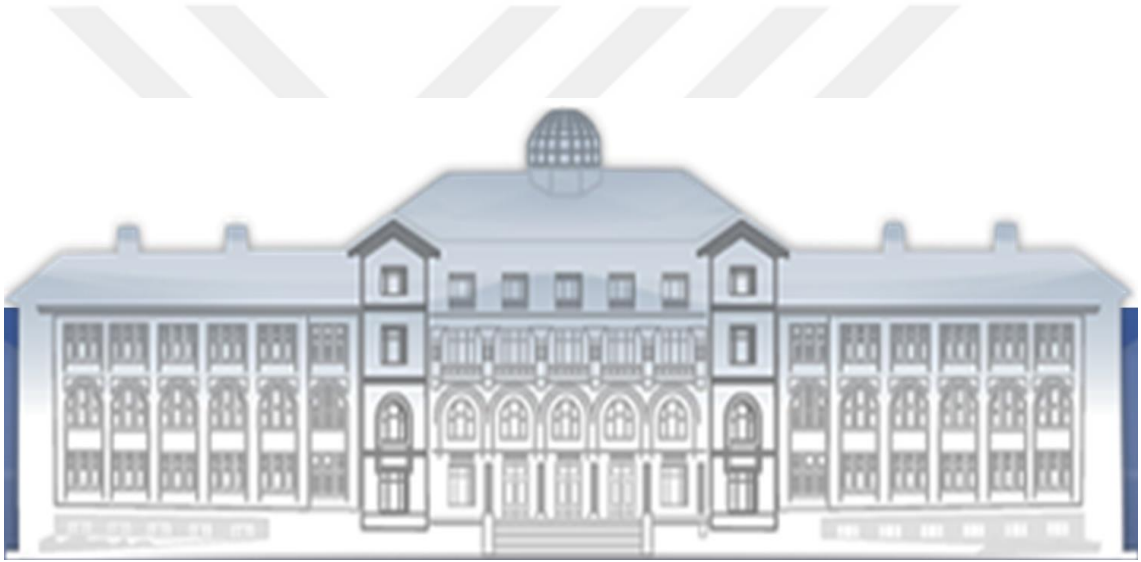
English, Turkish, Arabic

Publications

Mirdan, Mustafa Nabel Mirdan. Noma, Samir Abbas Ali. Ateş, Burhan. and Alayli Altundaş, Aliye. (2019). *Synthesis of 1-benzyl-4-phenyl-1H-1,2,3-trizole derivatives and investigation of its biological activity*. Poster presented at the 7th Drug Chemistry Conference: Design, Synthesis, Production and Standardization of Drug Active Substances.

Hobbies

Swimming, martial art, table tennis



GAZİ GELECEKTİR..